



**US Army Corps  
of Engineers®**  
Engineer Research and  
Development Center

**ERDC**  
INNOVATIVE SOLUTIONS  
for a safer, better world

## **Minimum Thickness of Concrete Pavement for the F-15 and C-17 Aircraft**

Carlos R. Gonzalez, Walter R. Barker, and  
Alessandra Bianchini

July 2013



**The US Army Engineer Research and Development Center (ERDC)** solves the nation's toughest engineering and environmental challenges. ERDC develops innovative solutions in civil and military engineering, geospatial sciences, water resources, and environmental sciences for the Army, the Department of Defense, civilian agencies, and our nation's public good. Find out more at [www.erdclibrary.usace.army.mil](http://www.erdclibrary.usace.army.mil).

To search for other technical reports published by ERDC, visit the ERDC online library at <http://acwc.sdp.sirsi.net/client/default>.



# **Minimum Thickness of Concrete Pavement for the F-15 and C-17 Aircraft**

Carlos R. Gonzalez, Walter R. Barker, and Alessandra Bianchini

*Geotechnical and Structures Laboratory  
US Army Engineer Research and Development Center  
3909 Halls Ferry Road  
Vicksburg, MS 39180-6199*

Final report

Approved for public release; distribution is unlimited.

Prepared for US Army Corps of Engineers  
Washington, DC 20314-1000

## Abstract

The procedure for the design of military rigid airfield pavements contained in the Unified Facilities Criteria 3-260-02 gives the minimum thickness of airfield concrete pavements as 6 in. The introduction of the C-17 aircraft and the requirement that dowel bars be used as load transfer mechanisms at joints for airfield pavements bring into question the validity of the 6 in. minimum thickness. With the objective of updating such minimum thickness criteria, a full-scale test section was constructed and trafficked with wheel loads simulating F-15, B-52, and C-17 aircraft traffic. Test section performance was evaluated by recording the number of passes to failure and by utilizing the falling weight deflectometer testing to measure the stiffness and load transfer capability of joints. In addition, strain gauges were installed on the vertical face of longitudinal joints and on the pavement surface on each side of the longitudinal joints. Evaluation of the test section performance and analysis of the strain data supported an Engineer Research and Development Center team recommendation that the minimum pavement thickness be 8 in. for any dowelled airfield pavement. The team further recommended that a minimum thickness of 11 in. be established for those pavements supporting C-17 aircraft.

**DISCLAIMER:** The contents of this report are not to be used for advertising, publication, or promotional purposes. Citation of trade names does not constitute an official endorsement or approval of the use of such commercial products. All product names and trademarks cited are the property of their respective owners. The findings of this report are not to be construed as an official Department of the Army position unless so designated by other authorized documents.

**DESTROY THIS REPORT WHEN NO LONGER NEEDED. DO NOT RETURN IT TO THE ORIGINATOR.**

# Contents

<b>Abstract.....</b>	<b>ii</b>
<b>Figures and Tables.....</b>	<b>v</b>
<b>Preface.....</b>	<b>viii</b>
<b>1 Introduction.....</b>	<b>1</b>
Background .....	2
Objective .....	3
Report content.....	3
<b>2 Test Section Design.....</b>	<b>4</b>
Thickness design.....	4
Geometric design .....	8
Test site.....	9
Site preparation.....	9
Concrete placement.....	11
Material properties.....	11
Subgrade .....	11
Subbase course.....	20
Concrete pavement.....	21
<b>3 Instrumentation.....</b>	<b>24</b>
Concrete strain measurement.....	24
Joint deflection gauges .....	24
<b>4 Accelerated Pavement Testing.....</b>	<b>29</b>
Traffic lane layout.....	29
F-15 Traffic.....	29
B-52 Traffic .....	29
C-17 Traffic (Lane 3).....	29
<b>5 Performance under Traffic.....</b>	<b>37</b>
General .....	37
Lane 1 Traffic (F-15 and B-52) .....	37
Lane 2 Traffic (F-15) – Items 1, 2, and 3.....	40
Lane 3 Traffic – Items 1, 2, and 3.....	40
<b>6 Analysis of Performance Data .....</b>	<b>45</b>
General .....	45
Falling Weight Deflectometer (FWD) data.....	45
Impulse stiffness modulus .....	46
Load transfer across joints .....	47

LVDT joint deflection gauges .....	49
Strain gauge data for Lane 1.....	52
Strain gauge data for Lane 3.....	55
<b>7 Conclusions and Recommendations .....</b>	<b>63</b>
Conclusions .....	63
Recommendations .....	64
<b>References.....</b>	<b>65</b>
<b>Appendix A: FWD Data .....</b>	<b>66</b>
<b>Report Documentation Page</b>	



# Figures and Tables

## Figures

Figure 1. Layout of the rigid pavement test section.....	5
Figure 2. Layout of the flexible pavement test section. ....	6
Figure 3. Front and aerial views of test facility.....	9
Figure 4. Placement of additional subbase material on the test section. ....	10
Figure 5. Surface of base at transition between Items 2 and 3. ....	10
Figure 6. Finished forms for the east paving lane.....	12
Figure 7. Dowel placement for the east paving lane.....	12
Figure 8. Beginning of concrete placement on March 15, 2010. ....	13
Figure 9. Concrete slump test, east paving lane.....	13
Figure 10. Cylinders and beams with concrete sampled on March 15, 2010.....	14
Figure 11. Center paving lane (from the north) on March 24, 2010.....	14
Figure 12. Sawing of transverse joint, center paving lane. ....	15
Figure 13. Sealed joint of two-week-old concrete. ....	15
Figure 14. Gradation curve for clay (CH) subgrade.....	16
Figure 15. Moisture-density curve for clay subgrade (ASTM 1557). ....	16
Figure 16. Relationship for strength as function of moisture content for subgrade material. ....	17
Figure 17. Stress-strain curves for compression tests.....	18
Figure 18. Construction of Mohr's circle for subgrade clay. ....	18
Figure 19. Correlation curve between CBR and soil reaction modulus for fine grain soils.....	19
Figure 20. Subbase aggregate blend gradations.....	20
Figure 21. Mohr's circles of the subbase material.....	21
Figure 22. Concrete mix design characteristics. ....	22
Figure 23. Strain gauge location layout on the test section.....	25
Figure 24. Strain gauge locations on each test item. ....	26
Figure 25. Strain gauge installation on the vertical face of the longitudinal joint. ....	26
Figure 26. Gauges being installed on the slab surface.....	27
Figure 27. Schematic of joint displacement gauge.....	27
Figure 28. Installation of a joint deflection gauge – concrete block-out and gauge mount. ....	28
Figure 29. Fitting of reference plate for joint displacement gauge. ....	28
Figure 30. Traffic lane layout.....	30
Figure 31. Heavy Vehicle Simulator – Aircraft (HVS-A) .....	31
Figure 32. Wheel path of the F-15 tire along longitudinal joint. ....	31
Figure 33. F-15 tire trafficking longitudinal joint of Item 1 (May 6, 2010). ....	32
Figure 34. Wheel path of B-52 traffic on Item 2. ....	32
Figure 35. C-17 traffic lane with guide lines.....	33

Figure 36. Configuration of the C-17 gear (simulated by load cart). .....	34
Figure 37. C-17 traffic pattern as defined by individual tires. ....	35
Figure 38. Combined distribution of traffic for a traffic pattern. ....	35
Figure 39. Corner break in Lane 1 Item 3 at 25,000 passes. ....	38
Figure 40. Corner break at 300 passes of B-52. ....	39
Figure 41. Lane 1 Item 3 corner break at conclusion of traffic (50,000 passes). ....	39
Figure 42. Lane 2 Item 3 at 1,000 passes of the F-15 tire. ....	41
Figure 43. Lane 2 Item 1 at 15,000 passes of the F-15 tire. ....	41
Figure 44. Corner break at transition joint between Items 2 and 3 at 1,303 passes. ....	42
Figure 45. Cracking pattern for Lane 3 Item 3 at 500 passes. ....	43
Figure 46. Cracking pattern for Lane 3 in Item 2 at 700 passes. ....	43
Figure 47. One of the two cracks in Item 1 – note load cart in the background. ....	44
Figure 48. Spalling along the top of dowel in Item 2 (orange dots are FWD test locations). ....	44
Figure 49. Data from LVDT joint deflection gauge Lane 1 Item 1 (longitudinal joint). ....	50
Figure 50. Data from LVDT joint deflection gauge traffic Lane 1 Item 3 (longitudinal joint). ....	50
Figure 51. Data from LVDT joint deflection gauge traffic Lane 3 Item 2 (longitudinal joint). ....	51
Figure 52. Enlargement of the plot for the relative joint deflection for Pass 2 Item 2 .....	51
Figure 53. Data from the LVDT deflection gauge for Lane 3 Item 3. ....	53
Figure 54. Enlargement of the plot for the relative joint deflection for Pass 2 Item 3. ....	53
Figure 55. Surface strain gauge response traffic Lane 1 Item 1 Passes 1-10. ....	54
Figure 56. Surface strain gauge response traffic Lane 1 Item 3 Passes 1-10. ....	54
Figure 57. Strain gauge data for C-17 on Lane 3 Item 1, Pass 1. ....	56
Figure 58. Strain gauge data for C-17 on Lane 3 Item 1, Passes 10 and 11. ....	56
Figure 59. Strain gauge data for C-17 on Lane 3 Item 2, Pass 1. ....	58
Figure 60. Strain gauge data for C-17 on Lane 3 Item 3, first 12 passes. ....	58
Figure 61. Strain gauge data for C-17 on Lane 3 Item 3, vertical face, Passes 1 and 2. ....	59
Figure 62. Strain gauge data for C-17 on Lane 3 Item 3, surface gauges, Passes 1 and 2. ....	59
Figure 63. Strain gauge data for C-17 on Lane 3 Item 3, all gauges, Pass 1. ....	60
Figure 64. Vertical face strain gauge data for C-17 on Lane 3 Item 3, Pass 5 and 6. ....	60
Figure 65. Surface strain gauge data for C-17 on Lane 3 Item 3, Pass 5 and 6. ....	61
Figure 66. Strain gauge data for C-17 on Lane 3 Item 3, Pass 5. ....	61
Figure 67. Strain gauge data for C-17 on Lane 3 Item 3, Pass 11. ....	62

## Tables

Table 1. Data on composite moduli collected during construction of the flexible pavement test section. ....	7
Table 2. Section details and traffic prediction for first crack failure. ....	8
Table 3. Material strength properties for subgrade. ....	19
Table 4. Strength of concrete at 28 days. ....	23
Table 5. Concrete modulus as determined by PSPA at 28 days. ....	23

Table 6. Traffic data for test section. ....	37
Table 7. Test section material properties. ....	38
Table 8. Impulse stiffness modulus for Lane 1 (F-15, B-52 single tire). ....	46
Table 9. Impulse Stiffness Modulus for Lane 3 (C-17) ....	46
Table 10. Deflection-based joint efficiency for Lane 1 Item 1. ....	47
Table 11. Deflection-based joint efficiency for Lane 1 Item 2. ....	48
Table 12. Deflection-based joint efficiency for Lane 1 Item 3. ....	48
Table 13. Deflection-based joint efficiencies for Lane 3 (center paving lane). ....	48
Table A1-1. FWD data Item 1 east paving lane on base course. ....	66
Table A1-2. FWD data Item 2 east paving lane on base course. ....	67
Table A1-3. FWD data Item 3 east paving lane on base course. ....	67
Table A1-4. FWD data Item 1 center paving lane on base course. ....	68
Table A1-5. FWD data Item 2 center paving lane on base course. ....	68
Table A1-6. FWD data Item 3 center paving lane on base course. ....	69
Table A1-7. FWD data Item 1 west paving lane on base course. ....	69
Table A1-8. FWD data Item 2 west paving lane on base course. ....	70
Table A1-9. FWD data Item 3 west paving lane on base course. ....	70
Table A2-1. FWD data for Lane 1 – Item 1 prior to traffic; 0 passes. ....	71
Table A2-2. FWD data for Lane 1 – Item 1 at 1,000 passes of F-15. ....	72
Table A2-3. FWD data for Lane 1 – Item 1 at 50,000 passes of F-15. ....	73
Table A3-1. FWD data for Lane 1 – Item 2 at 100 passes of B-52. ....	74
Table A3-2. FWD data for Lane 1 – Item 2 at 300 passes of B-52. ....	75
Table A3-3. FWD data for Lane 1 – Item 2 at 1,000 passes of B-52. ....	76
Table A4-1. FWD data for Lane 1 – Item 3 at 0 passes of F-15. ....	77
Table A4-2. FWD data for Lane 1 – Item 3 at 1,000 passes of F-15. ....	78
Table A4-3. FWD data for Lane 1 – Item 3 at 10,000 passes of F-15. ....	79
Table A5-1. FWD data for Lane 2 – Item 1 western free edge. ....	80
Table A5-2. FWD data for Lane 2 – Item 2 western free edge. ....	81
Table A5-3. FWD data for Lane 2 – Item 3 western free edge. ....	82
Table A6-1. FWD data for Item 1 at 0 passes. ....	83
Table A6-2. FWD data for Item 2 at 0 passes. ....	84
Table A6-3. FWD data for Item 3 at 0 passes. ....	85
Table A7-1. FWD data for Item 1 at 1,008 passes. ....	86
Table A7-2. FWD data for Item 2 at 1,008 passes. ....	87
Table A7-3. FWD data for Item 3 at 1,008 passes. ....	88

## Preface

Pavement minimum thickness values were established to prevent unrealistically thin pavement sections from being constructed as a result of the Department of Defense (DoD) design procedure applied to light loads, low volume of traffic, or a strong subgrade. In addition, the minimum thickness requirement allowed environmental conditions, material influences and construction feasibility to be taken into account. For rigid airfield pavements, the current minimum thickness allowed in design guidance is 6 in. Justification for the 6 in. minimum thickness could not be found in the literature review. Nevertheless, with current heavy wheel loads and high-pressure tires, investigating the validity of such a low minimum thickness was necessary. The study herein provides data to justify the recommended changes in the minimum thickness values of rigid airfield pavements.

Personnel of the US Army Engineer Research and Development Center (ERDC), Geotechnical and Structures Laboratory (GSL), Vicksburg, Mississippi, conducted research reported in this publication. The ERDC research team consisted of Dr. Walter R. Barker, SOL Engineering Service LLC, and Carlos R. Gonzalez, Airfields and Pavements Branch (APB), GSL. Gonzalez, Drs. Barker and Alessandra Bianchini prepared this publication under the supervision of Dr. Gary L. Anderton, Chief, APB; Dr. Larry N. Lynch, Chief, Engineering Systems and Materials Division; Dr. William P. Grogan, Deputy Director, GSL; and Dr. David W. Pittman, Director, GSL.

COL Kevin J. Wilson was Commander and Executive Director of ERDC. Dr. Jeffery P. Holland was Director at the time the research was conducted.



# 1 Introduction

The design of rigid airfield pavements is based on a mechanistic analysis of the concrete properties, subgrade support, and applied loadings. The following is an excerpt from the Unified Facilities Criteria (UFC) 3-260-02 for the design of pavements for airfield: “The pavement thickness requirement is calculated using a mechanistic fatigue analysis. Stresses under design aircraft are calculated using the Westergaard edge-loaded model. These calculated edge stresses are related to the concrete flexural strength and repetitions of traffic through a field fatigue curve based on full-scale accelerated traffic test of aircraft loads.” The UFC further states that “a wide variety of model tests, theoretical analyses and field measurements have demonstrated that part of the load applied to the edge of a pavement [edge meaning the edge of a slab with an adjacent slab] is transferred to and carried by the adjacent slab.” Taking into account the load transferred to the adjacent slab allows computing realistic estimates of stress with the Westergaard edge-load model. Thus in theory, the required thickness of pavement can be determined for all conditions of loads and subgrade support. If a rigid pavement performed exactly according to the analytical model, the mechanistic model could be relied on to provide accurate thicknesses for all design situations. In reality, the design model does not provide reasonable thicknesses for all design conditions. This is particularly true for conditions involving light loads, low volume of traffic, a strong subgrade, and high strength concrete for which the mechanistic model would calculate a very thin slab thickness.

For flexible pavements, the minimum asphalt thickness was established on the basis of observed performance. However, for rigid pavements, a thorough literature review did not indicate that specific performance studies were used to determine the value of 6 in. as the minimum thickness for plain concrete slabs. Several studies were conducted in the 1950s to determine optimal slab thickness in relation to aircraft loading, The Lockbourne No.1 Test Track Report (Ohio River Division, 1946) evaluated the effects of the variation in types of subgrade on the slab performance concentrating on 6-in.-thick slabs. The report concluded that a deep granular subgrade had a positive influence on slab performance when compared to the effects of the plastic subgrade existing at the test-section location. However, the report did not provide recommendations concerning

the minimum value of slab thickness to account for the subgrade quality. The Lockbourne No. 2 – Modification Multiple Wheel Study (Ohio River Division, 1950) recommended thickness between 15 and 20 in. for 150,000-lb, twin-tandem wheel load traffic. J. H. Stratton proposed that the thickness be restricted to 8 in. with an increased thickness in the gravel base in case of poor subgrade support (Stratton, 1945). Skinner and Martin (1955) supported a similar argument stating that “In general, experience has shown that the minimum thickness of an exposed airfield pavement slab should not be less than 8 in.” The report by Hutchinson (1966) suggested a minimum thickness of 6 in. for reinforced rigid pavements, although there was no mention about plain concrete slab thickness.

## Background

In the current UFC 3-260-02, the required minimum thickness of rigid pavement is 6 in. Although no minimum thickness values are directly specified for different aircraft, minimum values for criteria other than the type of aircraft are tied to pavement thickness. In Table 12-7 (UFC 3-260-02), the recommendation for transverse contraction joint spacing for pavements of 9 in. or less in thickness is 12.5 to 15 ft. This implies that pavements less than 9 in. thick can be constructed and that the joint spacing would not be less than 12.5 ft. Considering warping and curling, a joint spacing of 12.5 ft would indicate that the pavement thickness would be greater than 6 in.

Airfield rigid pavements require the presence of dowels along construction joints and in specific areas such as between existing and newly placed rigid pavements. Therefore, the dowel would influence the slab thickness. Table 12-8 (UFC 3-260-02) specifies a dowel diameter of 0.75 in. for pavement thickness of less than 8 in. and a diameter of 1 in. for pavement thickness between 8 and 11.5 in. Dowels are usually placed at the slab mid-thickness within a criteria-allowed tolerance of 0.5 in. If the slab is part of a reinforced concrete pavement, the UFC 3-260-02 specifies the position of the reinforcement steel in relation to the position of the dowels usually placed at the slab center. For steel placed within the slab, the American Concrete Institute (ACI) recommends a minimum concrete cover of 3 in. Taking into consideration all requirements, the minimum thickness for a 0.75-in. dowel results in 7.75 in. For a 1-in. dowel, it would be 8 in.

Based exclusively on the requirements for the joints and dowel placement, the conclusion is that the minimum thickness of rigid airfield pavements

should be 8 in. Nevertheless, additional investigations are needed to evaluate if there are structural issues that could dictate a different minimum thickness.

## **Objective**

The objectives of this study were to evaluate the current minimum thickness criteria of airfield rigid pavements and develop recommendations for establishing a minimum thickness when considering heavier aircraft. As part of the study, a full-scale test section was constructed at the Engineer Research and Development Center (ERDC) Vicksburg site. This full-scale testing allowed an evaluation of the performance of relatively thin concrete pavements when subjected to single- and multi-wheel aircraft traffic.

## **Report content**

Chapter 2 contains the details of the design of the rigid pavement test section. Chapter 3 describes the instrumentation installed in the test section. Chapter 4 covers the traffic patterns that were applied to the section. Chapter 5 describes the section performance under traffic. Chapter 6 contains summary and analyses of the falling weight deflectometer (FWD) data, linear displacement transducer (LDT) and strain gauge data. Chapter 7 presents a summary of the findings and recommendations.

## 2 Test Section Design

### Thickness design

The test section constructed for this project was designed to support both F-15 and C-17 traffic. The test section consisted of concrete pavements constructed on subbase material that was used in a previous full-scale flexible pavement test section (Gonzalez et al., in preparation).

The rigid pavement test section consisted of three test items. Each test item was 50 ft in length and 45 ft in width and included 9 slabs. The concrete thickness of Item 3 was 8 in., based on the premise that 8 in. is the minimum thickness that a dowelled pavement would be constructed. The concrete thickness of Items 1 and 2 were 11 in. with the total pavement thickness selected based on predicted traffic that the sections should sustain. Figure 1 shows the general layout of the rigid pavement test section.

The concrete pavement test section was built on the area that previously hosted a flexible pavement test section and over a portion of the flexible pavement layers. Data from field tests conducted on the granular layers during construction of the flexible pavement test section were used to determine thickness of the concrete slabs employed in this project. Data from additional tests after trafficking of the flexible test section or prior to constructing the rigid pavement section were not considered for the design of this test section. Figure 2 shows a general layout of the flexible pavement test section including layer thickness and CBR. In particular, the 8-in. test item was placed over Items 3 and 4 of the flexible pavement test section.

With regards to the aggregate layers and subgrade characteristics during construction of the original flexible pavement test section in the previous study, field plate-bearing tests were conducted on top of the base, subbase, and subgrade layers for measuring each layer's reaction modulus ( $K$ ). The plate-bearing tests were executed according the standard CRD-C 655-95 (1995). The CRD-C 655-95 recommends corrections to be applied to the reaction modulus to account for the banding of the plate and saturation. For these tests, the modulus was corrected exclusively for plate bending. Based on the CRD-C 655-95 method, the uncorrected modulus ( $K'_u$ ) is given by the formula:



Figure 1. Layout of the rigid pavement test section.

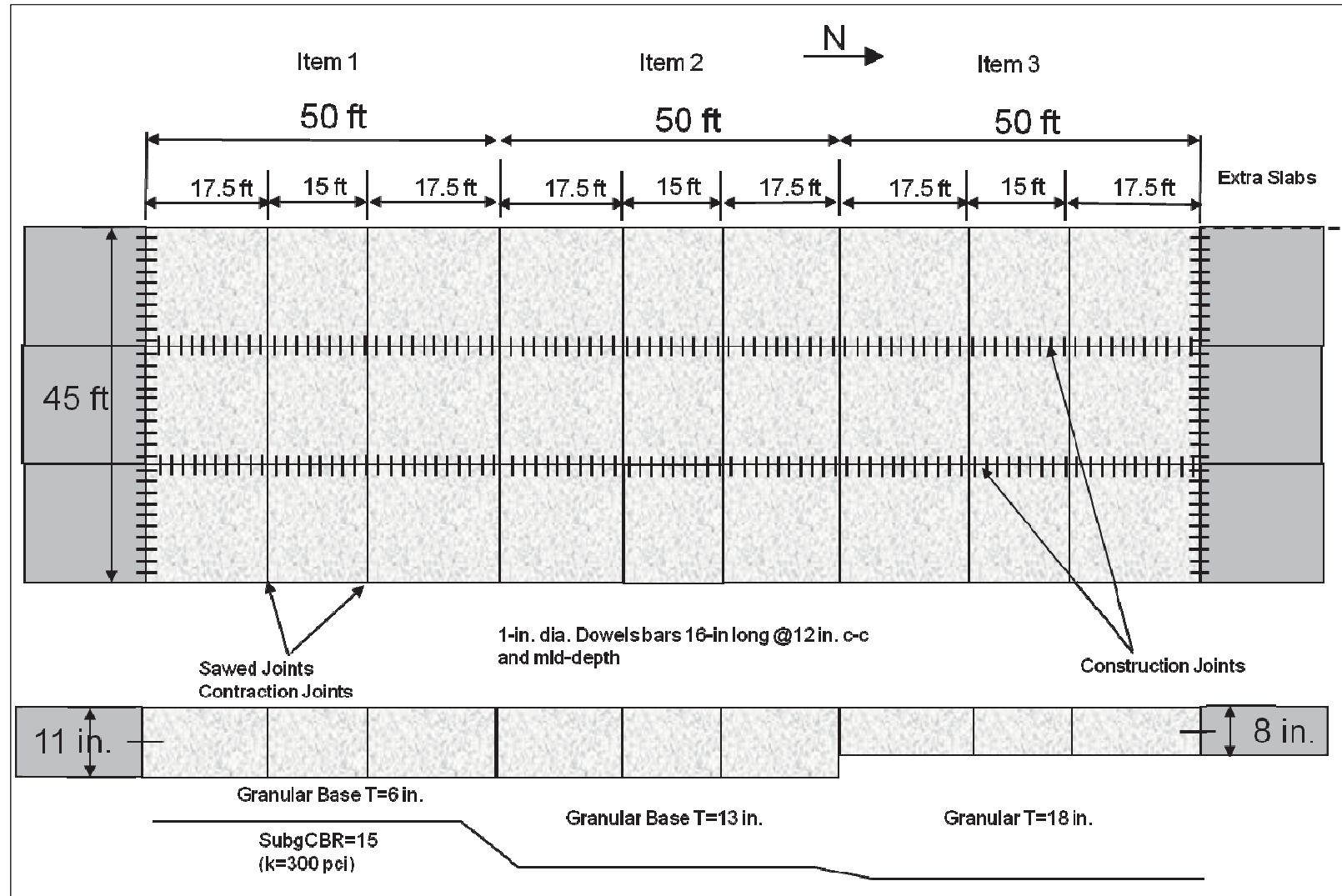
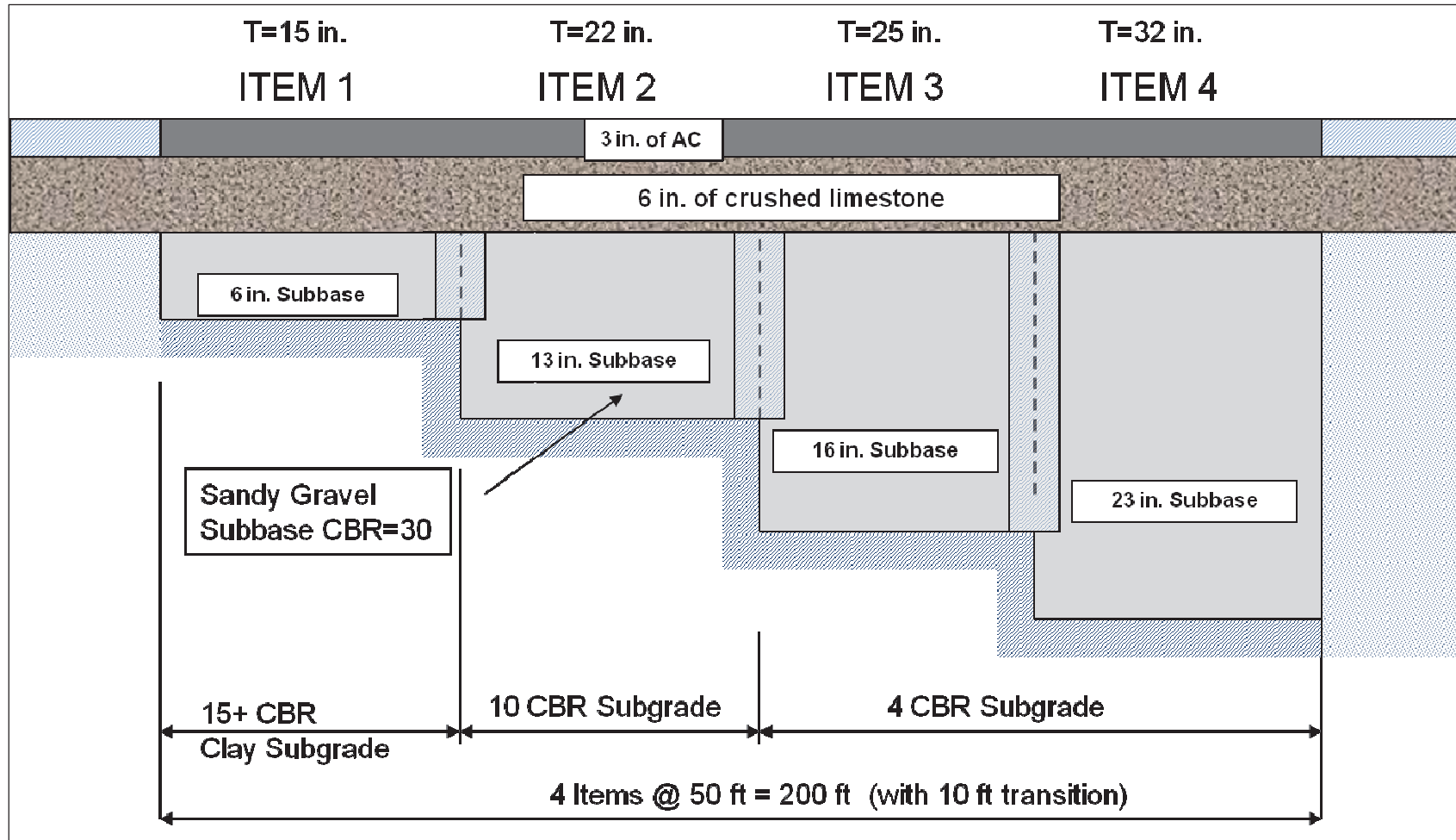


Figure 2. Layout of the flexible pavement test section.



$$K'_u = \frac{10 \text{ psi}}{\text{average deflection}} \quad (1)$$

The value of  $K'_u$  was corrected for bending of the loaded plate using the chart contained in the CRD-C 655-95. Table 1 contains the results of the tests. In the table,  $K_u$  is the corrected value of the soil reaction modulus.

Table 1. Data on composite moduli collected during construction of the flexible pavement test section.

Depth	Item 1			Item 2			Item 3			Item 4		
	$K'_u$ (pci)	Thickness Above Subgrade (in.)	$K_u$ (pci)	$K'_u$ (pci)	Thickness Above Subgrade (in.)	$K_u$ (pci)	$K'_u$ (pci)	Thickness Above Subgrade (in.)	$K_u$ (pci)	$K'_u$ (pci)	Thickness Above Subgrade (in.)	$K_u$ (pci)
Top of base	404	13	331	302	20	259	518	22	404	338	29	285
Tops of subbase	571	7	436	421	14	342	198	16	180	347	23	292
7 in. into subbase				417	7	340	99	9	99	312	16	267
15 in. into subbase								0	0	200	9	182
Top of subgrade	201	0	183	232	0	207	100	0	100	100	0	100

Examining Table 1, the data exhibit considerable scatter and contain a number of contradictions. The subgrade rated CBR for Items 1 and 2 were 15 and 10, respectively; yet the K value for Item 1 is less than the K value for Item 2. Based on the correlations in the Ohio River Division Laboratories (CRD-C 655-95, 1995; Ohio River Division 1943), the expected K for the subgrade of Item 1 would be 200 pci, whereas the expected K for Item 2 would be almost 300 pci. In contrast to the measured K at the top of the subgrade, the K values at the top of the subbase are greater for Item 1 than for Item 2 even if the Item 1 subbase thickness is greater than in Item 2. For Items 3 and 4, the K measured at the top of the subgrade for both was 100 pci, yet the K measured at 16 in. above the subgrade was 180 pci for Item 3 and 267 pci for Item 4.

In order to estimate the traffic the items were expected to support (passes to failure) and on the basis of the correlation between CBR and the data in Table 1, a K of 300 pci was assigned to the Item 1 subgrade; 200 pci was the K for the Item 2 subgrade; and 100 pci was the K for the Item 3 subgrade. The effective K was then determined based on the relationship between subgrade K and base thickness contained in the UFC 3-260-02. This resulted in the effective K values of 333 pci, 320 pci, and 265 pci for Items 1, 2, and 3, respectively.

Determining the predicted passes to failure for each item also required assumptions of concrete properties and selection of aircraft gross weights. The assumed concrete properties included a modulus of elasticity of 4,000,000 psi, a Poisson's ratio of 0.15, and a modulus of rupture of 650 psi. Load transfer across the joints was set at 25%. The aircraft gross weights were 585,000 lb for the C-17 and 81,000 lb for the F-15E.

Based on the traffic loads and assumed properties, the minimum pavement thicknesses were determined for Items 1 and 2 as 11 in. The concrete thickness for Item 3 was 8 in., based on the premise that 8 in. is the minimum thickness that a dowelled pavement would be constructed. Table 2 summarizes item properties and predicted traffic passes to failure. Failure was based on the development of the first crack (first crack criterion).

Table 2. Section details and traffic prediction for first crack failure.

Item	Item Properties				F-15			C-17		
	Subgrade K (pci)	Base Thickness (in.)	Effective K (pci)	Pavement Thickness (in.)	Load (lb)	Wander Width (in.)	Predicted Passes (first-crack criteria)	Load (lb)	Wander Width (in.)	Predicted Passes (first-crack criteria)
1	300	6	333	11	81,000	0	2204	585,000	70	2284
2	200	13	320	11			1847			1828
3	100	18	265	8			7			23

## Geometric design

The length of 50 ft for each test item was selected to match the length of the flexible pavement test items from the previous study. However, the width of the flexible test items was only 40 ft; and, in order to fit three concrete slabs with widths of 15 ft into the test section, the section width was increased to 45 ft. For both the 8- and 11-in.-thick pavements, the slab size of 15 ft is in accordance with the UFC 3-260-02. The length of the slabs was also adjusted to fit the 50-ft length of each test item. Thus, in each test item, the center slab was 15 ft by 15 ft in size, whereas the end slabs were 17.5 ft by 17.5 ft. The two longitudinal joints were dowelled; the dowels were 1 in. in diameter and 16 in. in length. Extra 17.5-ft-long slabs were placed at the end of the test section to provide a maneuvering area and assure confinement of the tested pavement. The only transverse joints that had dowels were those at the end of the test section, specifically between the test section and overrun slabs. Figure 2 shows the final layout of the test section.



## Test site

The full-scale test site was located at the US Army ERDC, Vicksburg. The testing area was in Hangar 4, covered and protected from precipitation, but not temperature controlled. Figure 3 shows the facility and location of the test sections.

Figure 3. Front and aerial views of test facility.



## Site preparation

As explained earlier, the test section for evaluating the rigid pavement minimum thickness was built over subgrade and subbase previously placed for the performance evaluation of flexible pavements.

For the flexible pavement test section, the layers above the subbase included 3 in. of asphalt and 6 in. of crushed stone base. Since the rigid pavement was placed directly over the subbase material, removal of the asphalt and base layers was necessary. To insure complete removal of the surface and base, 1 in. of subbase was also dislodged. Additional subbase material was added to level the subbase and bring the surface of each item to grade. The subbase course in Item 3 required 3 in. of additional material because the flexible pavement removed was 3 in. thicker than the proposed concrete slabs of Items 1 and 2. The subbase surface was compacted using a steel-wheel vibratory roller. Figure 4 shows the test section after removal of the asphalt and base layers and placement of the additional subbase material. The base layer for the rigid pavement section was completed February 25, 2010. Figure 5 shows the base surface at the transition between Items 2 and 3.

Figure 4. Placement of additional subbase material on the test section.



Figure 5. Surface of base at transition between Items 2 and 3.



## Concrete placement

The concrete was placed in three paving lanes along the length of the test section. The first paving lane was placed on the east side of the test section, the second paving lane was placed on the west side, and the third paving lane was a fill-in lane between the first two. The paving lanes were wooden forms in which the dowels were pre-placed. Figure 6 shows the finished forms for the east paving lane (Paving Lane 1). Figure 7 illustrates the method used to secure the dowels for the east lane. Paving of this lane was accomplished during the early morning of March 15, 2010. To avoid the operating equipment moving over the test section base, the concrete was placed using a concrete pump. Figure 8 shows the beginning of concrete placement. During placement operations, slump tests measured the concrete workability (Figure 9). Concrete cylinders and beams were also taken for later laboratory testing (Figure 10). The pavement was leveled using a mechanical screed and was broom finished. Transverse joints were sawed during the afternoon of March 15, 2010. After completion of the east lane, forms were placed for the west lane, and concrete placement was performed in a manner similar to that of the east lane. The west lane was completed March 19, 2010. With regard to the center lane, the dowel bars were greased on the ends extending towards the interior lane, and the base course was re-compacted in preparation for concrete placement (Figure 11). Concrete placement was completed March 24, 2010. The transverse joints were sawed at a concrete age of about 7 hr. Figure 12 shows the sawing of a joint for the center paving lane. Both longitudinal and transverse joints were sealed in the 2-week-old concrete (Figure 13) using Spectrem 900 SL, a traffic-grade, self-leveling silicone-type sealant.

## Material properties

### Subgrade

The subgrade of the test sections was heavy clay (Vicksburg Buckshot Clay). The material was extracted from a borrow pit about 10 miles south of Vicksburg. The soil had Liquid Limit (LL) of 79, Plasticity Index (PI) of 51, and was classified as high plasticity clay (CH), according to the Unified Soil Classification System (USCS). The soil specific gravity was 2.74. The soil gradation curve is contained in Figure 14. The results from laboratory compaction according to modified Proctor ASTM D1557 are summarized in Figure 15, which shows the clay moisture-density curve. Laboratory CBR tests were also executed based on the procedure ASTM D1883-07e2; the data are contained in Figure 16.



Figure 6. Finished forms for the east paving lane.



Figure 7. Dowel placement for the east paving lane.





Figure 8. Beginning of concrete placement on March 15, 2010.



Figure 9. Concrete slump test, east paving lane.





Figure 10. Cylinders and beams with concrete sampled on March 15, 2010.



Figure 11. Center paving lane (from the north) on March 24, 2010.





Figure 12. Sawing of transverse joint, center paving lane.



Figure 13. Sealed joint of two-week-old concrete.



Figure 14. Gradation curve for clay (CH) subgrade.

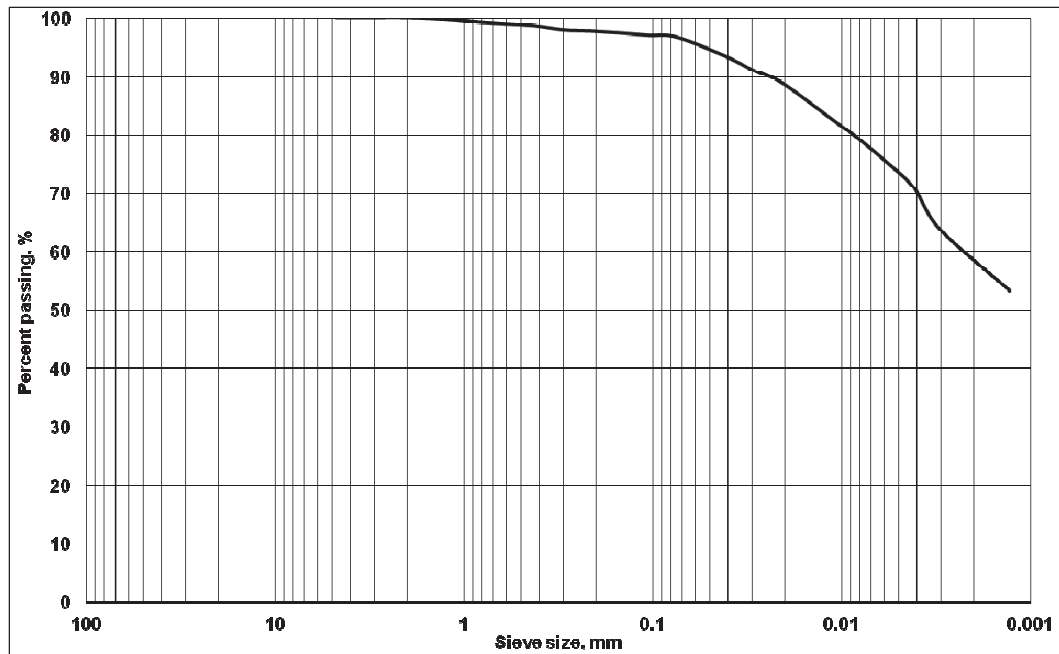


Figure 15. Moisture-density curve for clay subgrade (ASTM 1557).

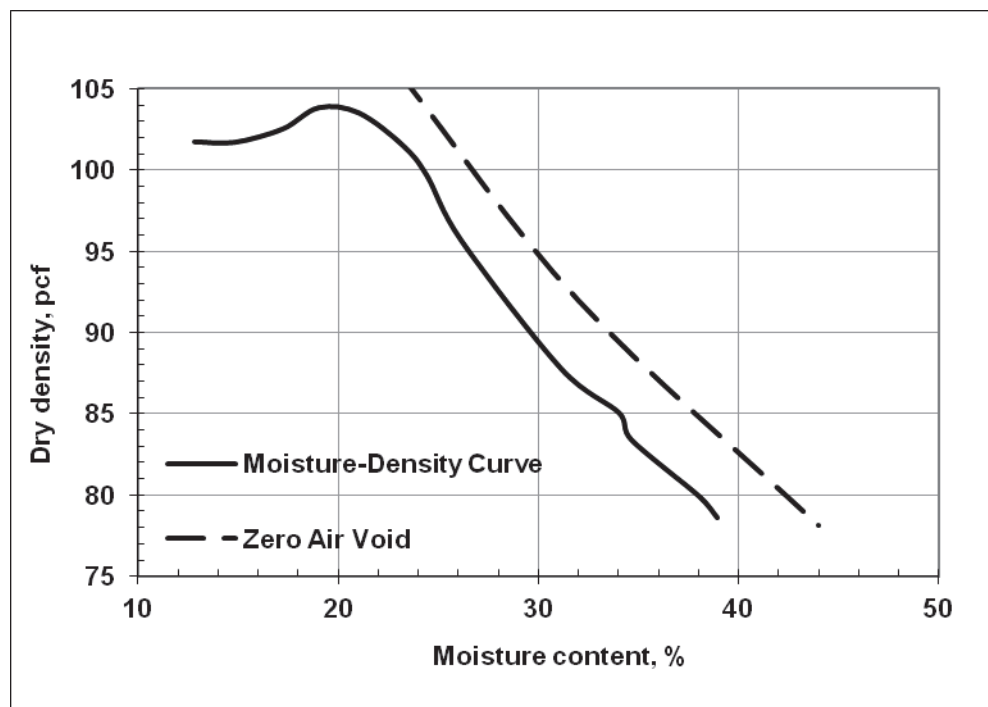
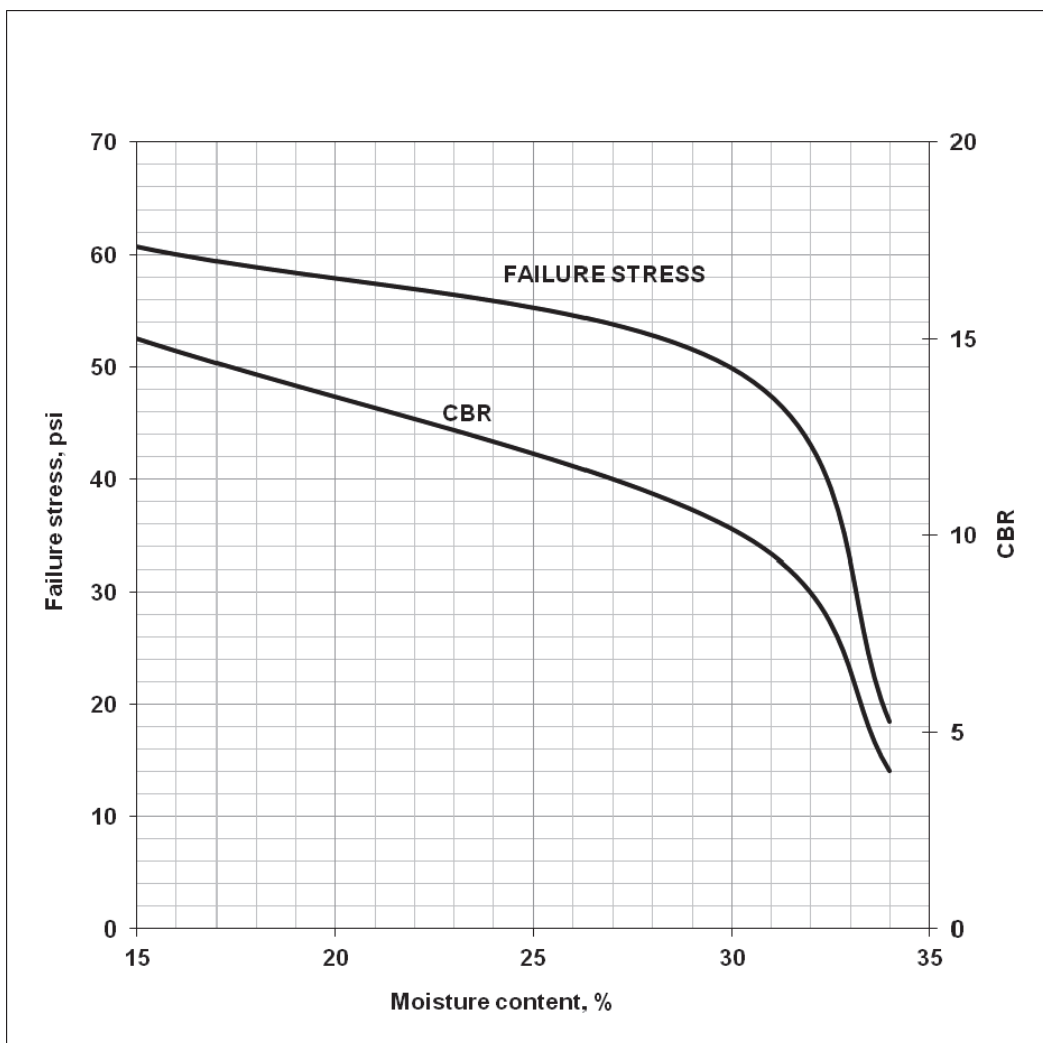




Figure 16. Relationship for strength as function of moisture content for subgrade material.



The subgrade CBR values selected for the previous flexible test section were 4, 10, and 15. The heavy clay water content was then determined from laboratory triaxial testing to reach these desired CBR values. The triaxial tests, with a confining pressure of 15 psi, were drained. Figure 16 shows the relationships between moisture content and CBR and failure stress. Figure 17 summarizes the deviator stress-strain curves of the triaxial test on the subgrade material characterized by CBR values of 4, 10, and 15 with respective moisture content of 34%, 30%, and 27%. Figure 18 presents the Mohr's circles of the material at different CBR values while tested under a confining pressure of 15 psi. Table 3 summarizes material characteristics for each CBR value.

Figure 17. Stress-strain curves for compression tests.

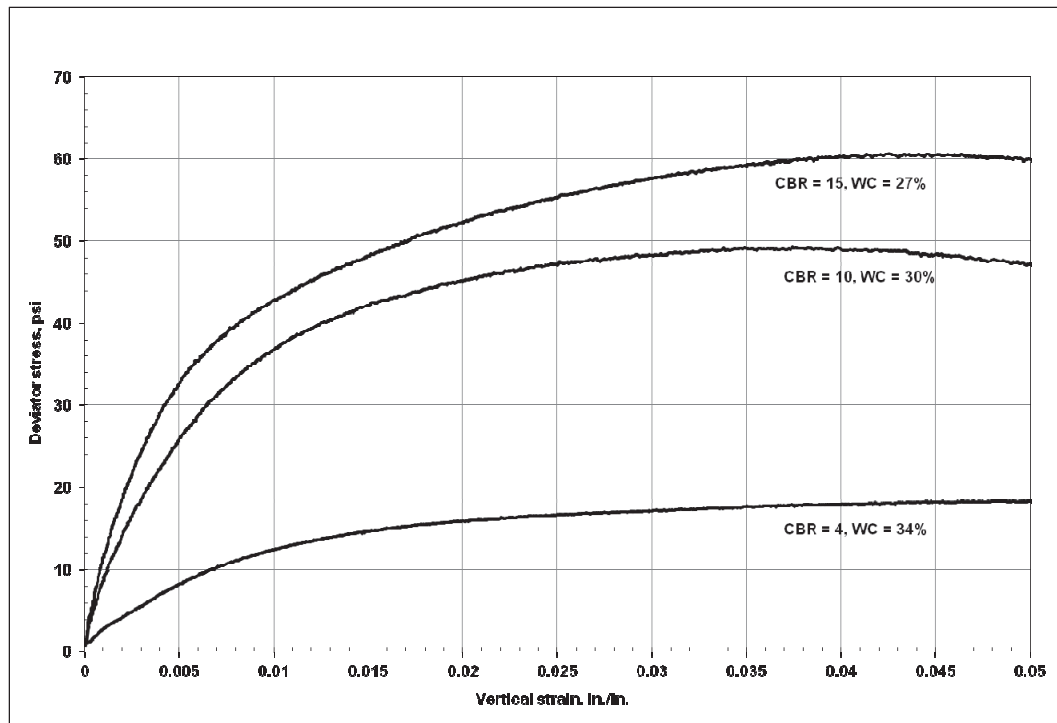


Figure 18. Construction of Mohr's circle for subgrade clay.

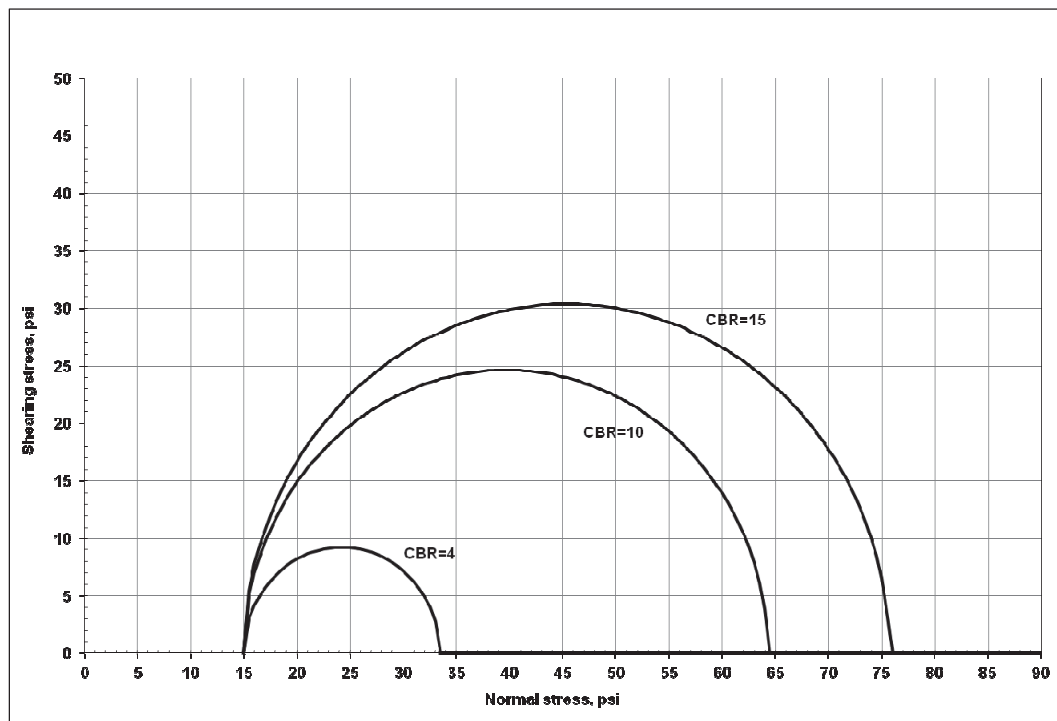


Table 3. Material strength properties for subgrade.

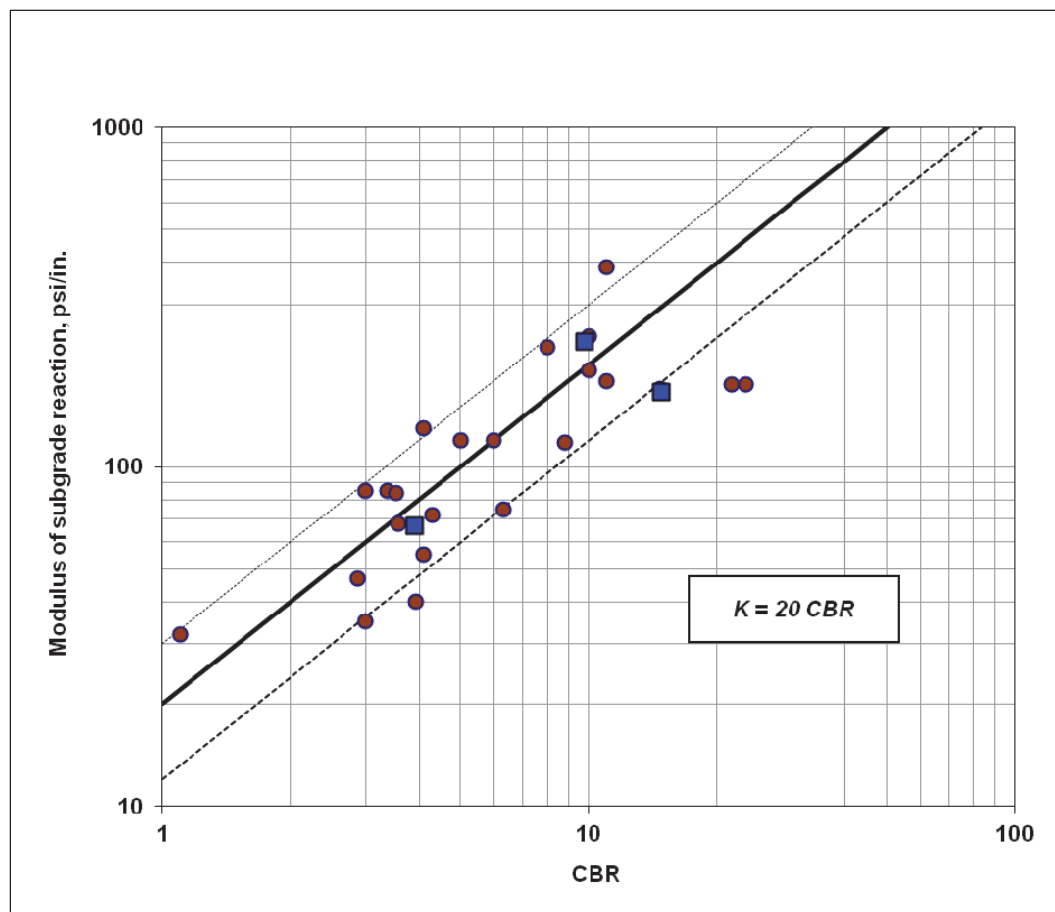
CBR	$(\sigma_1 - \sigma_3)_{ult}$ , psi	$(\sigma_1 - \sigma_3)_f$ , psi	c, psi	$\Phi$ , °	w, %
4	21.2	18.4	9.2	0	34
10	55.1	49.3	25.7	0	30
15	68.9	60.7	30.4	0	27

The CBR data and the results of field tests for determining the soil reaction modulus were analyzed. The inclusion of data points from previous projects allowed increasing the database and formulating the following relationship between CBR and soil reaction modulus (K) for fine grain soils:

$$K = 20 \text{ CBR} \quad (2)$$

Figure 19 shows data points and correlation curve. In the figure, the squares refer to the testing for the flexible pavement test section granular layers that were used for this rigid pavement full-scale testing. The circles refer to past full-scale test projects.

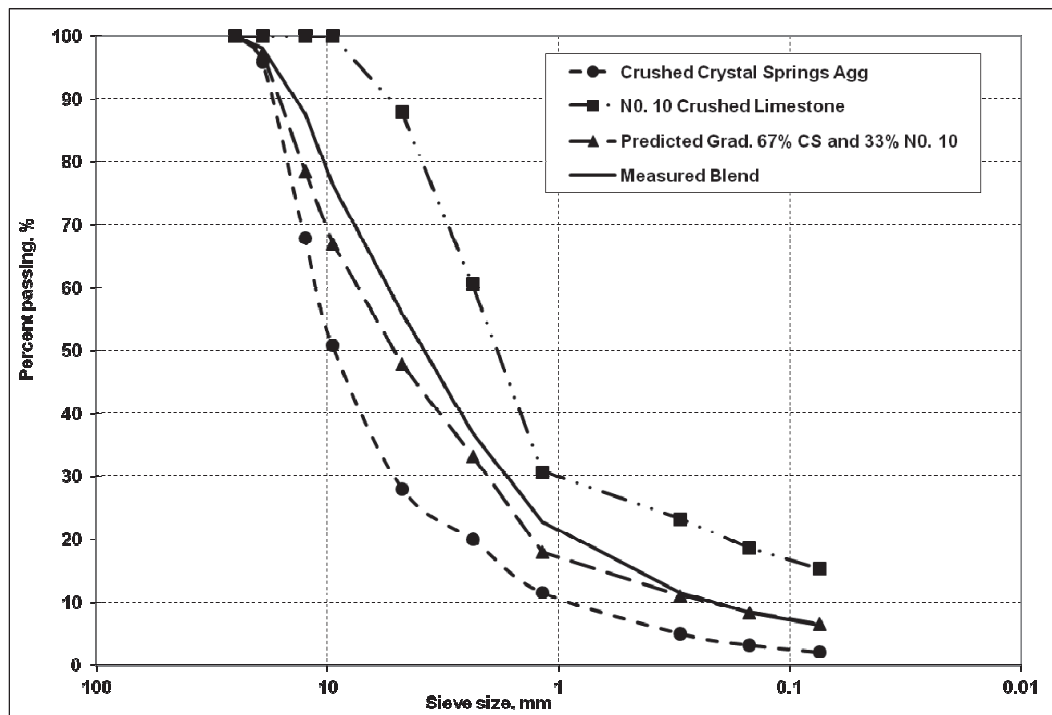
Figure 19. Correlation curve between CBR and soil reaction modulus for fine grain soils.



### Subbase course

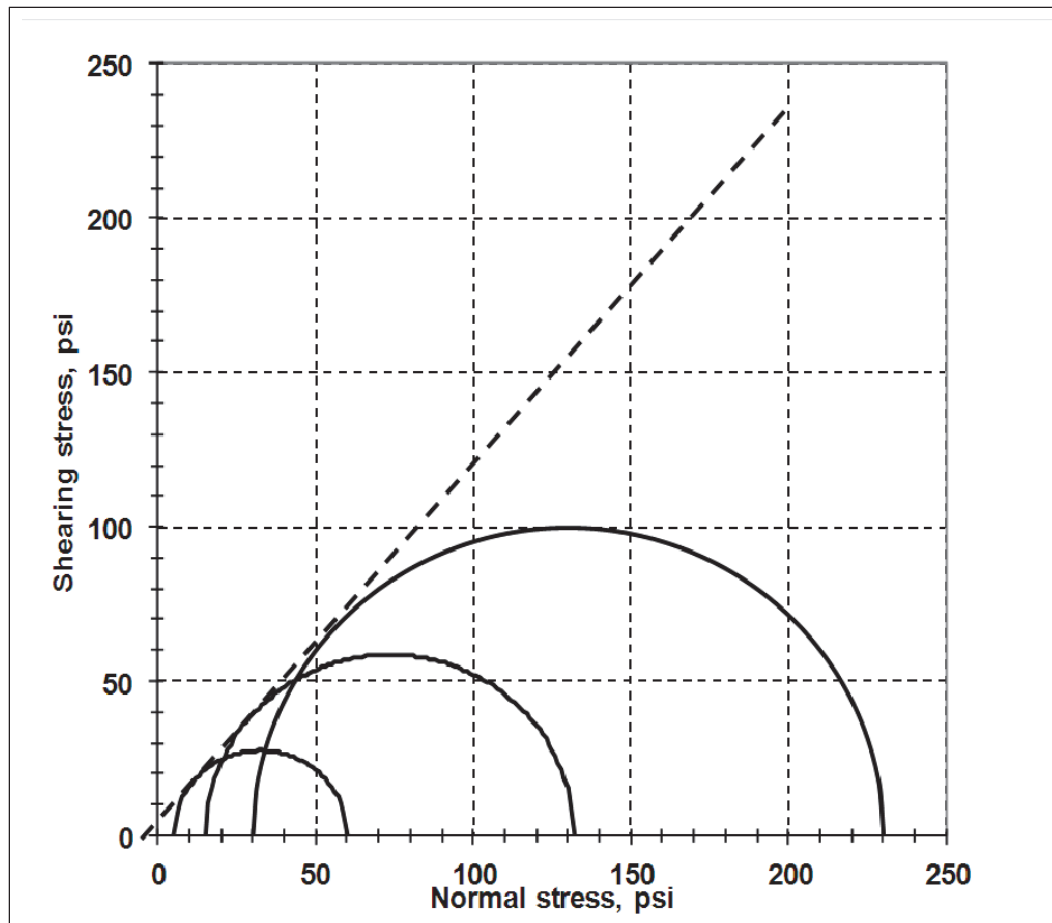
The subbase course consisted of a blended mix of crushed stone (67% by weight) and No. 10 crushed limestone (33% by weight). The aggregate material was obtained from local providers in Vicksburg and Crystal Springs, Mississippi. Figure 20 shows the gradation plots of the blending materials (represented by dashed lines with circle- and square-shaped markers), the predicted gradation of the blend (dashed line with triangle-shaped markers), and the measured gradation of the final blend that was used for construction (continuous line).

Figure 20. Subbase aggregate blend gradations.



The blended material underwent three series of triaxial tests under drained conditions and with confining pressures of 5 psi, 15 psi, and 30 psi, respectively. The tests were conducted in a controlled deformation (strain) rate mode. The strain rate was set at 1% strain per minute; the tests ended after a total deformation of 0.85 in. Figure 21 shows the Mohr's circles obtained from the triaxial tests at different confining-pressure values. The angle of internal friction was 48 deg, and the material cohesion was 8 psi. The test section subbase layer had thicknesses of 6 in., 13 in., and 18 in. for Items 1, 2, and 3, respectively.


Figure 21. Mohr's circles of the subbase material.



### Concrete pavement

The concrete was purchased from MMC Materials, Inc., and was produced at the local plant in Vicksburg. The distance from the plant to the test site is approximately 5 miles. Plant engineers performed the concrete mix design using Federal Aviation Administration (FAA) specifications for airport mixes. Figure 22 shows the data for the concrete mixture. The Material Testing Center at ERDC conducted the testing of the concrete cylinders and beams. Table 4 summarizes concrete strength as obtained from the cylinder and beam testing. The 28-day concrete was tested with a portable seismic pavement analyzer (PSPA) to determine the modulus of elasticity of the in-place concrete slabs. Table 5 shows the PSPA-measured modulus values. The Poisson's ratio was assumed equal to 0.18.

Figure 22. Concrete mix design characteristics.



Construction Type:	Paving	Project Description:	USACE
Constructor:	Diversified	Concrete Supplier:	MMC Materials
Mix Number:	V5041961	Specified Flexural Strength:	650 psi.
Specified Slump:	7 inches	Specified Air Content	3 to 6 %

**Material Properties and Source**

Cementitious Material	Type	Source	Specific Gravity
Portland Cement	II	Holcim	3.15
Fly Ash	C	Headwaters	2.59
GGBFS (Slag)			

Admixtures	Name	Supplier	Dosage, Fl. Oz.
Type A	322 N	BASF	1-3 per cwt.
Type F	7500	BASF	4-8 per cwt
AE	MB90	BASF	3% - 6%

Note: Dosage rate will require adjustments for field and environmental conditions.

Aggregate Size	Type	Supplier	Sp. Gr. SSD	Sp. Gr. OD	Absorption, %	F.M.
# 57	Stone	Vulcan	2.68	2.67	0.80	
Sand	Natural	Green Bro	2.60	2.58	0.66	2.65

**Batch Quantities**

Material	Quantities lb/yd <sup>3</sup> SSD	Absolute Volume ft <sup>3</sup>
Cement, lb.	489	2.49
Fly Ash, lb	122	0.75
Mix Water, lb.	245	3.93
Slag, lb.		
Coarse Aggr., lb.	1850	11.06
Fine Aggr., lb.	1225	7.55
Air Content, %	4.5	1.22
Total Mass, lb.	3931	27.00

Water / cementitious material ratio:		0.40
--------------------------------------	--	------

Mix Design Information:

Mix Class: 5000 psi. with Air

Comments: 650 Flex

Designed by: Andrew Lester

Title: Regional QA Manager

Organization: MMC Materials

**Table 4. Strength of concrete at 28 days.**

Test No.	West Lane		Center Lane		East Lane	
	Compressive Strength (psi)	Flexural Strength (psi)	Compressive Strength (psi)	Flexural Strength (psi)	Compressive Strength (psi)	Flexural Strength (psi)
1	7,115	953	6,201	879	6,541	743
2	6,723	1,058	6,422	842	6,493	782
3	7,036	953	6,318	865	6,558	778
4	7,331	956	6,273	926	6,657	744
Average	7,051	980	6,304	878	6,562	762

**Table 5. Concrete modulus as determined by PSPA at 28 days.**

West lane			Center lane			East lane			Poisson's ratio
Item 1 (ksi)	Item 2 (ksi)	Item 3 (ksi)	Item 1 (ksi)	Item 2 (ksi)	Item 3 (ksi)	Item 1 (ksi)	Item 2 (ksi)	Item 3 (ksi)	
4,960	4,680	5,320	5,190	4,470	4,350	3,700	4,590	4,820	0.18
4,890	4,560	5,350	5,220	4,420	4,510	3,680	4,530	4,780	0.18
5,000	4,540	5,320	5,220	4,480	4,290	3,670	4,540	4,800	0.18
5,100	5,160	5,300	4,800	4,830	5,120	5,770	4,990	5,380	0.18
5,060	5,160	5,350	4,770	4,780	5,110	5,770	4,950	5,340	0.18
5,070	5,210	5,290	4,780	4,780	5,030	5,820	5,030	5,420	0.18
4,910	4,720	5,070	5,120	4,700	5,220	5,170	5,480	5,130	0.18
4,870	4,690	5,000	5,130	4,670	5,190	5,130	5,370	5,070	0.18
4,910	4,640	5,040	5,150	4,630	5,110	4,990	5,310	5,000	0.18
		5,040							0.18
		4,990							0.18
		4,970							0.18
Average Modulus (ksi)									
4,974	48,17	5,170	5,042	4,640	4,881	4,885	4,976	5,082	
Average modulus for paving lane (ksi)									
4,987			4,854			4,997			0.18
Average modulus for the test section (ksi) 4,938									

### 3 Instrumentation

Instrumentation for monitoring pavement performance under traffic was installed throughout the test section. Instrumentation included joint deflection gauges, surface strain gauges, and embedded temperature sensors. Figure 23 shows the general layout of sensor location with respect to the slab joints.

#### Concrete strain measurement

The rigid pavement test section was outfitted to measure the concrete strain resulting from the applied loads. Four gauges were installed along each longitudinal construction joint between the three items. The 2-in.-long strain gauges were general-purpose constantan foil-type gauges with a thin, laminated, polyimide-film backing. Figures 23 and 24 show gauge-schematic locations on the pavement test section. The gauges had a temperature range between  $-100^{\circ}\text{F}$  and  $+200^{\circ}\text{F}$ . For each test item, two gauges were installed before placement of the center lane on the concrete slab vertical face in the east lane, and two gauges were installed on the vertical face of the west lane and placed horizontally to measure tensile or compressive strains induced by the moving loads over the pavement surface. Specifically at each location, one gauge was 1 in. from the bottom of the concrete slab and the other was 1 in. from the top of slab. Figure 25 shows installation details. After placing the center lane and before applying traffic, two other strain gauges were installed on the surface of the concrete slab directly above the gauges on the vertical face. The gauges were 1 in. from the longitudinal joint. Specifically, one gauge was on the center lane and the other was across the joint on the slab of the adjacent lane (on the west or east lane). Figure 26 details surface-gauge installation.

#### Joint deflection gauges

Joint deflection gauges were installed at two locations on the longitudinal joints of Item 2 to measure the differential movement between the concrete slab of the center lane and the slabs of east and west lanes. The joint deflection gauges were constructed by pre-forming rectangular holes in the concrete to install a linear variable differential transformer (LVDT) on one side of the joint and a reference plate on the other side.



Figure 23. Strain gauge location layout on the test section.

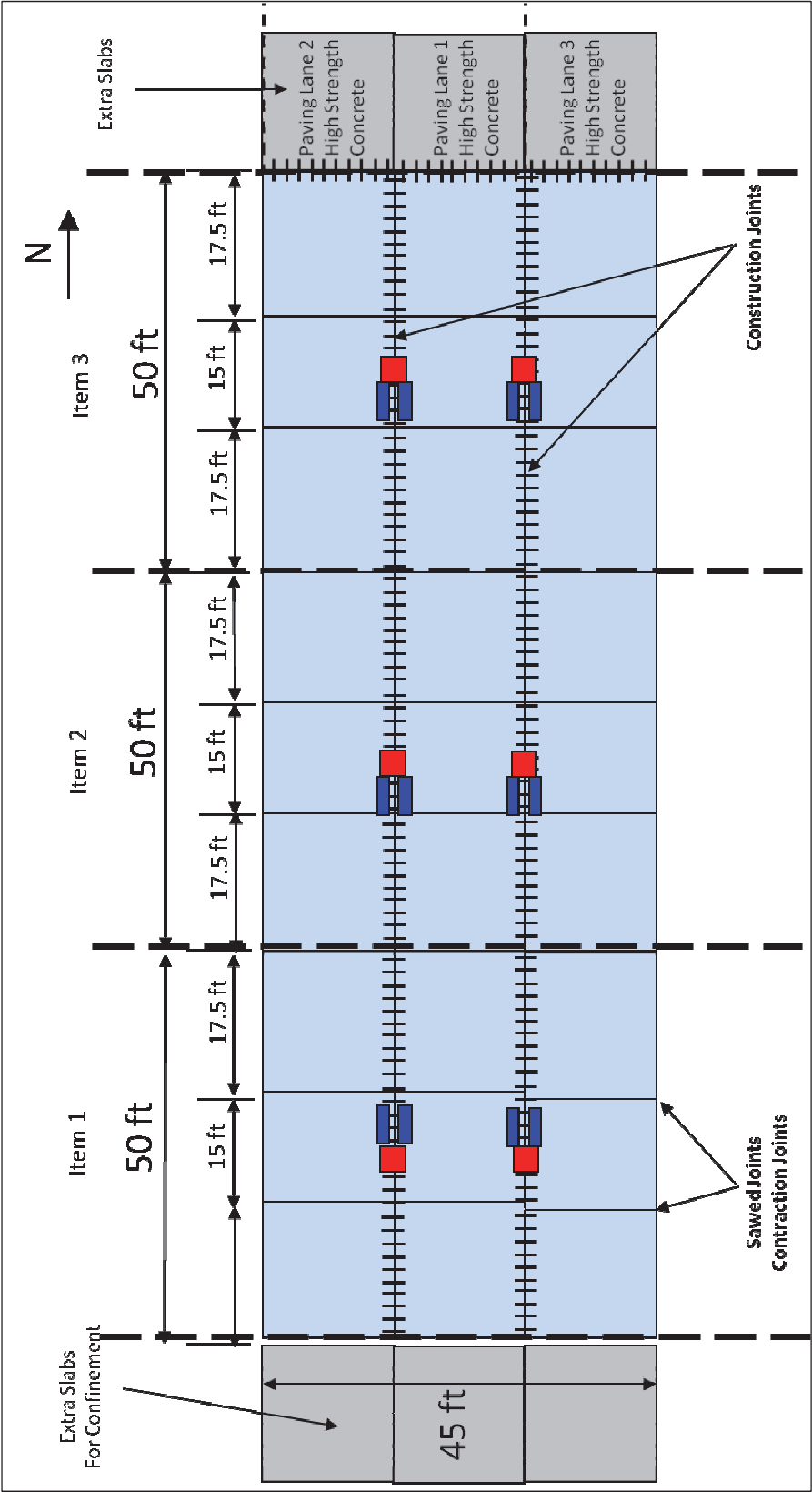


Figure 24. Strain gauge locations on each test item.

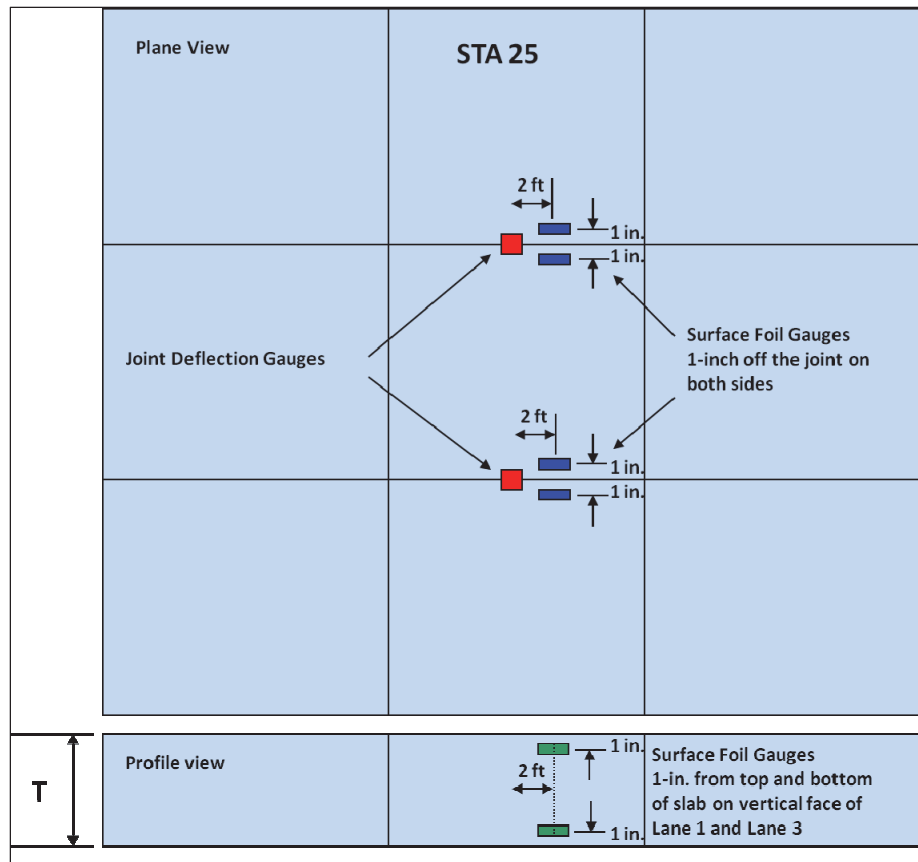


Figure 25. Strain gauge installation on the vertical face of the longitudinal joint.



Figure 26. Gauges being installed on the slab surface.



The LVDT had a measurement range of  $\pm 0.4$  in., allowing a total measurement range of 0.8 in. The construction of the joint deflection gauge allowed for adjustment of the vertical positioning of the LVDT during traffic. Figure 27 shows the schematic for the joint deflection gauges. Figures 28 and 29 are photographs of deflection-gauge installation.

Figure 27. Schematic of joint displacement gauge.

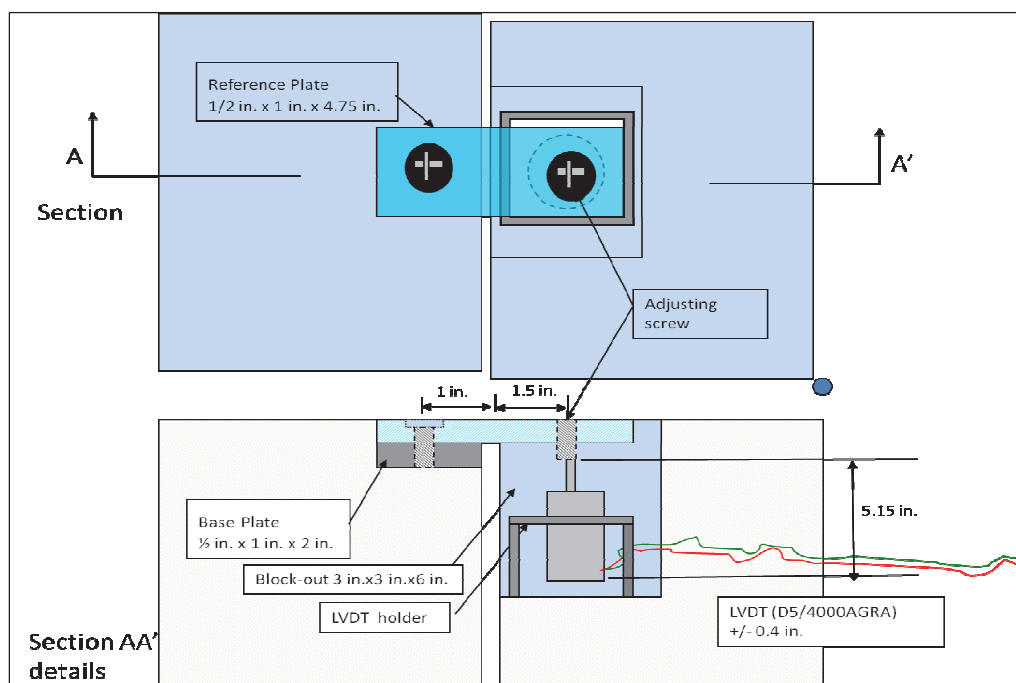




Figure 28. Installation of a joint deflection gauge – concrete block-out and gauge mount.



Figure 29. Fitting of reference plate for joint displacement gauge.



## 4 Accelerated Pavement Testing

### Traffic lane layout

Figure 30 shows the layout of the traffic lanes. Traffic was applied using ERDC's heavy vehicle simulator – aircraft (HVS-A) Mark V, manufactured by Dynatest International, along the west side of the longitudinal joint between the center and the west lanes, and along the west free edge of the test section. The HVS-A (Figure 31) was configured to simulate single-tire loading and channelized traffic. The longitudinal joint between the center and east paving lanes was trafficked using the C-17 load cart with a six-tire configuration simulating one side of the C-17 main gear.

### F-15 Traffic

The F-15 traffic was applied along the west free edge of Items 1, 2, and 3 (Lane 2) and along the west side of the longitudinal joint of Items 1 and 3 (Lane 1), between the west and the center lanes (Figure 30). The traffic of the F-15 tire was channelized with the tire edge located 2 in. from the joint or free edge (Figure 32). The HVS-A was configured to simulate the F-15 single tire loaded to 35,000 lb with a tire pressure of 325 psi (Figure 33). The computed tire contact area and width were 115 in.<sup>2</sup> and 9.4 in., respectively.

### B-52 Traffic

The B-52 channelized traffic was applied only in Item 2 along the west side of the longitudinal joint between the west and center lanes (Lane 1). The HVS-A tire was loaded with 62,000 lb and a tire pressure of 265 psi. The computed contact area and tire width were 234 in.<sup>2</sup> and 13.4 in., respectively. Figure 34 shows the wheel path of the B-52 tire directly along the west side of the joint.

### C-17 Traffic (Lane 3)

The C-17 multiple wheel load cart was used to simulate the C-17 main landing gear and apply the traffic to a portion of the east and center paving lanes (Lane 3). Figure 35 indicates the extent of the C-17 traffic across the lanes. The six painted lines in Figure 35 were guides for positioning the load cart during trafficking of the test section. These lines were spaced 18 in., the approximate width of the C-17 tire.

Figure 30. Traffic lane layout.

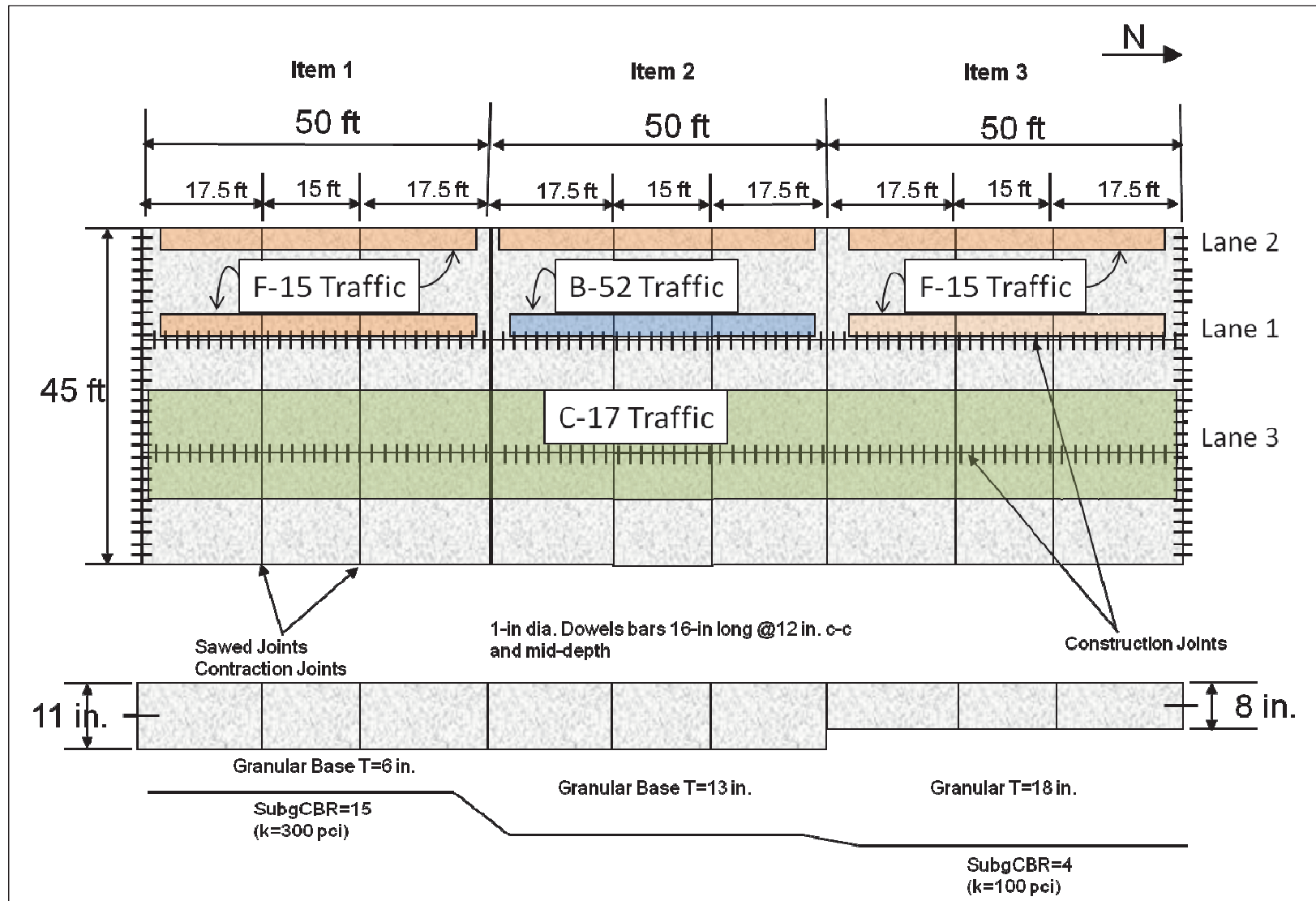




Figure 31. Heavy Vehicle Simulator – Aircraft (HVS-A)



Figure 32. Wheel path of the F-15 tire along longitudinal joint.



Figure 33. F-15 tire trafficking longitudinal joint of Item 1.



Figure 34. Wheel path of B-52 traffic on Item 2.





Figure 35. C-17 traffic lane with guide lines.



Figure 36 provides the layout of one gear of the C-17 aircraft, which was simulated with the load cart.

The outside width of the load cart gear, including the width of the tires, was 102 in. When the load cart moved across all six guide lines (Figure 35), the resulting width of the traffic lane was equal to 192 in. (Figure 37). The guide lines were used to ensure lateral traffic distribution encountered on taxiways.

Figure 37 shows tracks of the individual tires as the load cart maneuvered across the traffic lane. The traffic pattern consisted of 28 load-cart passes. The passes were distributed as follows: Guide Lines 1 and 6 – 2 passes (one round trip); Guide Lines 2 and 5 – 4 passes; Guide Lines 3 and 4 – 8 passes. Since the C-17 gear consisted of tandem wheel, each pass of the load cart resulted in two surface coverages along the wheel path. The traffic distribution was obtained by combining the traffic of all the guide lines, as shown in Figure 38.

In trafficking the rigid pavement, placement of the tires relative to the longitudinal joint was an important aspect of the test. The purpose of the C-17 load cart position was to apply the maximum number of stress repetitions to the center lane along the longitudinal joint between the

center and east lanes. Figure 37 indicates that the wheel paths are discrete and result in a discontinuous traffic distribution. In reality, some random distribution was caused by the cart driver wandering from the guide lines. The trend line in Figure 38 represents a better estimate of the actual traffic distribution.

Figure 36. Configuration of the C-17 gear (simulated by load cart).

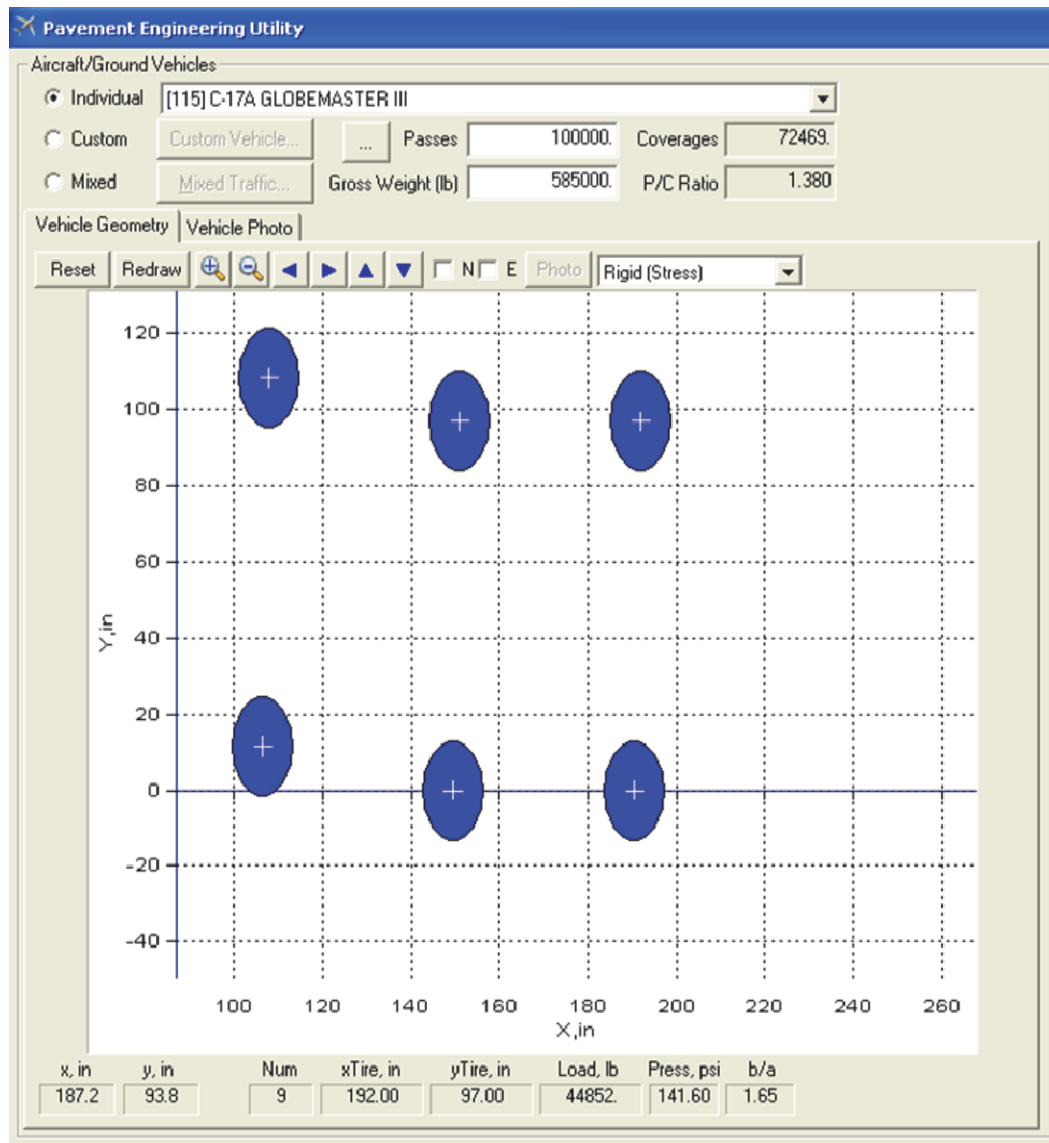


Figure 37. C-17 traffic pattern as defined by individual tires.

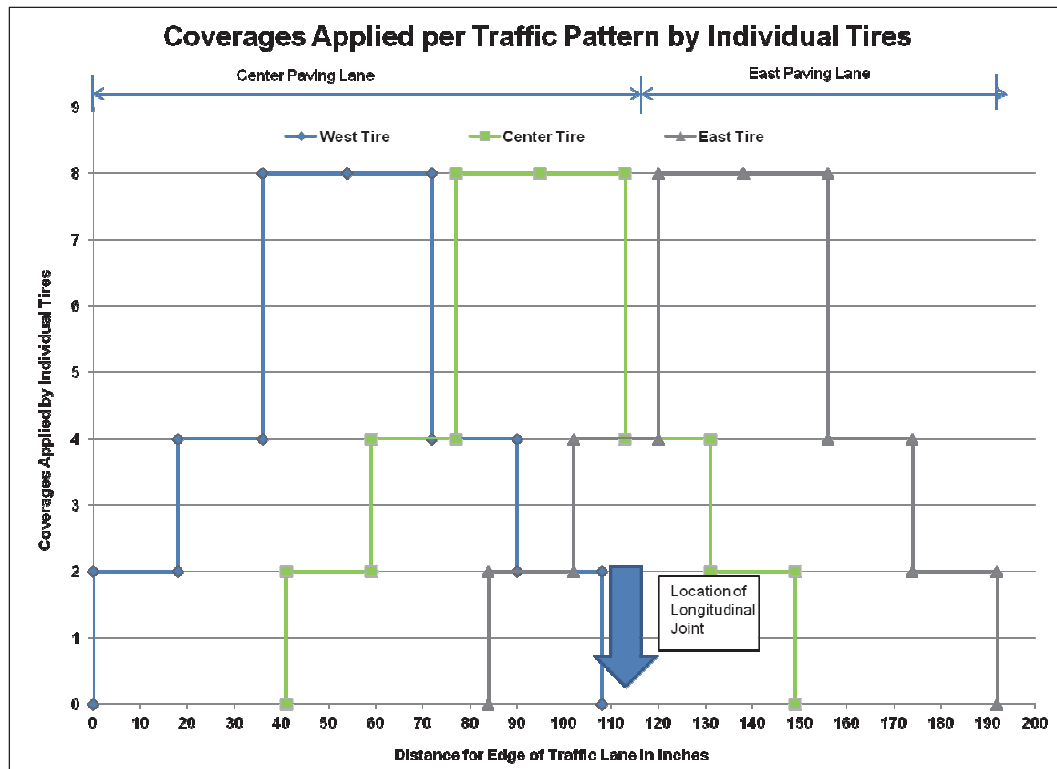
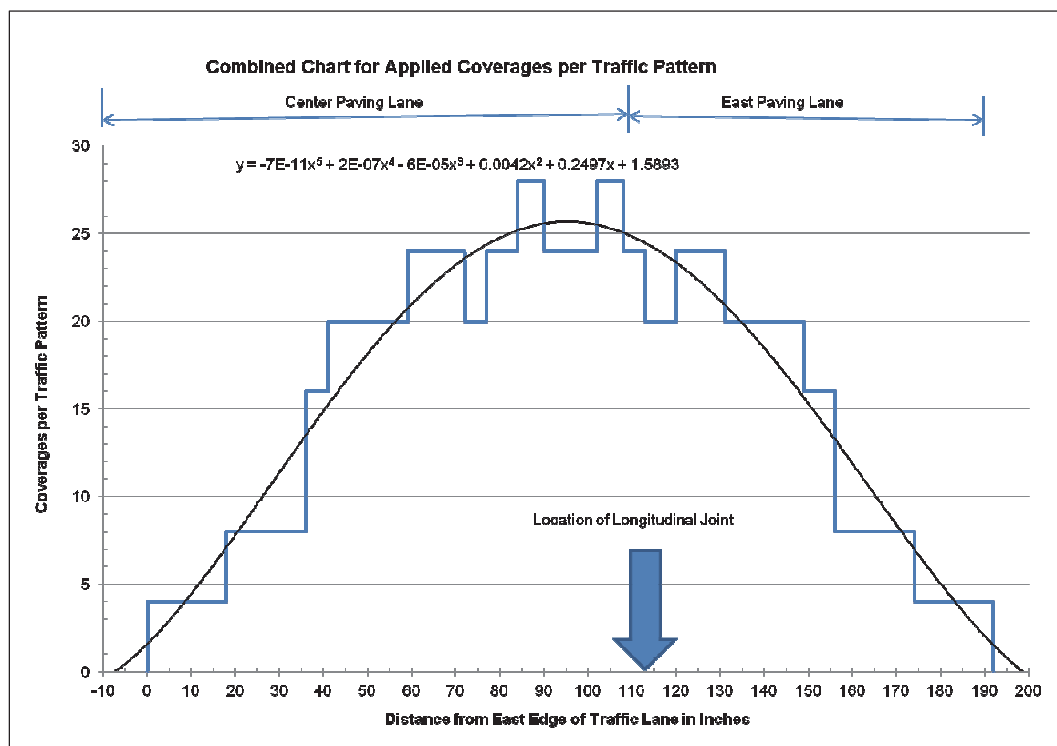


Figure 38. Combined distribution of traffic for a traffic pattern.



For the distribution in Figure 38, the pass-to-coverage ratio was calculated to be 1.1. Currently, the rigid pavement design criteria are based on the assumption that coverage is synonymous with pass, except for the case of tandem tires with spacing less than 6 ft. Examining the location of the individual tires (Figure 37) as the load cart moved laterally across the traffic lane provided reason to question the rationale of using coverages for stress repetitions. In fact, when the load cart follows the first guide line (far-left), the left tire is along the west edge of the traffic lane and the right tire is within 10 in. of the longitudinal joint. Likewise, when the load cart follows the sixth guide line, the far-right tire of the load cart is along the right edge of the traffic lane with the far-left tire within 5 in. of the joint. Further examination of Figure 37 showed that positioning the load cart at each of the other guide lines places a tire near the joint. For the traffic distribution applied to the test section, every pass of the load cart caused two significant stress repetitions along the joint. If the assertion that each pass of the load cart results in two significant stress repetitions is accepted, the effective pass-to-stress-repetition ratio would be 0.5, essentially doubling the number of stress repetitions vs. the number of coverages.

## 5 Performance under Traffic

### General

Lane 1 traffic was a single-wheel path along the western side of the longitudinal joint between the center and the west lanes; Lane 2 was a single-wheel path along the western free edge of the test section; and Lane 3 was distributed traffic along both sides of the longitudinal joint between the center and the east lanes (Figure 30). Table 6 summarizes the traffic applied to the test section. Table 7 provides a synthesis of the material properties.

### Lane 1 Traffic (F-15 and B-52)

Lane 1 traffic was a single-tire path along the western edge of the joint between the center and the western paving lanes (Figure 30). Lane 1 was trafficked with the F-15 tire in Items 1 and 3 and with the B-52 tire in Item 2. The traffic application started with the F-15 single tire on Item 1, where after 18,000 passes a corner break developed. Traffic continued to 50,000 passes without the appearance of additional pavement failures. At 50,000 passes, trafficking was discontinued.

Table 6. Traffic data for test section.

Lane Traffic	Test Load		Test Item	Applied Traffic, Passes		
	Gear Type	Gear Load (kips)		First Crack	Shattered Slab	Traffic Stopped
1	F-15	35	1	No failure	No failure	50,000
	B-52	62	2	100	300	1,000
	F-15	35	3	18,000	25,000	50,000
2	F-15	35	1	300 <sup>1</sup>	No failure	25,000
			2	504 <sup>2</sup>	700 <sup>3</sup>	1,303
			3	141	500	1,000
3	C-17	270	1	1,008	No failure	2,000
			2	308	1,008	2,000
			3	8	308	2,000

Notes:

1 First crack occurred at the corner of a transition joint between Items 1 and 2; no other crack developed;

2 First crack occurred at the corner of transition joint between Item 2 (11-in. slab) and Item 3 (8-in. slab);

3 Shattered condition in transition slab only; no cracks developed in the other two slabs.

Table 7. Test section material properties.

Test Item	Thickness (in.)		Modulus of Subgrade Reaction (pci)		
	PCC Slab	Base	Top of the Subgrade	Top of the Base	After Traffic
1	11	6	183	436	433
2	11	13	207	342	421
3	8	18	100	182	468

After the 11-in. pavement of Item 1 sustained such a high volume of traffic, the HVS-A was moved to the 8-in. pavement of Item 3, where the F-15 single-tire traffic was applied along the longitudinal joint. Corner breaks appeared on Item 3 at 18,000 passes. Item 3 reached the shattered slab condition after applying 25,000 passes (Figure 39). The shattered slab condition was defined when both corners contained multiple cracks and the slab was divided into four or more pieces. Traffic continued to 50,000 passes when it was terminated. There were no mid-slab cracks. Figure 40 shows a corner break after 300 B-52 passes. Figure 41 shows a corner break at the conclusion of traffic.

Figure 39. Corner break in Lane 1 Item 3 at 25,000 passes.





Figure 40. Corner break at 300 passes of B-52.

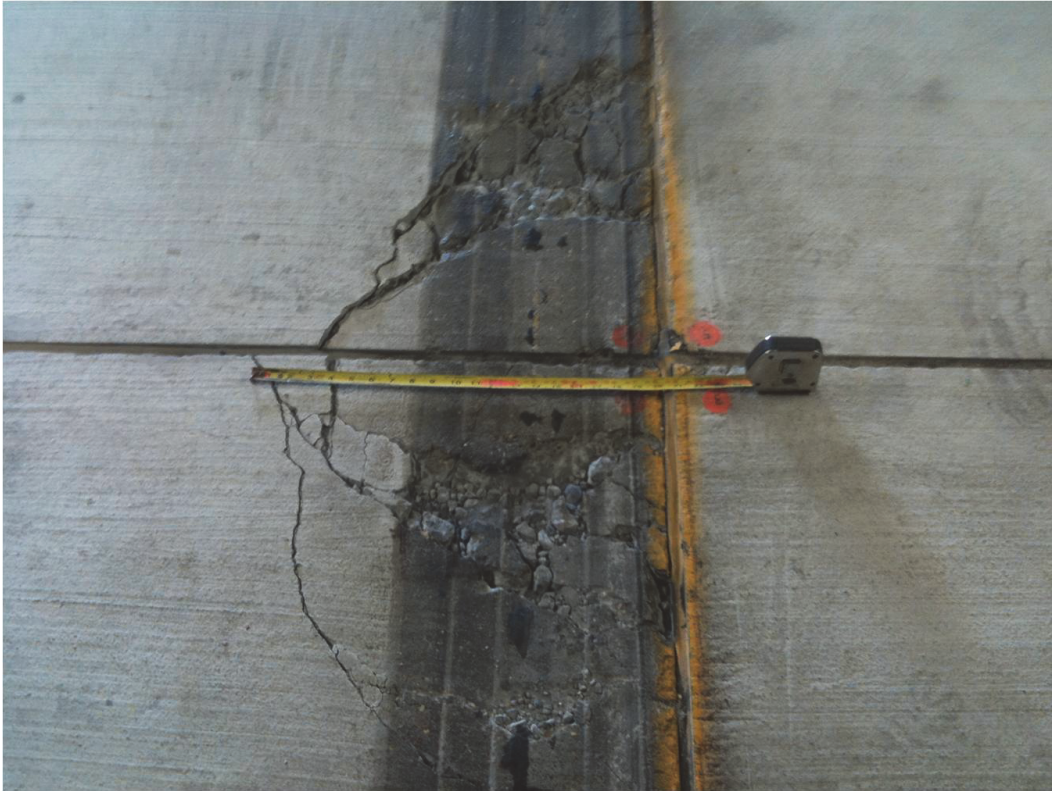


Figure 41. Lane 1 Item 3 corner break at conclusion of traffic (50,000 passes).



## **Lane 2 Traffic (F-15) – Items 1, 2, and 3**

Lane 2 Traffic was along the west free edge of the test section and was trafficked with the F-15 single tire loaded to 35,000 lb. The traffic was applied using the HVS-A along a single-tire path. Table 7 includes the performance summary for this traffic lane. There was a dramatic difference in the pavement performance between Lanes 1 and 2, both trafficked with the F-15 single tire. This was expected since Lane 2 traffic was along a dowelled longitudinal joint, whereas Lane 1 traffic was along a free edge of the test section. The concrete slab free edge was along the outer edge of the constructed subbase. Although not verified, the fact that limited subbase compaction was attained along this edge most likely had a negative influence on the pavement performance.

The F-15 traffic was first applied on Lane 2 Item 3 (8-in. slab thickness). The first crack occurred at 141 passes. At 500 passes, Item 3 was considered to have sufficient cracking to be in a shattered slab condition. Figure 42 shows the condition of the slabs after 1,000 passes, at which time the traffic was terminated.

After termination of traffic on Item 3, the HVS-A was moved successively to Item 1 and then to Item 2. On Item 1, a corner break developed at 300 passes but the crack did not progress to a shattered slab condition. No other cracks developed prior to termination of the traffic at 25,000 passes. Figure 43 shows the condition of the test section at 15,000 passes.

After trafficking Item 1, the HVS-A was moved to Item 2. After 504 passes, a corner crack developed at the transition joint between Items 2 and 3. The difference in slab thickness between Item 2, with 11-in. slabs, and Item 3, with 8-in. slabs, caused a discontinuity at the joint between the two items. Pavement deterioration was rapid at the corner break where a shattered slab condition was reached at 700 passes. At 1,303 passes, termination of traffic was necessary due to the corner break, which posed a risk to the tire (Figure 44). However, for Item 2 there were no additional cracks other than the corner break.

## **Lane 3 Traffic – Items 1, 2, and 3**

Traffic for Lane 3 was applied using the C-17 load cart, allowing traffic application to all three test items in a continuous fashion. The first crack



Figure 42. Lane 2 Item 3 at 1,000 passes of the F-15 tire.



Figure 43. Lane 2 Item 1 at 15,000 passes of the F-15 tire.



Figure 44. Corner break at transition joint between Items 2 and 3 at 1,303 passes.



occurred on Item 3 (8-in. slabs) after 8 passes. The first crack, a corner break, was of a different nature than the corner breaks resulting from single-wheel traffic. The corner breaks from the single-wheel traffic began at the dowel closest to the corner and advanced to the transverse joint about 1 ft from the corner. The corner break in Lane 3 began at the longitudinal joint at about 1/3 of the slab length from the corner and propagated to about mid-slab on the transverse joint. The location where the crack initiates corresponds with the location of the maximum tensile stress at the top of the slab. The maximum tensile stress would occur as one set of the C-17 tires is near the transverse joint and the other set is near the center of the slab. Item 3 was in the shattered slab condition after 308 passes. Figure 45 shows the cracking pattern at 500 passes for Item 3.

The first crack for Items 1 and 2 (11-in. slabs) were at 308 and 1,008 passes, respectively. The shattered slab condition was reached at 1,008 for Item 2, whereas Item 1 did not reach shattered slab condition before traffic was terminated at 2,000 passes. During the 2,000 passes, only two cracks appeared in Item 1. Figures 46 and 47 show the cracking pattern at 700 passes for Item 2 and one of the two cracks in Item 1, respectively.

Some minor spalling of the pavement occurred in Item 2 over a dowel near the corner (Figure 48).



Figure 45. Cracking pattern for Lane 3 Item 3 at 500 passes.



Figure 46. Cracking pattern for Lane 3 in Item 2 at 700 passes.

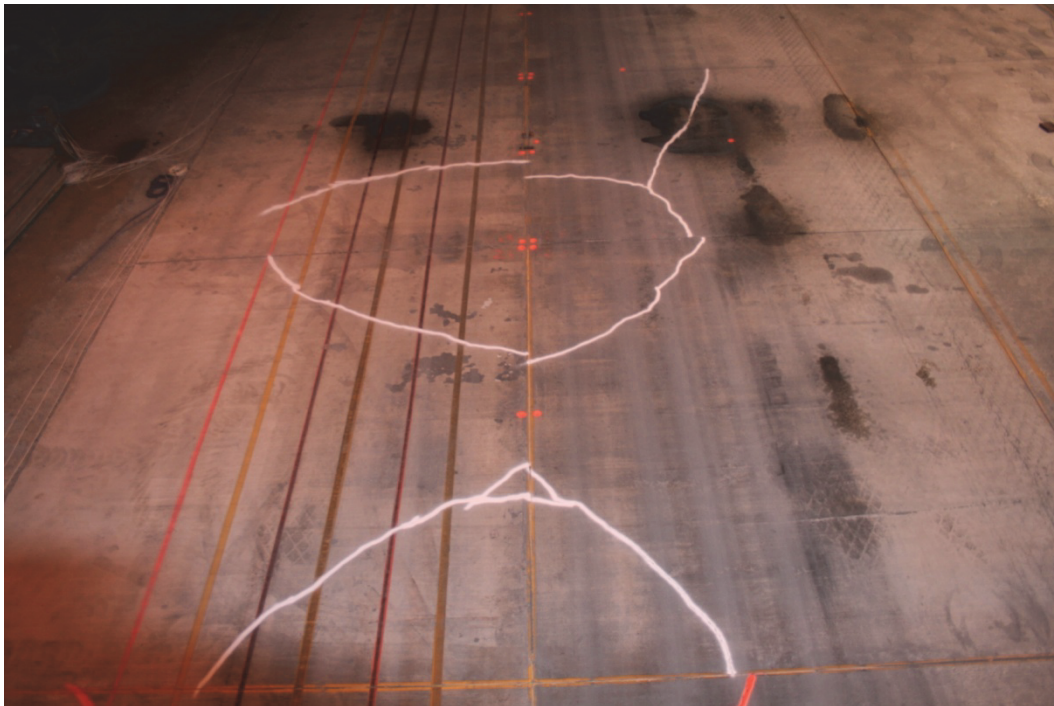


Figure 47. One of the two cracks in Item 1 – note load cart in the background.



Figure 48. Spalling along the top of dowel in Item 2 (orange dots are FWD test locations).



## 6 Analysis of Performance Data

### General

The performance data were recorded during various stages of the construction and testing of the pavement test section. The following data are available for additional studies: FWD testing data, LVDT data from sensors measuring the joint movement, strain data from gauges installed on the vertical face of the longitudinal joint between the east and center paving lanes and on concrete surface on the east and center paving lanes.

### Falling Weight Deflectometer (FWD) data

Appendix A includes selected data from the FWD testing. The FWD data in Appendix A are divided in relation to the testing phase. The data in Part 1 are those collected at the top of the base course, along the length of the test section, prior to placement of the concrete. Tables A1-1 through A1-3 are for the east paving lane; Tables A1-4 through A1-6 are for the center paving lane; and Tables A1-7 through A1-9 are for the west paving lane. The FWD plate diameter was 17.7 in. (45 cm), and testing of the base course included six drops for each testing location. The remaining FWD testing at the pavement surface was conducted using the standard 11.8-in. (30-cm) plate. The first three drops were at the maximum drop height, with each drop being at sequentially lower drop heights. The deflections were measured at the center of the plate and at 12-in. intervals out to 72 in. from the center of the plate. As would be expected for FWD tests on base courses, the results were highly variable; nevertheless, the three items were of similar stiffness.

Parts 2, 3, and 4 of Appendix A are FWD data for Lane 1 on Items 1, 2, and 3, respectively. Lane 1 traffic consisted of F-15 single tire for Items 1 and 3 and the B-52 single tire on Item 2. The FWD data were taken at different levels of traffic; Appendix A includes tables for these different levels. Each table includes FWD data for four different stations with Station 1 being the center of the middle slab of the item, Station 2 being across the north transverse joint, Station 3 being across the south transverse joint, and Station 4 being across the longitudinal joint adjacent to the traffic lane.

Part 5 of the appendix is the FWD data taken during the trafficking of Lane 2 for Items 1, 2, and 3. The data were taken perpendicular to the free



edge of the test section, with the test locations at the center of the traffic lane. These data represent a free edge condition, thus the measured deflections are much greater than the deflections at the interior of the test section.

Part 6 of Appendix A includes the FWD data for Lane 3 traffic, Items 1, 2, and 3. Traffic on Lane 3 was applied simultaneously across all the test items using the C-17 load cart. With traffic applied in this manner, the FWD testing was conducted on all test items after the same pass levels. The FWD tests were on the center slab of each test item and along the south transverse joint, the north transverse joint, and the east longitudinal joint.

## Impulse stiffness modulus

The impulse stiffness modulus (ISM) is defined as the measured FWD load applied to the plate divided by the measured center plate deflection. These values provide a measure of the overall pavement system when subjected to the impulse load. Tables 8 and 9 include the average ISM values for the test conducted during trafficking Lanes 1 and 3. The data represent the average of all drops at the slab centers for each item.

**Table 8. Impulse stiffness modulus for Lane 1 (F-15, B-52 single tire).**

Item	ISM (lb/mils)		
	Traffic Level		
	Start of Traffic	Mid-way Through Traffic	Near End of Traffic
1	3,086	2,059	3,015
2	2,558	2,652	2,462
3	2,372	2,383	2,403

**Table 9. Impulse Stiffness Modulus for Lane 3 (C-17)**

Item	ISM (lb/mils)		
	Traffic Level, Passes		
	0	300	1,000
1	3,492	<sup>a</sup>	3,468
2	3,711	3,447	3,095
3	2,749	2,566	2,571

<sup>a</sup> No data collected.

The data taken during trafficking of Lane 1 (slabs in the west lane) indicate no influence of the traffic on the impulse stiffness modulus. This was expected, since the traffic was along the joint and there was no damage noted at the slab centers. The data indicate a difference in stiffness among test items, with Item 1 being the stiffest, followed by Item 2 and Item 3.

## Load transfer across joints

The joint efficiency (or deflection ratio) is defined as the deflection measured at the Number 2 sensor (12 in. from the center of the plate) divided by the deflection measured at the plate center. Precisely, the Number 2 sensor is across the joint from the deflection plate and at an equal distance from the joint as the plate center. The joint efficiency is a measure of the amount of load transferred from the loaded slab to the adjacent slab. In pavement evaluation, the joint efficiency value allows one to quantify the load reduction factor by use of Figures 4-11 in the UFC 3-260-03. A joint efficiency of 0.76 yields a load reduction factor of 1.00, which corresponds to a load transfer across the joint of 25%; a joint efficiency of 0.00 yields a load reduction factor of 0.75, which corresponds to no load transfer across the joint.

Tables 10, 11, and 12 include the joint efficiency data for Lane 1 and Items 1, 2, and 3, respectively. The joint efficiencies are greater for the sawed transverse joints than for the longitudinal construction joints. With the exception of the longitudinal construction joint of Item 3, the joint efficiencies for Lane 1 were unaffected by the traffic.

Table 10. Deflection-based joint efficiency for Lane 1 Item 1.

Station	Joint	Joint Efficiency		
		0 (F-15 Passes)	1,000 (F-15 Passes)	50,000 (F-15 Passes)
1	Center slab	0.92	0.91	0.91
2	North transverse	0.96	0.92	0.94
3	South transverse	0.99	0.98	0.97
4	East longitudinal	0.81	0.85	0.83

Table 11. Deflection-based joint efficiency for Lane 1 Item 2.

Station	Joint	Joint Efficiency		
		100 (B-52 Passes)	300 (B-52 Passes)	1,000 (B-52 Passes)
1	Center slab	0.92	0.91	0.91
2	North transverse	0.96	0.92	0.94
3	South transverse	0.99	0.98	0.97
4	East longitudinal	0.81	0.85	0.83

Table 12. Deflection-based joint efficiency for Lane 1 Item 3.

Station	Joint	Joint Efficiency		
		0 (F-15 Passes)	10,000 (F-15 Passes)	50,000 (F-15 Passes)
1	Center slab	0.85	0.88	0.88
2	North transverse	0.94	0.96	0.87
3	South transverse	0.99	1.00	0.99
4	East longitudinal	0.88	0.73	0.74

Table 13 includes the joint efficiencies for Lane 3. As shown in Table 13, most joint efficiencies after 300 passes were above 0.76; however, some joints had very low measured efficiencies.

Table 13. Deflection-based joint efficiencies for Lane 3 (center paving lane).

Item	Station	Joint	Joint Efficiency		
			0 (C-17 Passes)	300 (C-17 Passes)	1,000 (C-17 Passes)
1	1	Center slab	0.88	<sup>a</sup>	0.91
	2	South transverse	0.68	<sup>a</sup>	0.08
	3	North transverse	0.96	<sup>a</sup>	0.58
	4	East longitudinal	0.86	<sup>a</sup>	0.7
2	5	Center slab	0.90	0.90	1.01
	6	South transverse	0.86	0.37	0.48
	7	North transverse	0.77	0.42	0.51
	8	East longitudinal	0.75	0.76	0.71
3	9	Center slab	0.87	0.88	0.94
	10	South transverse	0.98	0.87	0.92
	11	North transverse	0.93	0.65	0.60
	12	East longitudinal	0.96	0.83	0.81

<sup>a</sup> No data collected.



## LVDT joint deflection gauges

The LVDT joint deflection gauges allowed the direct measurement of the relative movement across the longitudinal dowelled construction joint. Figure 49 shows the data for the F-15 single tire on Item 1 of Lane 1.

The data were collected during passes 1 through 10 and passes 50,000 through 50,010. During the initial traffic, the relative movement across the joint was 0.0026 in. The movement at the end of traffic was 0.0036 in., which represents a significant increase of the joint relative movement. The estimated joint efficiency for the initial traffic was 0.82, whereas 0.81 was the joint efficiency at the end of the traffic. These estimated joint efficiencies were in agreement with joint efficiency values determined from the FWD data. Even though the relative deflection increased with traffic, the joint efficiency did not change. This is due to the fact that while the relative deflection was increasing with traffic, the total deflection of the loaded slab was also increasing.

Figure 50 shows the data for the relative longitudinal construction joint deflection for F-15 traffic applied on Lane 1 for Item 3. The relative joint movements were much greater for Item 3 as compared to the movements for Item 1. For the initial traffic, the relative movement was 0.004 in., which increased to 0.0065 in. after 12 passes, and to 0.0085 in. after 10,000 passes. The estimated joint efficiency for the first pass was 0.86, 0.77 for 12 passes and 0.77 for 10,000 passes. These estimated efficiencies are in agreement with the joint efficiencies determined from FWD data.

Figure 51 shows the data for relative deflection across the longitudinal construction joint for Item 2 in Lane 3. The data are for the first 12 passes of the C-17 load cart, with the location of the load shifted laterally with each forward pass. In Figure 51, it is possible to note that the relative deflection across the joint is influenced by the location of the load cart: the highest relative deflections occurred during Passes 1, 2, 5, 6, 9, and 10. The maximum relative deflection of 0.017 in. occurred during Pass 2. The relative deflections were small during passes when some of the C-17 tires were across the joint. Figure 52 provides an enlarged plot of the relative joint deflections for Pass 2. The responses for the load-cart drive tires as well as the individual sets of three tires are evident and labeled in the figure.

Figure 50. Data from LVDT joint deflection gauge traffic Lane 1 Item 3 (longitudinal joint).

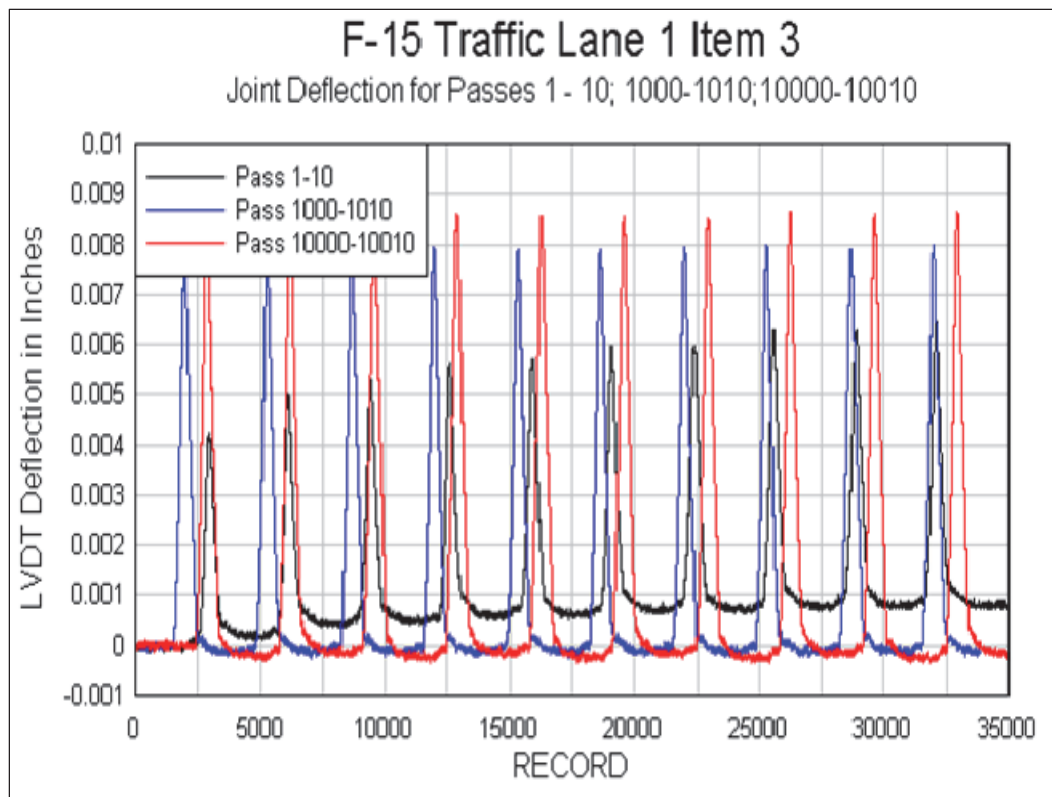


Figure 49. Data from LVDT joint deflection gauge Lane 1 Item 1 (longitudinal joint).

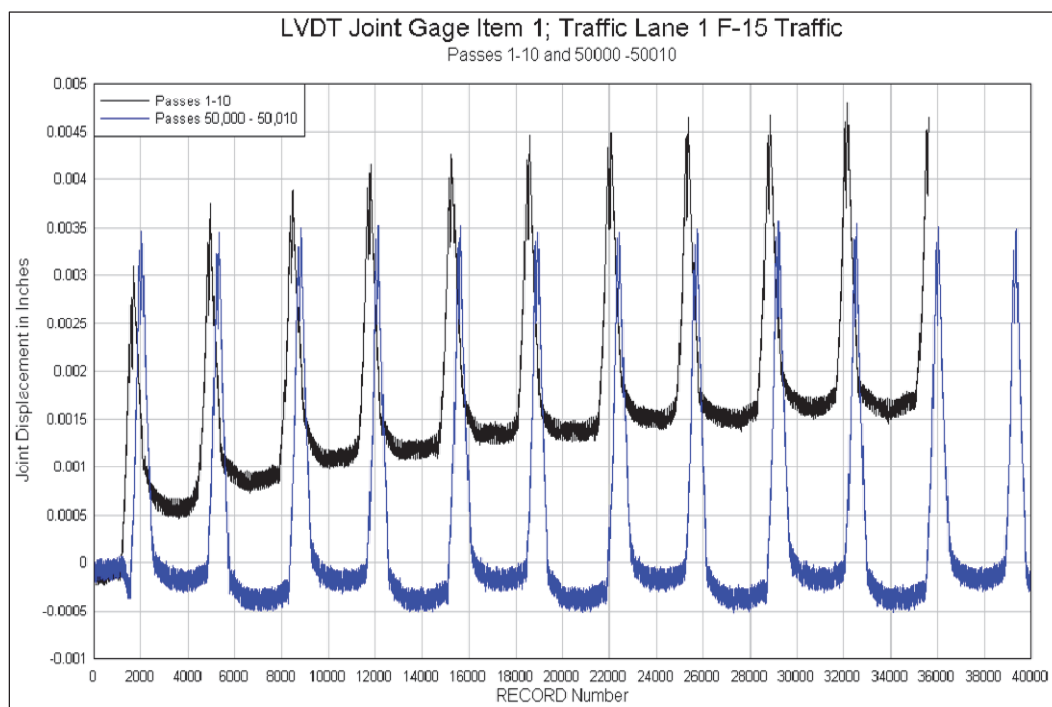


Figure 51. Data from LVDT joint deflection gauge traffic Lane 3 Item 2 (longitudinal joint).

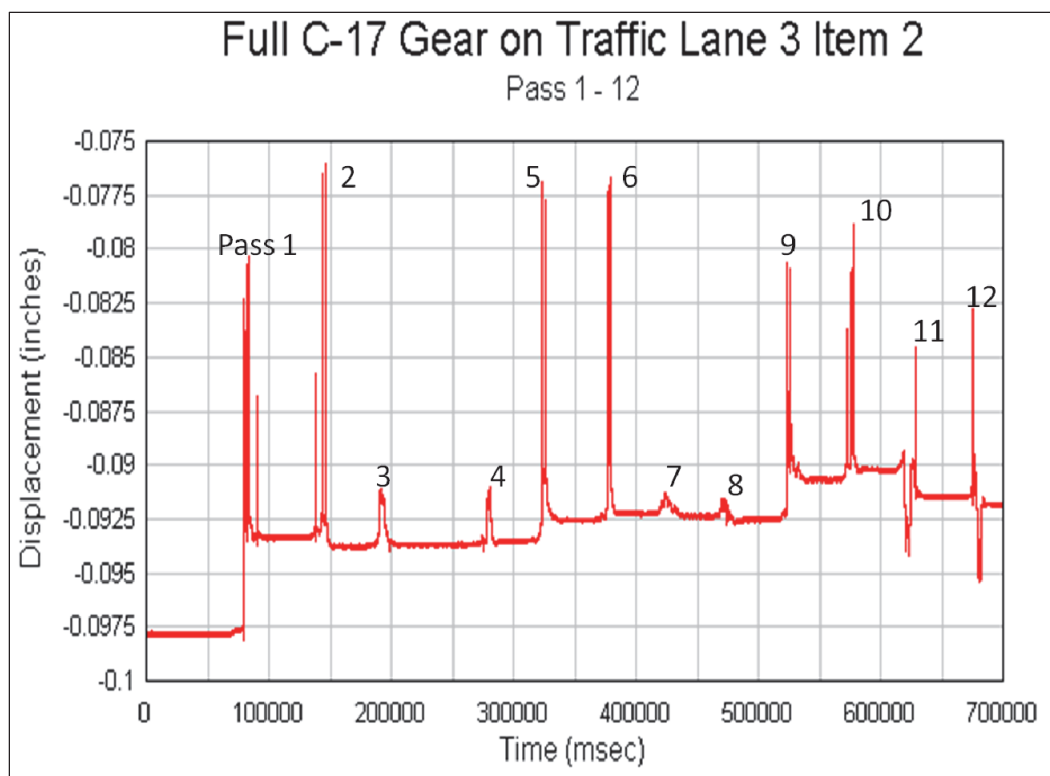
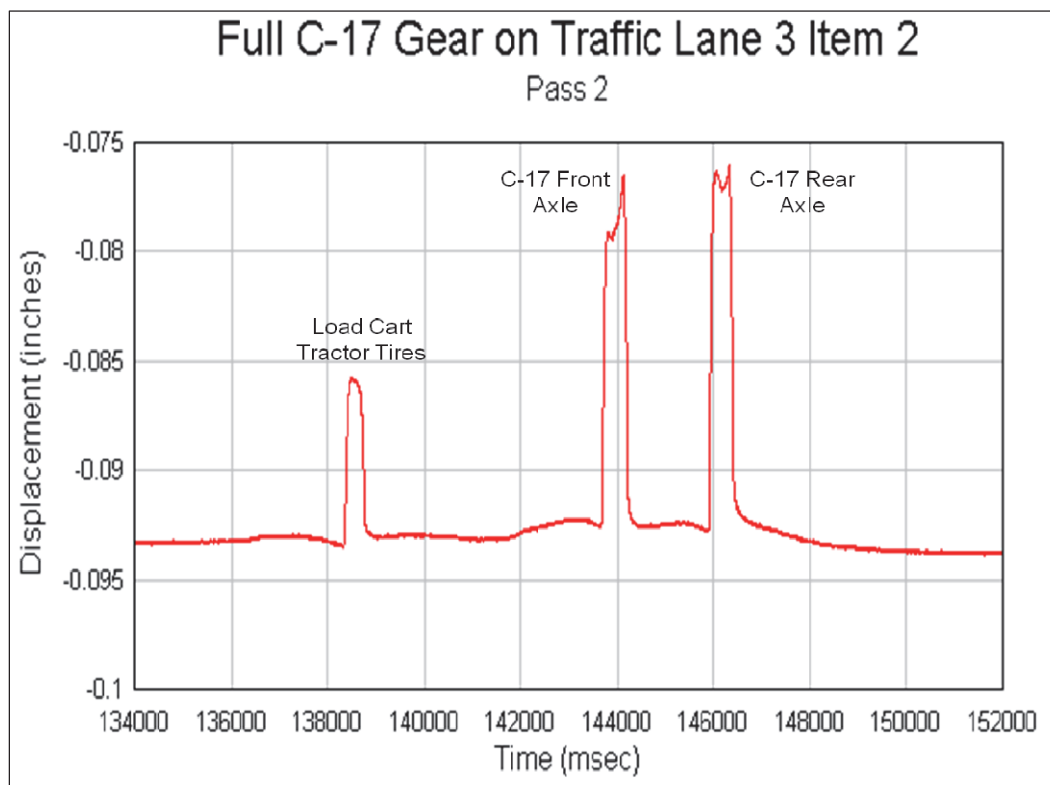


Figure 52. Enlargement of the plot for the relative joint deflection for Pass 2 Item 2 (longitudinal joint).



Figures 53 and 54 show the data for the relative longitudinal joint deflection in Item 3. As with the gauge response for Item 2, the maximum deflection of 0.021 in. occurred during Pass 2, which is greater than the maximum deflection in Item 2. In addition to having higher relative joint deflection, the permanent deformation that developed during the first 12 passes was greater in Item 3 than in Item 2. This was expected due to the reduced thickness of Item 3 as compared to Item 2.

### Strain gauge data for Lane 1

Figures 55 and 56 show the data from the surface strain gauge installed in Items 1 and 3 on Lane 1 (Figure 24). In these figures, positive strain represents tensile strain and negative strain represents compression strain. Although not all the gauges functioned properly, the data in Figures 55 and 56 appear to be an accurate representation of the strain distribution. Some of the malfunctions of the gauges on the vertical face of the longitudinal joint were most likely caused by moisture from the placement of the center lane. Many of the surface gauges malfunctioned early in the traffic testing due to tire abrasion. However, the gauges on Items 1 and 3 performed well.

Figure 55 shows the measured cyclic strain for which the strain pulse repeats every two passes. A single-strain pulse was not symmetric, nor was the strain magnitude measured when the tire moved north (odd passes) or south (even passes). A possible reason for the asymmetrical strain pulses is that the strain gauges were closer to the south transverse joint than to the north transverse joint. The difference in strain magnitude would indicate a difference in the applied load for the different directions of travel, which can be explained through the geometrics of the load carriage, load distribution of front and rear gear, or dynamic forces.

The strain measured in the unloaded slab is a measure of the load transferred from the loaded slab to the unloaded slab, since the strains are directly proportional to the stresses and the load through the Young modulus (in a layered elastic model). The load transfer is computed from the measured strain by using Equation 3. Using the data in Figures 55 and 56, load transfer of 20% and 27% are computed for Items 1 and 3, respectively.

$$\%LoadTransfer = \left( \frac{\epsilon_{unloaded\ slab}}{\epsilon_{unloaded\ slab} + \epsilon_{loaded\ slab}} \right) 100 \quad (3)$$

Figure 53. Data from the LVDT deflection gauge for Lane 3 Item 3.

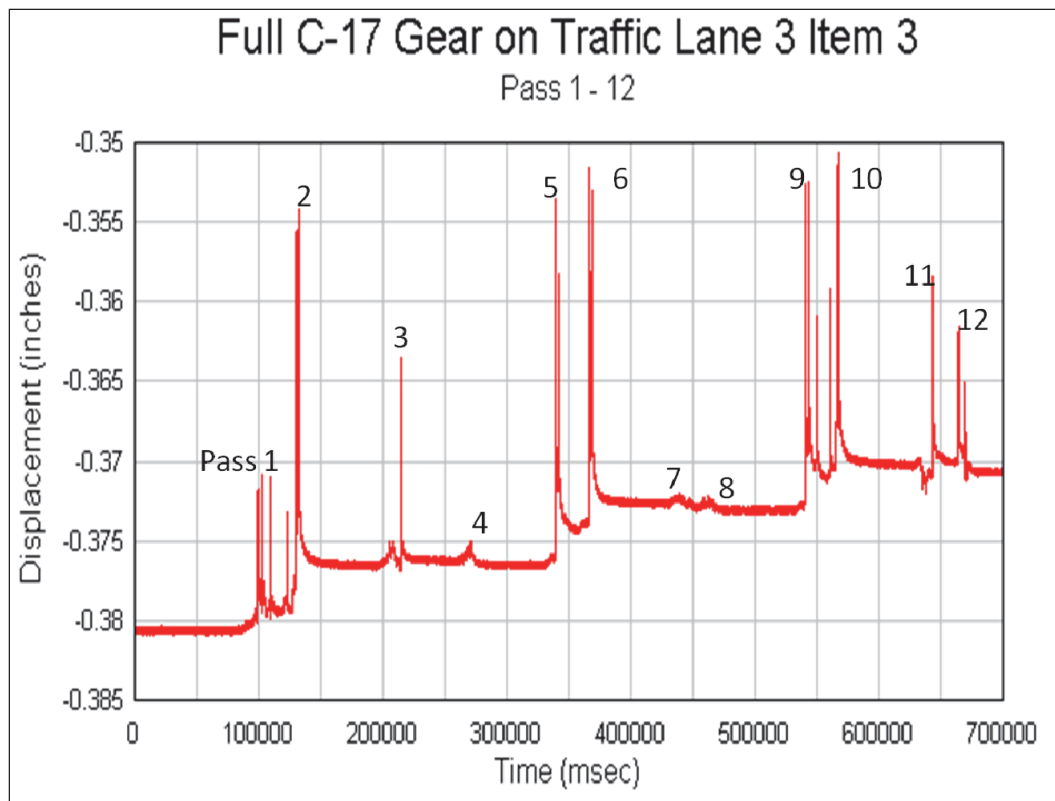


Figure 54. Enlargement of the plot for the relative joint deflection for Pass 2 Item 3.

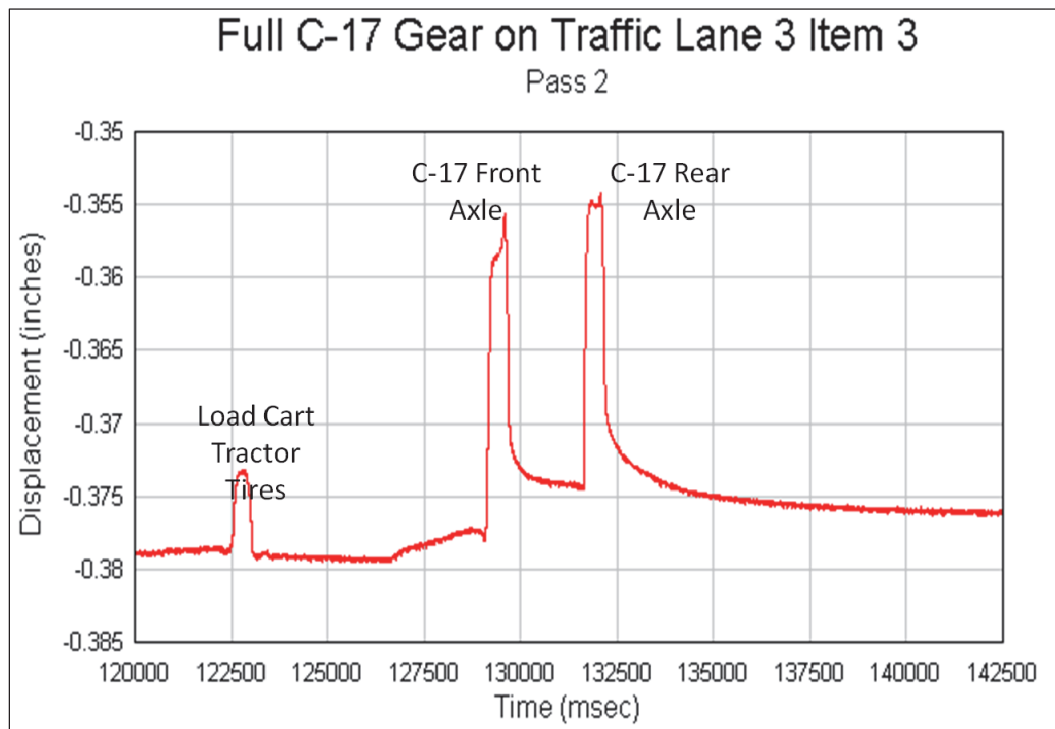


Figure 55. Surface strain gauge response traffic Lane 1 Item 1 Passes 1-10.

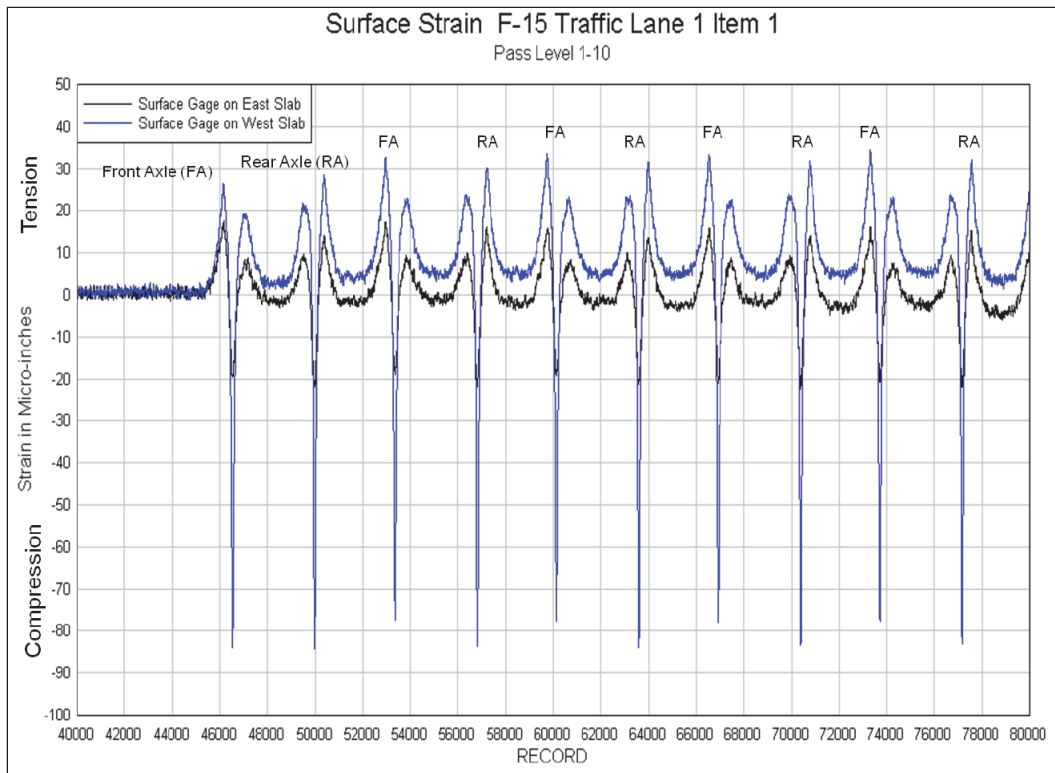
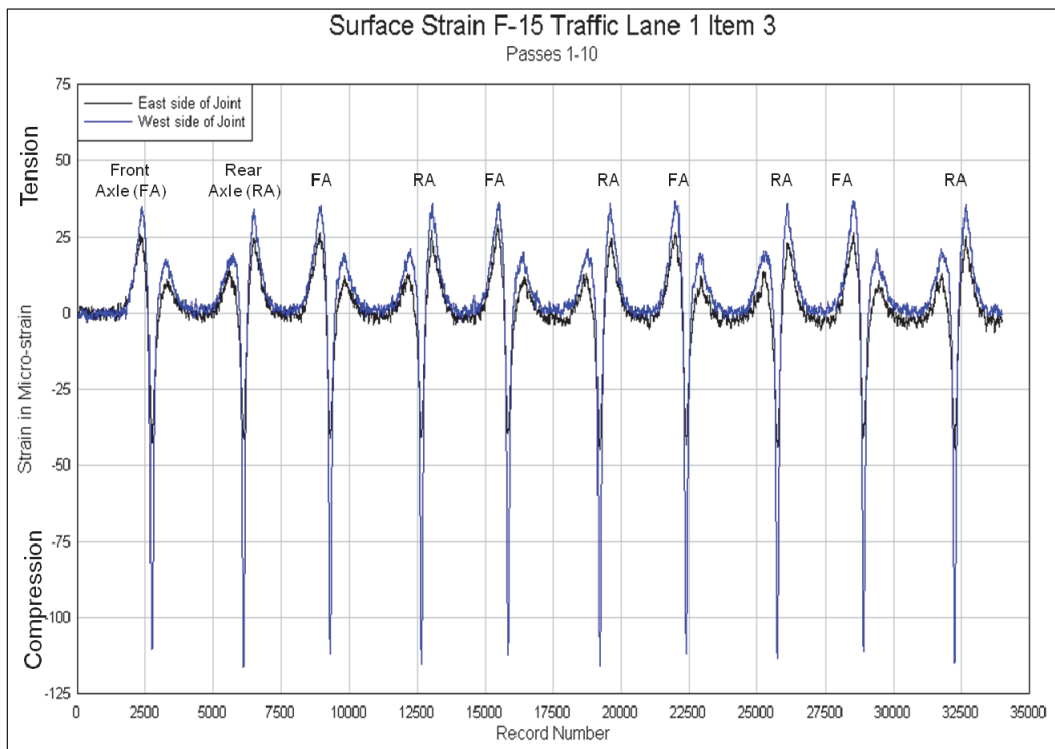


Figure 56. Surface strain gauge response traffic Lane 1 Item 3 Passes 1-10.



where

$\epsilon_{\text{unloaded slab}}$  = strain measured on the unloaded slab

$\epsilon_{\text{loaded slab}}$  = strain measured on the loaded slab

Another aspect of the data is that strain changes from tensile strain to a compressive strain, as the tire approaches and moves over the gauges. This action results in a strain difference, from tensile to compressive strain that is significantly greater than just the measured tensile or compressive strain. In Figure 55, it is also noted that in Item 1 there is a small amount of permanent strain that develops during the first 10 passes. The magnitude of the permanent strain does not appear significant. However, no permanent strain was noted in Item 3.

### Strain gauge data for Lane 3

Surface strain gauges were installed on the slab surface and on both sides of the longitudinal joint for Lane 3. The joint was the dowelled construction joint between the east and center lane. For each pavement item, the two gauges on the vertical face of the east lane were installed just prior to the placement of the center lane. Two surface gauges, one on each side of the joint, were installed on each item before the start of trafficking. The gauges for Items 1 and 2 provided erratic data from the first pass (Figure 57). It appears that the bottom gauge on the vertical face provided erratic data even before the tires moved over the gauges. The data from the top gauge on the vertical face continued to be reasonable and consistent. The data from the remaining three gauges appeared to be reliable, with the three gauges tracking each other until the loaded C-17 tires crossed the gauges. After the C-17 gear passed, only one surface gauge and the top vertical face gauge appeared to work properly.

After Passes 10 and 11, one surface and one vertical face gauge were still working and provided the data in Figure 58. The gauge readings were consistent in indicating significant tensile strains developing at the surface of the slab as the C-17 load cart approached. The data show a response to the test cart drive wheels as well as response to the loaded C-17 tires. With the load cart traveling to the north, the C-17 tires are in front of the drive wheel tires (odd passes), thus the first two gauge responses are for the C-17 tires. The response for the tractor drive tires was smaller than the one obtained for the load tires. The width of the drive tires is 28 in., with the inside of the drive tires in line with the inside of the outer C-17 tires. The longitudinal

Figure 57. Strain gauge data for C-17 on Lane 3 Item 1, Pass 1.

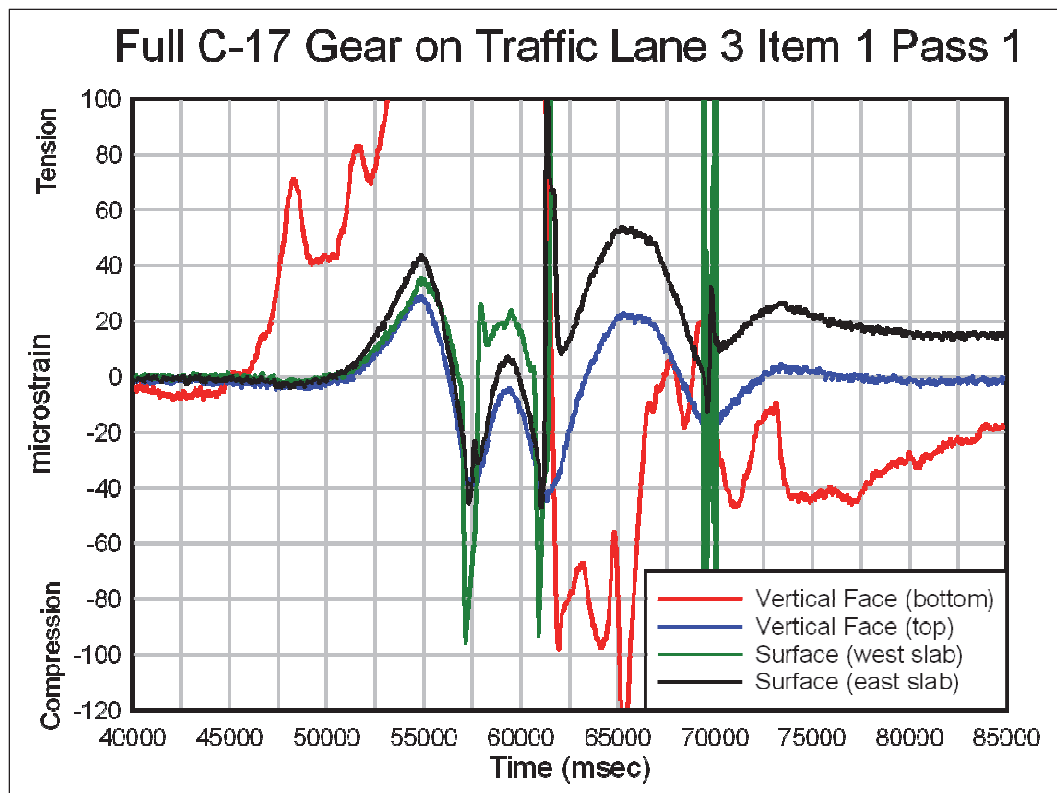
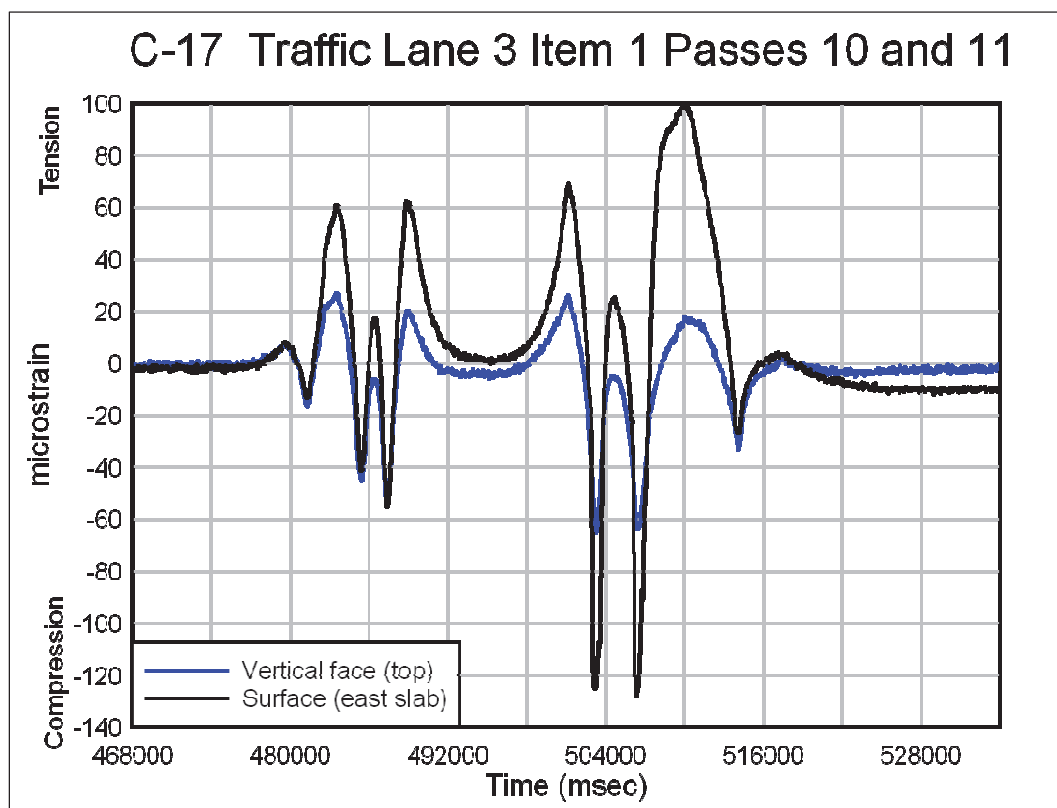


Figure 58. Strain gauge data for C-17 on Lane 3 Item 1, Passes 10 and 11.





distance between the C-17 tires is 97 in. (Figure 37), and the longitudinal distance from the leading set of C-17 tires to the drive tires of the tow vehicle is 18 ft and 5 in. By using these distances as reference, Figure 58 indicates that the maximum tensile strain measured by the surface gauges occurred when the front axle was approximately 5 ft from the gauge. This distance would place the lead C-17 tires at the south transverse joint. This is not the maximum tensile strain along the joint, but it is the maximum tensile strain at the gauge location, at a distance of 6.5 ft from the joint when the leading tires are located at the joint. The observed cracking of the slabs due to C-17 traffic (Figures 45 and 46) were corner breaks occurring about 4 ft from the corner. These corner breaks were likely caused by tensile stress at the top of the slab induced by the loading of the transverse joints. Therefore, the maximum tensile stress at the top of the slab occurred about 4 ft from the transverse joint.

Figure 59 shows the strain gauge data for the first pass of the C-17 gear on Item 2. These gauges were destroyed by abrasion from the C-17 tire. The data appeared good as the tire approached the gauge, but erratic readings were obtained when the tire crossed the gauge. The observed trends of Item 2 were similar to those for Item 1, although the data for Item 2 show larger tensile strains than those measured strains in Item 1.

The gauges installed in Item 3 performed much better than those in Items 1 and 2. Figure 60 provides an overview of the surface strain gauges for the first 12 passes of the C-17 load cart for Item 3. In these first 12 passes, the tensile strains reached the value of  $80\ \mu\epsilon$ , while the compressive strain reached  $120\ \mu\epsilon$ . For Passes 1 and 2, Figures 60 and 61 provide the data for the gauges on the vertical face and on the surface, respectively. The data for Pass 1 in Figure 61 indicate a tensile strain of  $75\ \mu\epsilon$  when the lead C-17 tires are located on the south transverse joint. The strains are only  $52\ \mu\epsilon$  when the trailing C-17 tires are located on the north transverse joint. The strain gauges are located closer to the south transverse joint (6.5 ft) than to north transverse joint (8.5 ft). This trend was consistent for the collected data, indicating that the gauge-joint distance has an influence on the magnitude of the tensile strain measured at the surface of the slab. This analysis would support the hypothesis that corner breaks occurring at a distance of about 4 ft from the joint were due to tensile stress at the top of the slab at that location. Figures 62 through 67 provide additional data on the collected strain data. At the surface of the slab, the tensile strain varied from about  $60\ \mu\epsilon$  to about  $80\ \mu\epsilon$ , and the compressive strain varied from about  $100\ \mu\epsilon$  to  $120\ \mu\epsilon$ .

Figure 59. Strain gauge data for C-17 on Lane 3 Item 2, Pass 1.

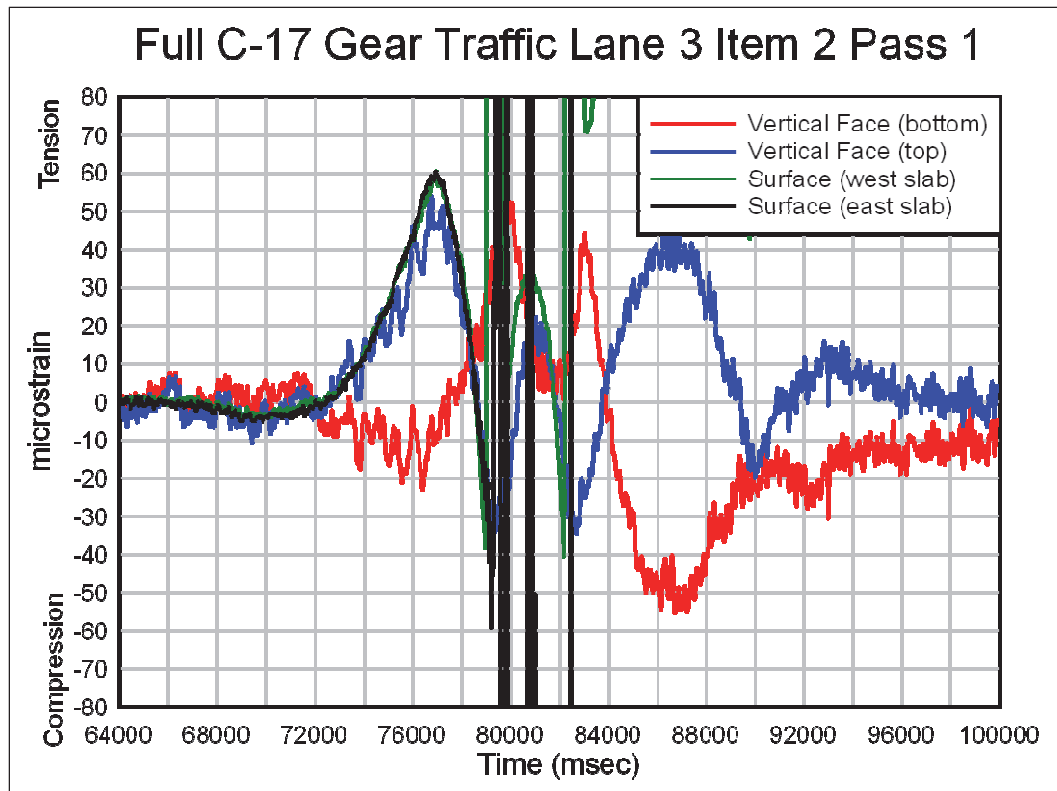


Figure 60. Strain gauge data for C-17 on Lane 3 Item 3, first 12 passes.

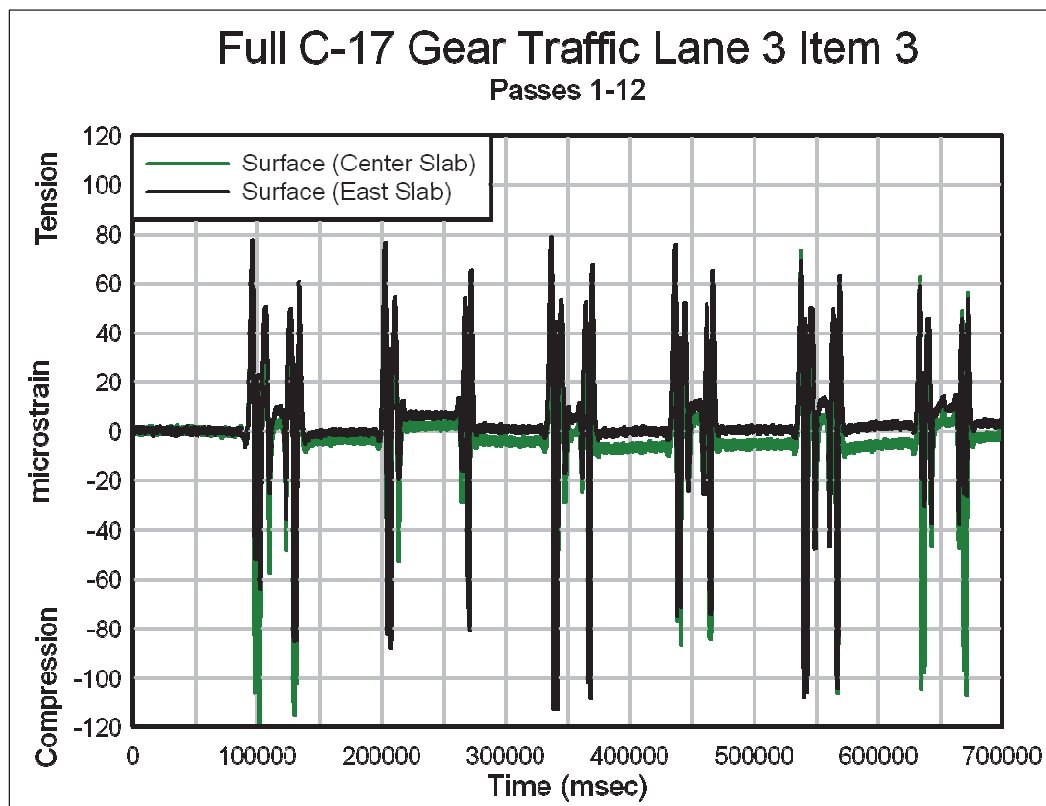


Figure 61. Strain gauge data for C-17 on Lane 3 Item 3, vertical face, Passes 1 and 2.

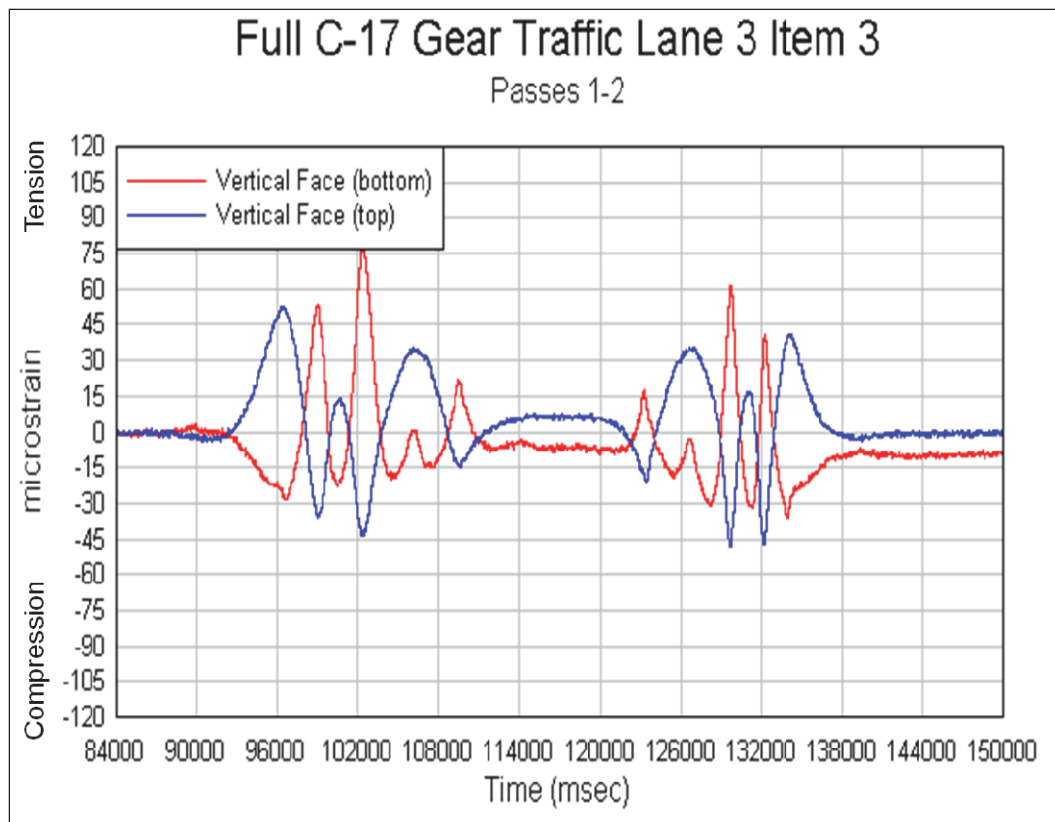


Figure 62. Strain gauge data for C-17 on Lane 3 Item 3, surface gauges, Passes 1 and 2.

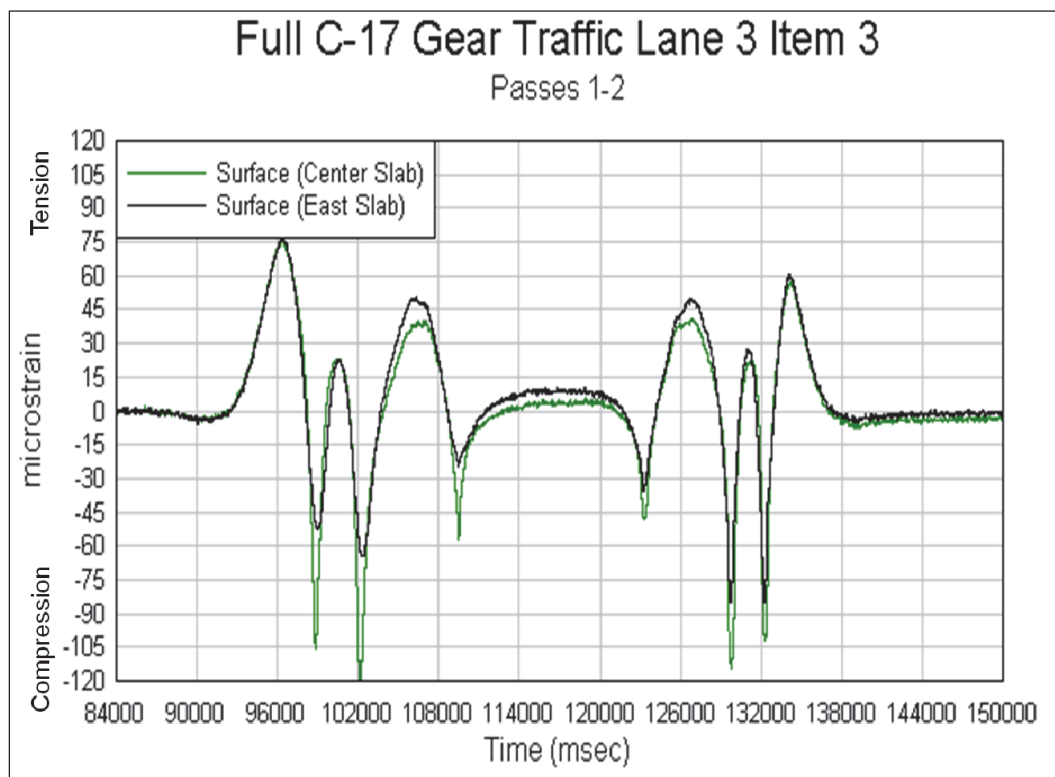


Figure 63. Strain gauge data for C-17 on Lane 3 Item 3, all gauges, Pass 1.

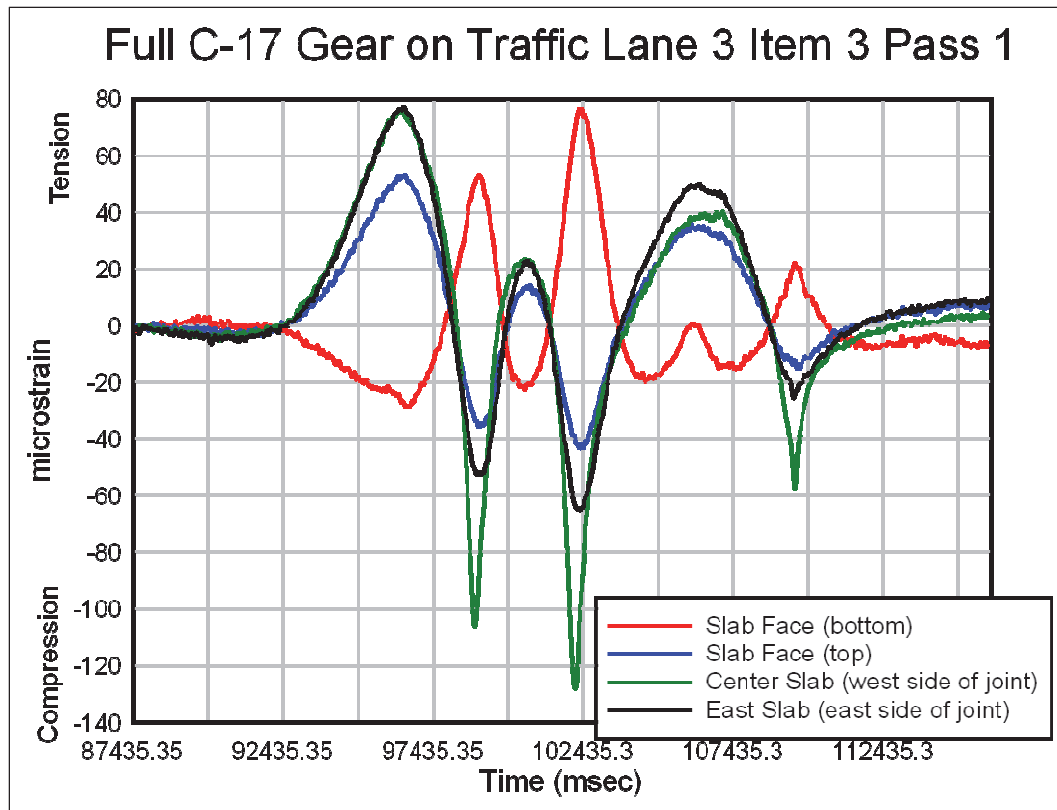


Figure 64. Vertical face strain gauge data for C-17 on Lane 3 Item 3, Pass 5 and 6.

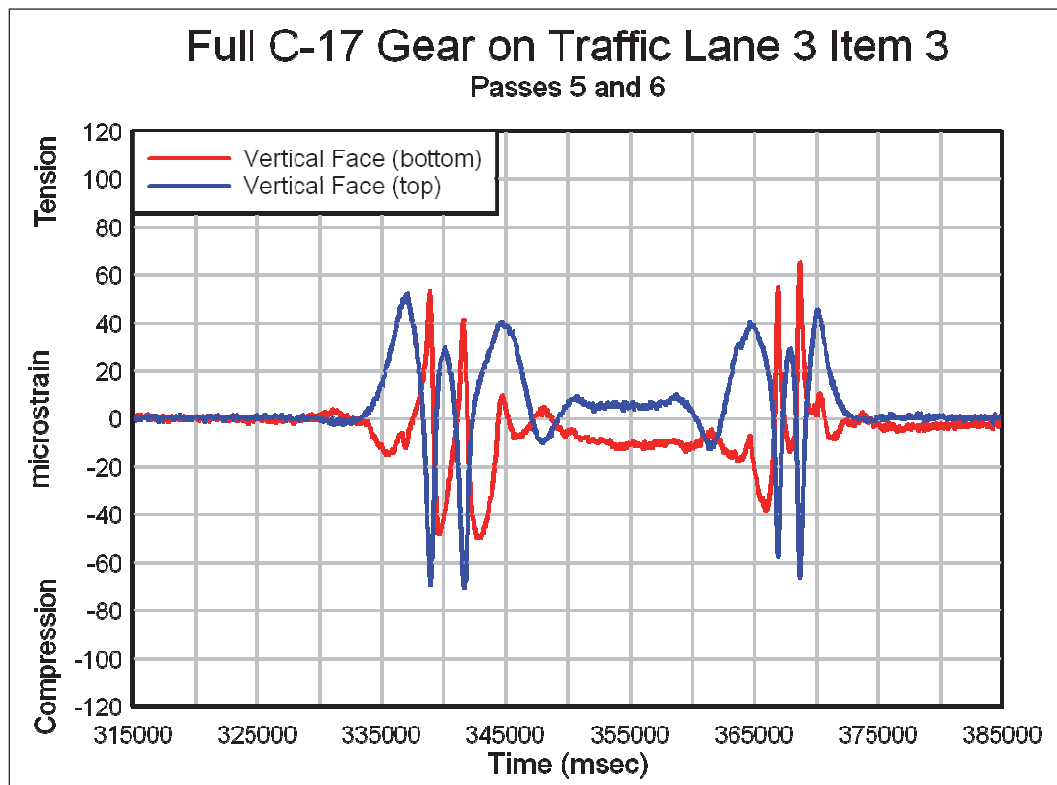


Figure 65. Surface strain gauge data for C-17 on Lane 3 Item 3, Pass 5 and 6.

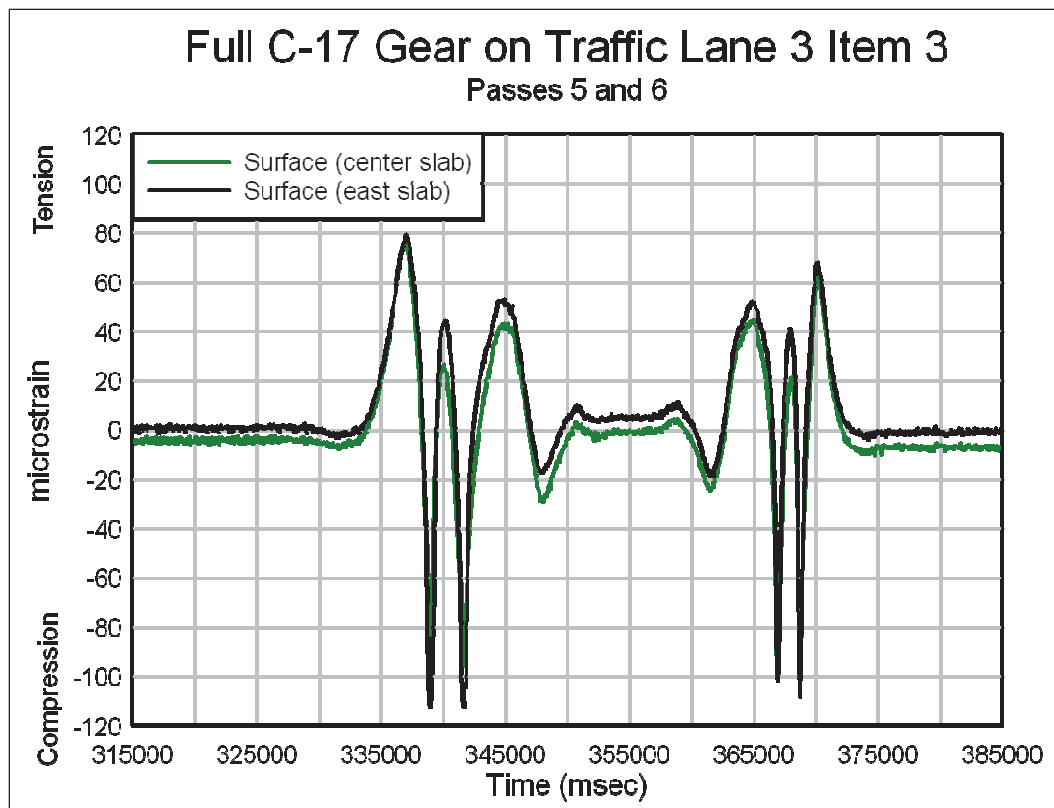


Figure 66. Strain gauge data for C-17 on Lane 3 Item 3, Pass 5.

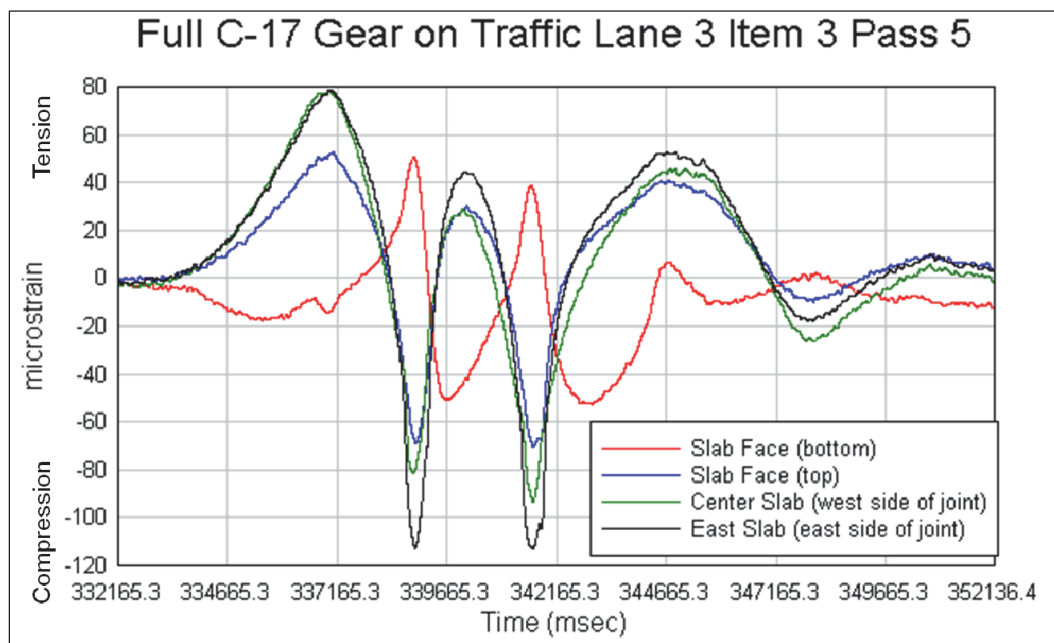
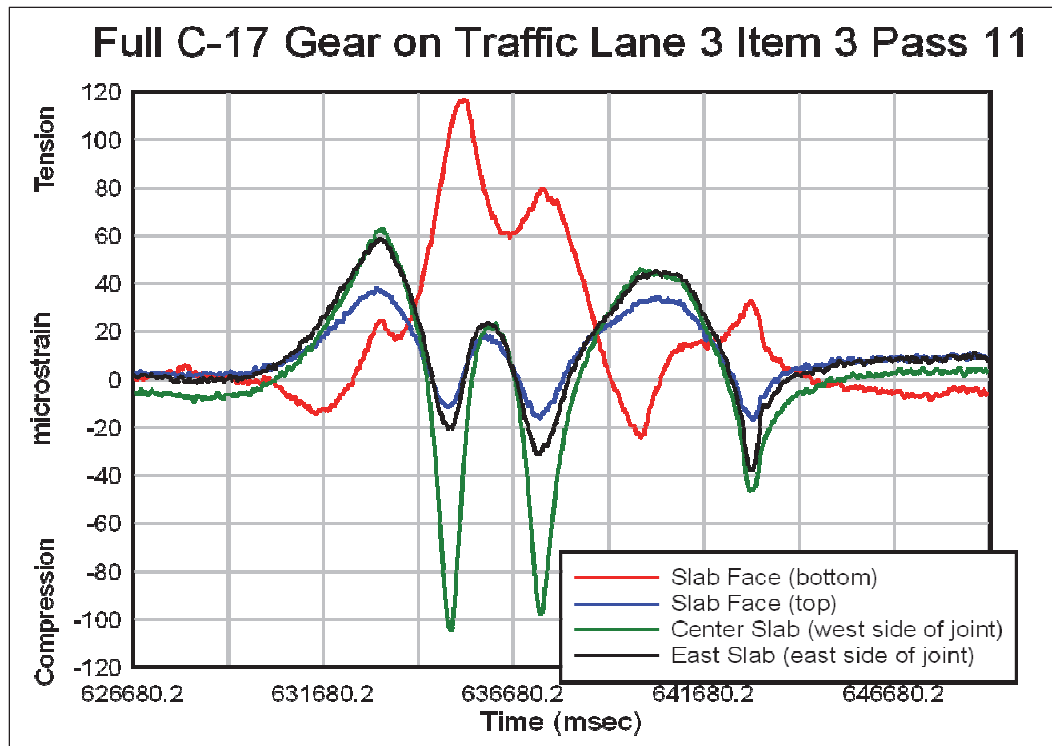




Figure 67. Strain gauge data for C-17 on Lane 3 Item 3, Pass 11.



## 7 Conclusions and Recommendations

This chapter presents conclusions and recommendations derived from the analysis of traffic and instrumentation data collected during full-scale field testing.

### Conclusions

Based on the observed behavior of the pavement test items and on the data obtained from the FWD, strain gauges, and joint deflection gauges, the following conclusions were drawn:

1. When trafficked with the simulated F-15 and B-52 single-wheel loads on a channelized traffic pattern along a dowelled longitudinal joint, the pavements performed better than expected. However, this traffic pattern did not represent actual field conditions and might indicate shortcomings with the analytical models.
2. For Item 3, the failures under the F-15 traffic were caused by cracking over the dowels adjacent to the transverse joint, indicating that the cover over the dowels should not be reduced.
3. When trafficked with the full C-17 gear, the pavements did not perform as well as expected. The failures were caused by corner breaks initiated by tensile stresses at the top of the slab along the longitudinal joint at a location 4 to 5 ft from the transverse joint.
4. The tensile strain at the top of the slab has a maximum value when the leading tires of C-17 gear have crossed the transverse joint and the rear axle tires remain on the adjacent slab. Since cracking occurred at 4 to 5 ft from the transverse joint, the maximum tensile strain obviously occurred 4 to 5 ft from the transverse joint.
5. Results of this testing indicate the current model used in the design and evaluation of rigid pavements does not adequately describe the pavement's behavior when it is subjected to loading of the C-17 aircraft.
6. Load transfer values at the joints measured by the FWD agree with the load transfer measured by the strain and joint deflection gauges.
7. Surface mounted strain gauges can give excellent response for the initial loadings of concrete pavements. These response data can provide valuable insight into behavior of concrete pavement under actual aircraft loading.

## Recommendations

Based on observations and results of this study, the following recommendations are made:

1. Based on dowel cover, the minimum thickness for any rigid airfield pavement should be set at 8 in.
2. Since early failures were experienced with the test pavements, minimum thickness of rigid pavement for the C-17 aircraft should be set at 11 in. At no time should the thickness be less than the thickness determined from the design criteria.
3. The rigid pavement response, when subjected to joint loading by the C-17 aircraft, should be further studied using more advanced models than those currently used by the military for design and evaluation of rigid pavements.
4. Additional test sections should be constructed and instrumented using surface-mounted strain gauges to quantify the critical response of rigid pavements to C-17 loading and other multi-wheel aircraft.

## References

- US Army Corps of Engineers (USACE). 1995. *Standard test method for determining the modulus of soil reaction*. Handbook for Concrete and Cement CRD-C 655-95. US Army Corps of Engineers.
- Gonzalez, Carlos R., W. R. Barker, and A. Bianchini. (n. d.). Reformulation of the CBR procedure, Volume 2 (in preparation) Vicksburg, MS: US Army Corps of Engineers, Waterways Experiment Station.
- Hutchinson, R. L. 1966. *Basis of rigid pavement design for military airfields*. Miscellaneous Paper 5-7. Cincinnati, OH: US Army Corps of Engineers, Cincinnati Testing Laboratory.
- Ohio River Division. 1943. *Field bearing tests on natural subgrade and prepared subbase using different bearing plates*. Cincinnati, OH: US Army Corps of Engineers, Cincinnati Testing Laboratory.
- Ohio River Division. 1946. *Lockbourne No. 1 – Test track final report, accelerated traffic tests of concrete pavements*. Mariemont, OH: US Army Corps of Engineers, Ohio River Division Laboratories.
- Ohio River Division. 1950. *Lockbourne No. 2 – Modification multiple wheel study*. Mariemont, OH: US Army Corps of Engineers, Ohio River Division Laboratories.
- Skinner, J. A. and F. R. Martin. 1954. Some considerations of airfield pavement design. In *Airport Engineering Division Meeting, Airport Paper 26*.
- Stratton, J. H. 1945. Construction and design problems. In *Transaction of the American Society of Civil Engineers, Military Airfields, A Symposium* 110 (2247):670-696.

## Appendix A: FWD Data

### Part 1: FWD Data for top of base course

Note: The force is measured in pounds, the deflections are measured in mils.

Table A1-1. FWD data Item 1 east paving lane on base course.

Item 1								
StationID	Force	D1	D2	D3	D4	D5	D6	D7
12.5	5585	43.52	8.84	4.31	2.31	1.91	1.29	1.08
	5389	24.16	8.46	3.94	2.30	1.75	1.30	1.09
	5353	20.98	8.43	3.80	2.30	1.74	1.32	1.10
	4443	17.61	6.93	3.19	1.96	1.41	1.07	0.98
	3312	13.47	5.04	2.30	1.42	1.00	0.74	0.73
	2223	9.28	3.27	1.58	0.95	0.69	0.54	0.53
25.0	5406	128.81	17.29	5.49	2.55	4.12	1.95	1.28
	5346	23.80	11.50	4.78	2.94	1.74	1.89	1.22
	5264	24.58	10.30	4.71	2.99	1.69	1.55	1.15
	4372	25.26	7.86	3.92	2.32	1.46	1.26	1.01
	3222	24.41	5.72	2.80	1.63	1.04	0.87	0.73
	2152	17.97	3.55	1.78	1.04	0.75	0.63	0.54
37.5	5371	38.58	10.07	5.19	3.15	16.84	1.73	1.39
	5257	69.49	9.77	4.95	2.89	2.20	1.55	1.25
	5239	24.35	9.54	4.75	2.83	2.13	1.51	1.24
	4336	20.69	7.80	3.91	2.31	1.71	1.28	1.09
	3187	15.37	5.46	2.82	1.65	1.20	0.92	0.85
	2159	10.59	3.60	1.90	1.14	0.82	0.65	0.54



Table A1-2. FWD data Item 2 east paving lane on base course.

Item 2								
StationID	Force	D1	D2	D3	D4	D5	D6	D7
12.5	5531	25.30	9.57	3.59	2.61	1.64	1.33	1.43
	5417	18.44	8.24	3.71	2.44	1.67	1.34	1.15
	5389	18.19	8.22	3.60	2.40	1.66	1.31	1.07
	4471	15.25	6.55	3.01	2.02	1.40	1.07	0.87
	3354	11.87	4.91	2.28	1.53	1.04	0.79	0.67
	2266	8.52	3.25	1.60	1.02	0.75	0.58	0.67
25.0	5371	79.20	11.98	4.68	2.41	1.98	1.50	0.87
	5435	21.24	9.48	3.65	2.27	1.86	1.64	0.92
	5424	20.43	8.69	3.63	2.24	1.69	1.38	0.95
	4525	18.33	7.19	3.10	1.91	1.32	1.16	0.83
	3354	14.95	5.33	2.31	1.42	0.97	0.67	0.55
	2241	10.63	3.33	1.39	0.97	0.63	0.65	0.47
37.5	5371	38.58	10.07	5.19	3.15	16.84	1.73	1.39
	5257	69.49	9.77	4.95	2.89	2.20	1.55	1.25
	5239	24.35	9.54	4.75	2.83	2.13	1.51	1.24
	4336	20.69	7.80	3.91	2.31	1.71	1.28	1.09
	3187	15.37	5.46	2.82	1.65	1.20	0.92	0.85
	2159	10.59	3.60	1.90	1.14	0.82	0.65	0.54

Table A1-3. FWD data Item 3 east paving lane on base course.

Item 3								
StationID	Force	D1	D2	D3	D4	D5	D6	D7
12.5	5471	48.77	25.48	4.21	5.57	2.04	1.36	2.41
	5560	28.98	47.01	3.76	3.89	1.85	1.16	1.09
	5578	23.58	23.99	3.76	2.44	1.85	1.23	1.15
	4621	19.56	15.61	3.05	30.64	1.55	1.02	0.91
	3437	15.69	6.57	2.12	1.35	1.13	0.84	0.68
	2302	11.99	2.61	1.41	2.34	0.72	0.61	0.61
25.0	5542	53.46	45.64	7.03	6.78	25.67	11.77	2.59
	5656	17.15	23.48	4.86	4.60	2.08	1.78	1.30
	5638	21.91	10.40	5.05	3.58	3.21	1.43	1.15
	4650	21.59	4.50	3.73	2.07	1.39	1.04	0.92
	3454	13.37	3.18	2.14	1.46	0.98	0.75	0.71
	2320	8.21	2.18	1.41	1.12	0.66	0.48	0.50
37.5	6131	55.26	31.97	9.24	6.84	2.07	3.29	4.46
	5728	39.36	7.15	3.30	4.62	1.82	1.53	2.01
	5667	23.51	5.56	3.27	4.25	1.76	1.98	1.98
	4775	11.13	4.35	2.81	1.89	1.54	1.24	2.69
	3551	8.97	3.12	2.04	1.66	0.74	0.76	0.64
	2384	6.40	1.96	2.90	1.03	0.43	0.56	0.65

Table A1-4. FWD data Item 1 center paving lane on base course.

Item 1								
StationID	Force	D1	D2	D3	D4	D5	D6	D7
12.5	5738	52.37	9.69	4.00	3.13	2.14	1.29	1.19
	5828	101.56	7.57	4.04	2.54	1.96	1.26	1.03
	5810	70.69	7.59	3.90	2.47	1.85	1.24	1.00
	4953	63.83	6.22	3.22	2.05	1.46	1.02	0.82
	3694	49.03	4.31	2.47	1.52	1.07	0.75	0.58
	2473	55.63	2.77	1.77	1.02	0.71	0.50	0.41
25.0	5613	100.60	5.78	3.38	2.76	4.39	3.78	1.15
	5720	78.69	5.84	3.45	2.69	2.71	2.55	1.13
	5781	86.04	6.03	3.54	2.60	2.52	2.10	1.00
	4818	63.56	5.02	2.98	2.25	1.77	1.40	0.83
	3604	68.07	3.81	2.28	1.72	1.84	0.94	0.61
	2420	38.94	2.69	1.58	1.07	0.96	0.54	0.39
37.5	5460	45.39	6.01	3.54	2.32	1.73	1.24	1.10
	5549	39.96	6.22	3.50	2.55	1.80	1.28	1.06
	5549	36.15	6.26	3.58	2.52	1.80	1.28	1.04
	4657	31.59	5.15	3.00	1.76	1.37	1.00	0.85
	3497	29.69	3.81	2.31	1.44	1.06	0.77	0.65
	2355	24.69	2.38	1.56	0.93	0.72	0.59	0.50

Table A1-5. FWD data Item 2 center paving lane on base course.

Item 2								
StationID	Force	D1	D2	D3	D4	D5	D6	D7
12.5	5674	50.33	15.14	3.15	2.26	1.81	1.58	1.05
	5667	45.69	128.97	3.15	2.38	1.81	1.46	1.22
	5674	42.84	6.97	3.13	2.13	1.78	1.44	1.03
	4764	40.82	5.13	2.79	1.77	1.54	1.12	0.91
	3544	36.92	4.15	2.01	1.46	1.10	0.83	0.72
	2366	30.34	2.98	1.39	1.07	0.80	0.56	0.65
25.0	5692	29.48	14.31	3.00	2.78	1.59	1.50	46.10
	5542	21.09	7.70	2.92	2.25	1.53	1.22	1.13
	5489	20.20	8.19	2.93	2.30	1.39	1.08	1.52
	4614	17.17	6.47	2.56	1.93	1.21	0.91	3.11
	3472	13.63	4.70	2.01	1.51	0.93	0.73	1.09
	2330	9.89	3.06	1.46	1.03	0.69	0.73	2.15
37.5	5710	20.24	10.28	3.76	2.54	1.94	1.56	1.17
	5460	18.17	8.09	3.66	2.32	1.88	1.44	1.11
	5453	17.63	8.20	3.35	2.43	1.73	1.36	1.05
	4604	15.19	7.06	2.99	2.02	1.47	1.13	0.87
	3437	11.85	4.87	2.23	1.48	1.07	0.84	0.68
	2330	8.59	3.27	1.53	1.09	0.80	0.62	0.50

Table A1-6. FWD data Item 3 center paving lane on base course.

Item 3								
StationID	Force	D1	D2	D3	D4	D5	D6	D7
12.5	5246	128.98	9.43	5.44	2.70	2.19	4.94	1.34
	5656	27.48	3.19	3.54	2.81	2.07	1.76	1.32
	5631	16.28	7.56	4.57	3.04	2.01	1.48	1.06
	4711	15.52	4.18	2.90	2.27	1.73	1.28	0.94
	3462	11.69	3.86	2.37	1.65	1.13	0.83	0.69
	2320	9.13	2.78	1.68	1.13	1.20	1.71	1.61
25.0	5353	82.12	73.38	5.59	5.96	4.90	5.01	1.65
	5531	31.86	16.39	4.37	2.81	1.96	1.37	1.57
	5496	35.45	7.14	4.43	2.87	2.18	1.54	1.50
	4561	22.39	8.56	3.49	2.24	1.56	1.28	1.30
	3347	18.65	4.26	2.52	1.69	1.33	0.87	0.88
	2213	15.37	2.80	1.68	1.09	2.07	1.51	0.71
37.5	5514	86.36	129.00	10.06	18.44	3.45	2.61	1.76
	5649	36.37	16.18	3.79	5.42	3.01	1.31	1.46
	5596	26.15	30.59	4.94	4.31	2.31	1.74	2.09
	4686	43.60	5.89	3.60	2.04	1.32	1.04	0.89
	3462	10.22	3.73	2.51	1.59	1.08	1.00	0.48
	2302	7.24	2.50	1.73	1.30	0.74	0.63	0.31

Table A1-7. FWD data Item 1 west paving lane on base course.

Item 1								
Station ID	Force	D1	D2	D3	D4	D5	D6	D7
12.5	5506	128.96	15.69	5.63	3.56	2.52	2.05	1.56
	5424	83.57	23.12	42.12	3.29	2.37	1.89	1.41
	5399	112.37	15.76	11.02	3.27	2.39	2.00	1.42
	4543	70.09	13.08	6.09	2.72	2.03	1.67	1.31
	3372	55.76	8.68	3.67	2.04	1.53	1.20	0.94
	2284	90.92	7.57	11.00	1.42	1.06	0.79	0.90
25.0	5567	44.65	9.96	11.02	4.09	2.66	1.85	1.29
	5514	20.39	10.66	6.03	3.46	2.44	1.93	2.43
	5478	73.11	10.87	5.41	3.46	2.34	1.65	1.36
	4561	80.65	9.12	4.30	2.61	1.77	1.33	1.04
	3337	21.88	5.91	2.97	1.78	1.14	0.97	0.79
	2284	22.36	3.84	2.11	1.23	0.76	0.67	0.53
37.5	5506	63.64	7.63	4.38	2.80	2.03	1.63	1.17
	5346	19.72	8.11	3.67	2.63	1.81	1.57	1.16
	5317	20.17	8.02	3.56	2.59	1.69	1.48	1.14
	4436	17.02	6.70	3.01	2.14	1.43	1.21	0.95
	3283	12.89	4.81	2.34	1.57	1.09	0.89	0.64
	2259	9.21	3.26	1.69	1.15	0.79	0.63	0.48

Table A1-8. FWD data Item 2 west paving lane on base course.

Item 2								
StationID	Force	D1	D2	D3	D4	D5	D6	D7
12.5	5328	29.49	8.49	3.43	2.42	1.77	1.54	1.39
	5257	21.46	8.74	3.31	2.35	1.73	1.52	1.23
	5239	22.25	8.85	3.27	2.34	1.74	1.46	1.18
	4382	44.25	7.38	2.85	2.02	1.42	1.20	0.96
	3319	67.71	5.39	2.33	1.55	1.12	0.87	0.68
	2213	56.78	3.47	1.67	1.11	0.81	0.65	0.52
25.0	5246	32.48	9.21	3.74	2.57	2.05	1.72	1.31
	5150	24.43	8.61	3.53	2.58	2.04	1.63	1.24
	5103	23.19	8.96	3.57	2.61	2.03	1.65	1.25
	4257	19.41	7.43	3.10	2.18	1.68	1.39	0.98
	3222	15.21	5.61	2.34	1.66	1.26	1.02	0.73
	2170	10.85	3.68	1.66	1.17	0.94	0.69	0.51
37.5	5310	74.12	43.91	3.99	2.65	2.11	1.68	1.46
	5282	54.18	12.12	3.74	2.65	2.00	1.58	1.31
	5317	52.25	8.77	3.70	2.69	1.86	1.55	1.27
	4454	50.28	7.53	3.87	2.27	1.71	1.21	1.05
	3354	71.65	5.67	2.95	1.76	1.29	0.97	0.86
	2284	33.25	3.61	1.79	1.23	0.97	0.71	0.71

Table A1-9. FWD data Item 3 west paving lane on base course.

Item 3								
StationID	Force	D1	D2	D3	D4	D5	D6	D7
12.5	5210	128.80	12.73	4.63	3.04	2.31	1.75	1.44
	5406	51.54	9.96	7.79	2.89	2.26	1.60	1.36
	5417	58.54	9.63	4.66	2.76	1.91	1.50	1.25
	4532	78.01	7.93	3.23	2.33	1.62	1.33	1.15
	3401	39.15	5.84	2.34	1.66	1.20	0.96	0.80
	2277	30.85	3.93	1.89	0.85	0.24	0.01	0.00
25.0	5381	40.97	12.06	3.61	3.31	2.29	1.94	1.72
	5567	23.55	10.65	4.09	5.70	2.28	1.99	2.11
	5656	21.76	10.26	3.89	2.97	2.32	1.71	1.38
	4775	19.43	8.65	3.45	2.58	2.04	1.50	1.26
	3551	15.79	6.65	2.65	1.97	1.56	1.18	0.94
	2330	11.51	4.69	1.90	1.41	1.09	0.83	0.72
37.5	5942	95.01	7.64	4.64	2.70	1.85	1.41	1.31
	5799	45.44	6.60	3.62	2.61	1.67	1.33	1.04
	5738	22.19	6.33	3.48	2.48	1.63	1.34	1.03
	4864	24.00	5.30	2.74	1.96	1.28	1.04	0.80
	3586	25.63	4.10	2.18	1.59	1.08	0.84	0.62
	2402	23.87	2.84	1.61	1.12	0.78	0.60	0.44

## Part 2: FWD data for Lane 1 - Item 1

Note: The force is measured in pounds; the deflections are measured in mils.

Table A2-1. FWD data for Lane 1 – Item 1 prior to traffic; 0 passes.

Station 1 Center of Test Item 1							
Load(lbs)	D1	D2	D3	D4	D5	D6	D7
23859	7.85	7.15	6.32	5.42	4.54	3.69	3.02
23489	7.63	7.01	6.19	5.33	4.47	3.67	3.04
23344	7.61	6.97	6.14	5.29	4.42	3.62	3.00
19239	6.21	5.71	5.03	4.33	3.64	2.99	2.49
13711	4.39	4.00	3.58	3.04	2.53	2.07	1.70
8823	2.75	2.52	2.23	1.91	1.61	1.33	1.14
Station 2 North Transverse Joint of Test Item 1							
Load(lbs)	D1	D2	D3	D4	D5	D6	D7
22887	16.24	15.66	12.58	10.07	7.64	5.64	4.24
23077	16.03	15.54	12.49	9.98	7.56	5.59	4.20
23042	16.06	15.51	12.51	9.98	7.56	5.60	4.21
19009	13.40	12.89	10.36	8.31	6.28	4.65	3.46
13450	9.87	9.44	7.67	6.09	4.63	3.39	2.52
8419	6.21	5.91	4.85	3.84	2.96	2.18	1.63
Station 3 South Transverse Joint of Test Item 1							
Load(lbs)	D1	D2	D3	D4	D5	D6	D7
22903	14.98	15.18	12.31	9.98	7.61	5.65	4.22
22971	14.85	14.85	12.28	9.55	7.56	5.61	4.40
22979	14.83	14.80	12.28	9.83	7.58	5.62	4.19
18937	12.39	12.24	10.33	8.07	6.38	4.71	4.72
13002	8.98	8.98	7.55	6.00	4.66	3.47	4.30
8300	5.74	5.51	4.83	3.75	2.99	2.22	1.56
Station 4 West Longitudinal Joint of Test Item 1							
Load(lbs)	D1	D2	D3	D4	D5	D6	D7
22998	10.80	9.03	7.44	5.98	4.82	3.83	3.15
23378	10.76	8.86	7.35	5.89	4.79	3.79	3.08
23399	11.04	8.84	7.35	5.89	4.79	3.79	3.09
19402	8.93	7.22	6.03	4.83	3.96	3.13	2.56
13795	6.49	5.11	4.34	3.47	2.85	2.24	1.85
9239	4.30	3.34	2.76	2.35	1.86	1.46	1.29



Table A2-2. FWD data for Lane 1 – Item 1 at 1,000 passes of F-15.

Station 1 Center of Test Item 1							
Load(lbs)	D1	D2	D3	D4	D5	D6	D7
23478	7.78	7.06	6.20	5.30	4.45	3.63	3.01
23692	7.71	7.03	6.17	5.30	4.46	3.64	3.04
23700	7.77	7.05	6.17	5.32	4.46	3.65	3.04
19299	6.29	5.71	5.00	4.30	3.61	2.97	2.50
13772	4.51	4.10	3.58	3.09	2.63	2.13	1.73
9021	2.87	2.60	2.30	1.99	1.69	1.38	1.14
Station 2 North Transverse Joint of Test Item 1							
Load(lbs)	D1	D2	D3	D4	D5	D6	D7
22926	16.80	15.53	12.61	10.00	7.66	5.69	4.32
23058	16.84	15.48	12.45	9.96	7.57	5.64	4.26
23050	16.67	15.47	12.40	9.94	7.55	5.60	4.22
19048	13.94	12.88	10.31	8.31	6.30	4.68	3.50
13553	10.31	9.43	7.60	6.07	4.64	3.43	2.56
8768	6.72	6.14	5.01	4.00	3.05	2.24	1.67
Station 3 South Transverse Joint of Test Item 1							
Load(lbs)	D1	D2	D3	D4	D5	D6	D7
22796	15.56	15.55	12.69	10.22	7.82	5.81	4.37
22804	15.42	15.38	12.46	10.07	7.72	5.75	4.38
22820	15.42	15.25	12.60	10.13	7.76	5.74	4.34
18942	12.93	12.74	10.63	8.45	6.53	4.81	3.62
13656	9.72	9.33	8.07	6.32	4.93	3.67	2.81
8712	6.38	6.16	5.19	4.13	3.19	2.39	1.81
Station 4 West Longitudinal Joint of Test Item 1							
Load(lbs)	D1	D2	D3	D4	D5	D6	D7
23074	12.01	10.29	8.48	6.92	5.49	4.44	3.91
23272	11.66	10.05	8.28	6.72	5.47	4.33	3.55
23248	11.65	9.99	8.28	6.63	5.50	4.30	3.54
19045	9.55	8.16	6.78	5.40	4.54	3.52	2.89
13585	6.90	5.88	4.89	4.02	3.26	2.58	2.11
8826	4.32	3.64	3.10	2.46	2.11	1.58	1.26

Table A2-3. FWD data for Lane 1 – Item 1 at 50,000 passes of F-15.

Station 1 Center of Test Item 1							
Load(lbs)	D1	D2	D3	D4	D5	D6	D7
22974	7.86	7.03	6.19	5.38	4.50	3.62	2.94
23391	7.72	7.12	5.96	5.44	4.60	3.60	2.81
23410	7.76	7.07	5.93	5.39	4.57	3.61	2.81
19294	6.31	5.74	4.89	4.40	3.76	2.97	2.34
13838	4.57	4.13	3.52	3.17	2.71	2.17	1.67
8895	2.86	2.64	2.17	2.01	1.72	1.33	1.02
Station 2 North Transverse Joint of Test Item 1							
Load(lbs)	D1	D2	D3	D4	D5	D6	D7
22673	14.45	13.20	10.78	8.54	6.63	5.03	3.86
22812	13.99	13.19	10.71	8.52	6.61	4.96	3.92
22868	13.94	13.19	10.67	8.53	6.62	4.96	3.87
18977	11.63	10.95	8.84	7.11	5.51	4.11	3.13
13640	8.58	8.04	6.53	5.24	4.06	3.03	2.30
8818	5.57	5.19	4.22	3.39	2.65	1.98	1.53
Station 3 South Transverse Joint of Test Item 1							
Load(lbs)	D1	D2	D3	D4	D5	D6	D7
22677	13.73	13.44	11.00	8.71	6.77	5.04	3.78
22788	13.70	13.44	10.83	8.78	6.72	4.96	3.57
22796	13.74	13.45	10.72	8.80	6.64	4.93	3.46
18823	11.38	11.10	8.96	7.23	5.52	4.09	2.89
13478	8.54	8.23	6.67	5.38	4.11	3.09	2.37
8803	5.65	5.44	4.43	3.57	2.74	2.06	1.59
Station 4 West Longitudinal Joint of Test Item 1							
Load(lbs)	D1	D2	D3	D4	D5	D6	D7
23137	12.69	9.58	8.15	6.67	5.47	4.42	3.66
23339	11.28	9.24	7.94	6.41	5.28	4.25	3.48
23462	11.32	9.31	7.85	6.42	5.29	4.24	3.46
19069	9.03	7.52	6.41	5.24	4.35	3.48	2.85
13680	6.25	5.44	4.74	3.84	3.17	2.52	2.09
9088	3.74	3.36	3.02	2.41	2.02	1.61	1.30

### Part 3: FWD data for Lane 1 - Item 2

Note: The force is measured in pounds; the deflections are measured in mils.

Table A3-1. FWD data for Lane 1 – Item 2 at 100 passes of B-52.

Station 1 Center of Test Item 2							
Load(lbs)	D1	D2	D3	D4	D5	D6	D7
23240	9.30	8.09	6.93	5.79	4.83	3.92	3.17
23225	9.13	7.93	6.82	5.72	4.79	3.94	3.28
23244	9.13	7.78	6.87	5.71	4.78	3.85	3.09
19228	7.45	6.32	5.60	4.64	3.87	3.08	2.38
13902	5.31	4.58	4.00	3.34	2.79	2.27	1.86
9109	3.44	2.99	2.51	2.11	1.73	1.43	1.17
Station 2 North Transverse Joint of Test Item 2							
Load(lbs)	D1	D2	D3	D4	D5	D6	D7
22895	31.00	29.19	23.19	18.23	13.68	10.19	7.77
23066	30.62	29.10	23.02	18.14	13.62	10.19	7.71
23082	30.50	29.11	22.91	18.07	13.61	10.09	7.44
18990	27.38	26.00	20.62	16.28	12.27	8.75	6.33
13362	21.79	20.50	16.48	13.05	9.86	7.19	5.27
8633	15.05	13.99	11.46	9.18	7.03	5.16	3.87
Station 3 South Transverse Joint of Test Item 2							
Load(lbs)	D1	D2	D3	D4	D5	D6	D7
22630	24.91	22.40	18.43	15.00	11.65	8.87	6.82
22855	24.59	22.32	18.24	15.00	11.74	8.77	6.62
22918	25.66	22.22	18.26	14.96	11.69	8.81	6.59
18811	20.50	18.62	15.27	12.60	9.71	7.38	5.58
13561	15.38	14.06	11.53	9.46	7.39	5.56	4.22
8811	10.40	9.40	7.79	6.37	4.88	3.72	2.76
Station 4 West Longitudinal Joint of Test Item 2							
Load(lbs)	D1	D2	D3	D4	D5	D6	D7
22252	31.00	22.31	17.57	13.68	10.21	7.44	5.51
22281	30.61	22.43	17.48	13.77	10.19	7.46	5.45
22482	30.45	22.44	17.56	13.74	10.21	7.46	5.51
18700	26.41	19.38	15.22	11.91	8.80	6.44	4.78
13367	20.27	15.10	11.93	9.28	6.96	5.07	3.71
8612	13.37	10.11	8.31	6.35	4.85	3.51	2.43

Table A3-2. FWD data for Lane 1 – Item 2 at 300 passes of B-52.

Station 1 Center of Test Item 2							
Load(lbs)	D1	D2	D3	D4	D5	D6	D7
23220	8.92	7.94	6.84	5.77	4.80	3.94	3.27
23383	8.83	7.84	6.79	5.75	4.81	3.94	3.23
23410	8.83	7.89	6.79	5.74	4.80	3.97	3.35
19323	7.26	6.42	5.57	4.69	3.93	3.25	2.73
13732	5.11	4.62	3.98	3.34	2.81	2.32	1.98
9128	3.36	3.02	2.58	2.16	1.81	1.48	1.25
Station 2 North Transverse Joint of Test Item 2							
Load(lbs)	D1	D2	D3	D4	D5	D6	D7
22566	29.07	25.37	20.17	15.81	12.00	8.93	6.80
22649	29.09	25.38	20.09	15.83	12.00	8.89	6.72
22701	29.33	25.60	20.25	15.96	12.17	8.93	6.53
18874	26.22	22.51	17.69	13.89	10.60	7.68	5.44
13510	21.53	18.30	14.42	11.27	8.49	6.07	4.36
8612	15.22	12.76	10.29	8.12	6.13	4.45	3.30
Station 3 South Transverse Joint of Test Item 2							
Load(lbs)	D1	D2	D3	D4	D5	D6	D7
22614	23.88	23.65	19.66	16.32	12.98	10.03	7.64
22836	23.78	23.52	19.48	16.21	12.92	9.92	7.38
22807	23.71	23.43	19.42	16.14	12.81	9.85	7.30
18823	20.15	19.81	16.63	13.76	10.97	8.43	6.22
13553	14.94	14.78	12.60	10.35	8.28	6.34	4.91
8652	9.93	9.77	8.37	6.86	5.48	4.17	3.20
Station 4 West Longitudinal Joint of Test Item 2							
Load(lbs)	D1	D2	D3	D4	D5	D6	D7
22154	28.16	20.29	15.82	14.08	9.18	6.71	5.06
22305	35.52	20.26	15.80	12.44	9.18	6.68	4.96
22154	47.30	20.19	15.75	12.42	9.12	6.65	4.94
18585	24.22	17.58	13.67	10.77	7.90	5.80	4.28
13251	18.30	13.57	10.65	8.43	6.18	4.41	3.36
8490	11.87	9.10	7.37	5.65	4.29	3.15	2.08

Table A3-3. FWD data for Lane 1 – Item 2 at 1,000 passes of B-52.

Station 1 Center of Test Item 2							
Load(lbs)	D1	D2	D3	D4	D5	D6	D7
22836	9.57	8.48	7.19	6.20	5.19	4.33	3.66
23259	9.49	8.33	7.24	6.15	5.22	4.37	3.76
23272	9.55	8.33	7.28	6.21	5.30	4.37	3.71
19215	7.70	6.81	5.93	5.04	4.29	3.55	3.01
13815	5.37	4.85	4.26	3.61	3.07	2.54	2.16
8922	3.54	3.03	2.76	2.30	1.99	1.59	1.36
Station 2 North Transverse Joint of Test Item 2							
Load(lbs)	D1	D2	D3	D4	D5	D6	D7
22688	32.48	25.04	19.99	15.60	11.74	8.63	6.56
22855	27.78	25.39	20.07	15.67	11.84	8.74	6.54
22784	27.72	25.20	19.94	15.75	11.88	8.74	6.43
19025	25.09	22.42	17.46	13.87	10.39	7.46	5.09
13494	20.42	17.99	14.23	11.22	8.41	6.05	4.37
8585	13.85	12.19	9.79	7.79	5.90	4.26	3.01
Station 3 South Transverse Joint of Test Item 2							
Load(lbs)	D1	D2	D3	D4	D5	D6	D7
22741	20.97	20.19	16.55	13.36	10.31	7.65	5.79
22871	20.40	20.10	16.59	13.37	10.33	7.69	5.80
22836	20.31	20.06	16.51	13.22	10.36	7.65	5.72
18903	17.14	17.04	14.07	11.37	8.80	6.53	4.85
13664	12.81	12.86	10.67	8.61	6.73	4.99	3.68
8895	8.56	8.53	7.13	5.74	4.51	3.30	2.48
Station 4 West Longitudinal Joint of Test Item 2							
Load(lbs)	D1	D2	D3	D4	D5	D6	D7
22379	30.67	20.96	16.24	12.79	9.42	6.94	5.08
22482	29.66	20.94	16.21	12.78	9.41	6.91	4.98
22522	29.31	20.93	16.13	12.75	9.40	6.89	4.96
18644	25.37	18.02	13.94	11.07	8.15	5.96	4.26
13312	19.15	13.89	10.74	8.59	6.34	4.60	3.24
8628	12.69	9.76	7.43	6.08	4.46	3.26	2.24

## Part 4: FWD data for Lane 1 - Item 3

Note: The force is measured in pounds; the deflections are measured in mils.

Table A4-1. FWD data for Lane 1 – Item 3 at 0 passes of F-15.

Station 1 Center of Test Item3							
Load(lbs)	D1	D2	D3	D4	D5	D6	D7
23018	9.99	8.52	7.24	5.91	4.75	3.73	3.00
23407	9.81	8.40	7.20	5.88	4.77	3.76	3.00
23370	9.87	8.36	7.23	5.89	4.77	3.76	2.96
19323	8.07	6.96	5.88	4.83	3.91	3.08	2.48
13986	5.83	5.02	4.24	3.51	2.86	2.24	1.82
9064	3.71	3.12	2.70	2.17	1.77	1.38	1.06
Station 2 North Transverse Joint of Test Item 3							
Load(lbs)	D1	D2	D3	D4	D5	D6	D7
22654	24.57	23.07	18.33	14.42	10.69	7.67	5.63
22828	24.70	23.03	18.29	14.36	10.68	7.69	5.65
22799	24.60	22.98	18.22	14.30	10.63	7.64	5.59
18858	21.09	19.70	15.66	12.27	9.15	6.60	4.84
13470	16.09	15.13	12.06	9.48	7.11	5.12	3.76
8684	10.76	10.12	8.14	6.42	4.85	3.50	2.58
Station 3 South Transverse Joint of Test Item 3							
Load(lbs)	D1	D2	D3	D4	D5	D6	D7
22804	19.39	19.12	15.64	12.43	9.39	6.85	5.03
22923	19.55	19.20	15.60	12.43	9.40	6.80	5.03
22942	19.28	19.21	15.49	12.36	9.37	6.76	4.74
18937	16.50	16.37	13.28	10.63	8.04	5.79	4.24
13526	12.48	12.41	10.11	8.10	6.19	4.48	3.20
8744	8.39	8.31	6.85	5.50	4.23	3.05	2.21
Station 4 West Longitudinal Joint of Test Item 3							
Load(lbs)	D1	D2	D3	D4	D5	D6	D7
22384	17.74	15.79	12.36	9.81	7.37	5.61	4.27
22546	18.89	15.75	12.40	9.78	7.32	5.59	4.37
22590	17.81	15.80	12.47	9.80	7.39	5.64	4.39
18538	14.91	13.27	10.38	8.22	6.17	4.68	3.57
13581	11.24	9.84	7.81	6.03	4.63	3.48	2.62
8755	7.27	6.44	5.11	3.94	2.99	2.25	1.76



Table A4-2. FWD data for Lane 1 – Item 3 at 1,000 passes of F-15.

Station 1 Center of Test Item 3							
Load(lbs)	D1	D2	D3	D4	D5	D6	D7
22812	9.73	8.53	7.21	6.00	4.98	3.99	3.24
23106	9.71	8.52	7.19	6.02	4.98	4.02	3.29
23125	9.74	8.55	7.20	5.99	4.96	4.01	3.29
19215	8.02	7.01	5.93	4.94	4.08	3.29	2.67
13803	5.72	5.01	4.28	3.54	2.94	2.34	1.88
8842	3.61	3.19	2.68	2.23	1.83	1.46	1.17
Station 2 North Transverse Joint of Test Item 3							
Load(lbs)	D1	D2	D3	D4	D5	D6	D7
22443	26.87	25.98	20.73	16.63	12.81	9.67	7.49
22617	26.72	25.76	20.33	16.38	12.62	9.44	7.26
22622	26.63	25.56	20.36	16.26	12.50	9.38	7.22
18776	22.61	21.87	17.58	13.99	10.76	7.89	5.98
13394	17.26	16.38	13.36	10.68	8.24	6.08	4.59
8562	11.08	10.58	8.82	7.01	5.46	3.99	3.00
Station 3 South Transverse Joint of Test Item 3							
Load(lbs)	D1	D2	D3	D4	D5	D6	D7
22828	20.73	20.87	17.31	14.14	11.09	8.30	6.37
22876	20.63	20.74	17.05	14.00	10.87	8.30	6.08
22903	20.52	20.60	17.02	13.91	10.79	8.17	5.86
18895	17.49	17.52	14.52	11.87	9.26	6.93	5.26
13632	13.26	13.30	11.01	9.02	7.06	5.30	4.01
8625	8.81	8.82	7.37	6.02	4.71	3.57	2.61
Station 4 West Longitudinal Joint of Test Item 3							
Load(lbs)	D1	D2	D3	D4	D5	D6	D7
22360	24.87	17.92	14.20	11.13	8.44	6.29	4.87
22506	24.55	17.88	14.20	11.10	8.41	6.28	4.86
22471	23.95	17.76	14.13	11.08	8.37	6.24	4.82
18649	20.62	15.21	12.05	9.40	7.07	5.26	4.03
13545	15.98	11.48	9.17	7.08	5.35	3.98	3.07
8620	10.76	7.69	6.19	4.81	3.63	2.66	2.00

Table A4-3. FWD data for Lane 1 – Item 3 at 10,000 passes of F-15.

Station 1 Center of Test Item 3							
Load(lbs)	D1	D2	D3	D4	D5	D6	D7
22895	9.68	8.46	7.28	6.16	5.14	4.25	3.53
23082	9.67	8.45	7.29	6.16	5.17	4.22	3.51
23148	9.60	8.43	7.28	6.14	5.17	4.20	3.46
19037	7.85	6.94	5.92	5.00	4.17	3.39	2.74
13534	5.57	4.97	4.26	3.61	3.02	2.44	1.94
8760	3.59	3.18	2.74	2.29	1.90	1.53	1.28
Station 2 North Transverse Joint of Test Item 3							
Load(lbs)	D1	D2	D3	D4	D5	D6	D7
22416	22.40	20.07	15.62	11.98	10.66	6.55	5.03
22641	22.44	20.20	15.45	11.90	8.86	6.48	4.95
22617	23.22	20.11	15.33	12.08	8.89	6.49	4.90
18596	19.40	17.02	13.19	10.36	7.65	5.54	4.19
13267	14.98	12.83	10.13	7.83	5.85	4.20	3.19
8538	10.34	8.59	6.80	5.28	3.96	2.84	2.12
Station 3 South Transverse Joint of Test Item 3							
Load(lbs)	D1	D2	D3	D4	D5	D6	D7
22646	20.16	20.16	16.20	13.54	10.74	7.86	5.44
22688	20.03	19.89	16.01	13.36	10.55	7.76	5.39
22784	20.13	19.83	16.12	13.36	10.53	7.78	5.50
18565	17.02	16.72	13.74	11.34	8.81	6.61	4.84
13251	12.83	12.65	10.52	8.61	6.75	5.06	3.82
8422	8.51	8.35	6.98	5.70	4.49	3.36	2.48
Station 4 West Longitudinal Joint of Test Item 3							
Load(lbs)	D1	D2	D3	D4	D5	D6	D7
22332	23.56	17.33	13.52	10.72	7.96	5.94	4.59
22474	23.28	17.37	13.50	10.68	7.98	5.95	4.57
22447	22.85	17.37	13.41	10.64	7.96	5.87	4.38
18522	20.19	14.77	11.58	9.10	6.74	4.99	3.76
13098	15.50	11.41	8.87	6.94	5.16	3.77	2.78
8419	10.39	7.89	6.15	4.91	3.59	2.64	1.95

## Part 5: FWD data for Lane 2 (F-15) - Items 1, 2 and 3

Note: The force is measured in pounds; the deflections are measured in mils.

Table A5-1. FWD data for Lane 2 – Item 1 western free edge.

Passes - 0							
Force	D1	D2	D3	D4	D5	D6	D7
22455	27.05	22.13	17.22	13.65	10.36	7.83	6.13
22752	27.20	22.24	17.44	13.89	10.60	7.91	5.80
22807	27.02	22.48	17.60	13.97	10.64	7.97	5.93
18839	23.15	18.80	14.75	11.67	8.89	6.62	4.77
13653	17.02	13.85	10.90	8.62	6.59	4.87	3.56
8673	10.50	8.56	6.80	5.34	4.09	3.04	2.28
Passes - 100							
Force	D1	D2	D3	D4	D5	D6	D7
22340	30.91	24.54	19.42	15.67	11.67	8.71	6.61
22482	43.24	24.35	19.12	15.28	11.68	8.63	6.25
22482	27.79	24.15	19.03	15.17	11.54	8.57	6.27
18839	24.50	19.94	15.80	12.50	9.48	7.09	5.43
13410	17.78	14.47	11.49	9.06	6.89	5.15	3.90
8744	11.05	8.98	7.17	5.61	4.27	3.19	2.39
Passes - 1000							
Force	D1	D2	D3	D4	D5	D6	D7
22471	31.40	24.40	19.28	15.26	11.57	8.68	6.70
22543	29.63	24.12	19.00	15.05	11.47	8.64	6.67
22554	29.77	24.04	18.99	14.95	11.65	8.63	6.66
18850	24.44	19.91	15.77	12.40	9.59	7.14	5.44
13248	17.58	14.33	11.37	8.93	6.90	5.11	3.89
8562	10.89	8.93	7.17	5.57	4.38	3.21	2.39
Passes - 25000							
Force	D1	D2	D3	D4	D5	D6	D7
22363	28.25	23.15	18.42	14.54	11.12	8.36	6.53
22606	27.68	23.40	18.36	14.64	11.18	8.41	6.16
22614	30.19	23.32	18.35	14.62	11.17	8.44	6.11
18807	23.54	19.17	15.18	12.01	9.21	6.96	5.28
12926	16.72	13.57	10.80	8.53	6.55	4.95	3.72
8466	10.14	8.30	6.62	5.22	4.00	3.00	2.28

Table A5-2. FWD data for Lane 2 – Item 2 western free edge.

Passes - 0							
Force	D1	D2	D3	D4	D5	D6	D7
22202	23.83	18.27	14.33	10.99	8.30	6.20	4.80
22487	23.76	18.74	14.41	11.36	8.48	6.38	4.51
22522	23.36	18.81	14.59	11.38	8.56	6.42	4.62
18585	19.59	15.86	12.28	9.64	7.20	5.40	3.85
13050	14.60	11.68	9.11	7.04	5.30	3.94	2.79
8216	9.26	7.48	5.79	4.44	3.35	2.46	1.84
Passes -10							
Force	D1	D2	D3	D4	D5	D6	D7
22300	27.87	22.35	17.43	13.50	9.93	7.40	5.78
22511	61.83	22.50	17.28	13.48	10.08	7.34	5.25
22403	27.57	22.14	17.17	13.32	9.96	7.32	5.33
18454	22.98	18.37	14.35	11.07	8.34	6.03	4.52
13042	16.80	13.48	10.48	8.08	6.09	4.40	3.23
8335	10.59	8.48	6.67	5.11	3.79	2.80	2.11
Passes -1303							
Force	D1	D2	D3	D4	D5	D6	D7
22070	34.38	28.11	21.79	16.93	12.57	9.19	6.91
22149	35.14	28.23	21.96	17.09	12.66	9.19	6.40
22213	35.11	28.26	21.86	17.02	12.60	9.13	6.30
18263	31.30	23.63	18.24	14.22	10.55	7.68	5.54
13066	21.40	17.26	13.50	10.45	7.79	5.65	4.17
8450	13.72	11.11	8.75	6.74	5.02	3.63	2.61

Table A5-3. FWD data for Lane 2 – Item 3 western free edge.

Passes - 0							
Force	D1	D2	D3	D4	D5	D6	D7
21773	32.78	25.67	19.42	14.48	10.41	7.46	5.57
22102	30.41	26.74	20.07	14.93	10.81	7.63	5.12
22138	32.35	27.39	20.58	15.26	11.09	7.82	5.18
18308	30.63	24.01	18.11	13.31	9.71	6.77	4.26
13220	24.01	18.89	14.22	10.55	7.56	5.25	3.65
8541	16.39	12.93	9.77	7.18	5.17	3.55	2.47
Passes - 10							
Force	D1	D2	D3	D4	D5	D6	D7
21662	49.11	37.42	28.01	20.89	14.85	10.33	7.56
21908	44.96	36.48	27.45	20.65	14.71	10.08	7.16
21861	44.72	36.20	27.35	20.51	14.63	10.09	7.25
18232	38.92	31.04	23.51	17.66	12.55	8.56	6.07
13209	30.05	23.93	18.17	13.70	9.70	6.54	4.53
8641	20.58	16.37	12.48	9.38	6.64	4.43	3.02
Passes - 100							
Force	D1	D2	D3	D4	D5	D6	D7
21710	58.22	45.78	34.05	25.64	18.30	12.69	9.17
21911	56.04	44.09	33.08	24.95	17.87	12.36	8.67
21935	53.36	43.26	32.71	24.67	17.67	12.23	8.52
18300	45.77	36.96	28.21	21.31	15.17	10.46	7.14
13240	35.37	28.55	21.93	16.54	11.84	8.11	5.56
8485	24.11	19.54	15.09	11.32	8.12	5.52	3.73
Passes - 300							
Force	D1	D2	D3	D4	D5	D6	D7
21734	57.33	47.10	34.25	25.70	18.39	12.99	9.47
21853	53.50	45.71	34.38	25.95	18.56	12.82	8.69
21880	56.19	45.52	34.44	25.87	18.61	12.81	8.68
18276	49.58	39.64	30.24	22.71	16.33	11.13	7.50
13045	39.32	31.50	24.10	18.15	12.98	8.86	6.08
8308	27.14	21.86	16.91	12.71	9.13	6.22	4.19
Passes - 1000							
Force	D1	D2	D3	D4	D5	D6	D7
21348	63.00	59.96	6.15	5.77	4.84	4.26	2.45
21623	62.19	54.16	5.44	4.91	4.33	3.71	3.15
21681	61.39	52.76	5.22	4.78	4.23	3.66	3.12
17930	50.91	44.03	4.32	4.00	3.50	2.98	2.47
12955	37.64	32.39	3.28	2.98	2.59	2.17	1.76
8268	24.43	20.84	2.11	1.93	1.65	1.37	1.10

## Part 6: FWD data for Lane 3; 0 passes of C-17 traffic

Note: The force is measured in pounds; the deflections are measured in mils.

Table A6-1. FWD data for Item 1 at 0 passes.

Station 1 Center of Test Item 1							
Load(lbs)	D1	D2	D3	D4	D5	D6	D7
23414	6.74	5.91	5.24	4.61	3.95	3.35	2.82
23512	6.72	6.02	5.13	4.62	3.92	3.31	2.81
23436	6.86	5.89	5.17	4.57	3.91	3.30	2.57
19280	5.39	4.80	4.18	3.69	3.19	2.67	2.19
13473	3.83	3.37	2.98	2.63	2.27	1.92	1.46
8847	2.52	2.17	1.86	1.69	1.43	1.20	1.04
Station 2 Center of South Transverse Joint							
Load(lbs)	D1	D2	D3	D4	D5	D6	D7
22889	17.13	12.82	10.47	8.41	6.46	4.92	3.90
23009	17.06	12.50	10.24	8.21	6.32	4.85	3.78
23020	17.13	12.31	10.22	8.13	6.35	4.82	3.56
18766	14.59	10.09	8.28	6.68	5.22	3.96	2.81
13342	11.31	7.19	5.98	4.83	3.82	2.89	1.88
8552	7.78	4.39	3.81	2.98	2.41	1.80	1.18
Station 3 Center of North Transverse Joint							
Load(lbs)	D1	D2	D3	D4	D5	D6	D7
23031	12.11	11.71	9.50	7.83	6.20	4.56	3.20
23173	11.97	11.68	9.23	7.78	5.95	4.36	2.92
23162	11.98	11.46	9.35	7.69	5.93	4.46	3.18
18843	9.97	9.57	7.73	6.43	4.89	3.61	2.40
13473	7.24	7.02	5.71	4.67	3.67	2.82	2.16
8661	4.69	4.43	3.70	3.00	2.34	1.77	1.31
Station 4 Center of East Longitudinal Joint							
Load(lbs)	D1	D2	D3	D4	D5	D6	D7
23228	16.58	10.85	8.70	7.32	5.86	4.70	3.78
23206	11.80	10.79	8.72	7.25	5.83	4.68	3.81
23370	11.83	10.83	8.77	7.28	5.85	4.68	3.76
19083	9.84	8.92	7.19	5.92	4.80	3.83	3.05
13550	7.22	6.39	5.17	4.26	3.44	2.74	2.15
8956	4.64	4.11	3.37	2.74	2.22	1.75	1.43



Table A6-2. FWD data for Item 2 at 0 passes.

Station 5 Center of Test Item 2							
Load(lbs)	D1	D2	D3	D4	D5	D6	D7
23632	6.48	5.82	5.24	4.57	3.94	3.30	2.70
23917	6.37	5.79	5.26	4.53	3.91	3.30	2.78
23906	6.43	5.78	5.27	4.51	3.91	3.31	2.77
19477	5.24	4.72	4.24	3.69	3.20	2.68	2.29
13725	3.73	3.37	3.05	2.65	2.30	1.96	1.65
9022	2.38	2.17	1.89	1.92	1.45	1.20	1.13
Station 6 Center of South Transverse Joint							
Load(lbs)	D1	D2	D3	D4	D5	D6	D7
22889	15.98	14.22	11.70	9.13	7.05	5.26	3.93
22943	15.91	14.05	11.52	9.03	6.97	5.17	3.91
23009	16.07	13.90	11.46	8.98	6.98	5.08	3.54
18843	13.64	11.81	9.60	7.56	5.84	4.30	3.20
13440	10.30	8.70	7.17	5.64	4.33	3.15	2.30
8617	6.85	5.67	4.76	3.70	2.87	2.05	1.42
Station 7 Center of North Transverse Joint							
Load(lbs)	D1	D2	D3	D4	D5	D6	D7
22790	16.95	13.56	11.13	8.94	6.96	5.39	4.17
22911	16.86	13.25	11.08	8.85	6.94	5.34	4.18
22889	16.85	13.60	10.96	8.88	6.81	5.27	4.24
18788	14.34	11.11	9.04	7.35	5.61	4.33	3.40
13440	10.81	7.87	6.56	5.25	4.07	3.17	2.53
8814	7.20	5.02	4.24	3.39	2.61	2.03	1.57
Station 8 Center of East Longitudinal Joint							
Load(lbs)	D1	D2	D3	D4	D5	D6	D7
23064	15.37	13.17	10.56	8.69	6.92	5.36	4.28
23173	37.36	13.06	10.69	8.63	6.89	5.34	4.28
23228	16.59	13.15	10.51	8.68	6.88	5.33	4.28
19028	12.93	10.91	8.76	7.13	5.66	4.37	3.51
13768	9.59	7.99	6.45	5.20	4.15	3.21	2.55
9011	6.22	5.26	4.28	3.42	2.71	2.06	1.56

Table A6-3. FWD data for Item 3 at 0 passes.

Station 9 Center of Test Item 3							
Load(lbs)	D1	D2	D3	D4	D5	D6	D7
22801	8.42	7.37	6.49	5.52	4.67	3.84	3.23
23162	8.38	7.38	6.51	5.47	4.65	3.82	3.23
23195	8.50	7.41	6.36	5.52	4.62	3.78	3.02
19160	6.86	6.06	5.27	4.51	3.76	3.10	2.47
13484	4.91	4.29	3.74	3.20	2.68	2.22	1.81
8891	3.19	2.74	2.46	2.08	1.77	1.46	1.25
Station 10 Center of South Transverse Joint							
Load(lbs)	D1	D2	D3	D4	D5	D6	D7
22714	16.15	15.83	12.86	10.33	7.96	6.12	4.82
22911	16.19	15.90	12.91	10.35	8.02	6.12	4.74
22834	16.21	15.90	12.93	10.25	8.24	6.09	4.43
18766	13.77	13.54	11.00	8.84	6.83	5.19	3.99
13342	10.19	9.98	8.24	6.54	5.20	3.86	2.96
8738	6.84	6.67	5.54	4.43	3.44	2.57	2.01
Station 11 Center of North Transverse Joint							
Load(lbs)	D1	D2	D3	D4	D5	D6	D7
22572	14.01	13.13	10.55	8.40	6.44	4.98	3.94
22714	14.04	13.19	10.51	8.40	6.41	4.95	3.89
22692	14.06	13.22	10.54	8.43	6.43	4.93	3.91
18799	11.80	10.94	8.94	7.00	5.51	4.08	3.16
13451	8.60	7.94	6.64	5.16	4.14	3.00	2.21
8639	5.71	5.21	4.43	3.41	2.74	1.98	1.52
Station 12 Center of East Longitudinal Joint							
Load(lbs)	D1	D2	D3	D4	D5	D6	D7
22626	16.33	16.21	12.36	9.32	7.14	5.43	4.11
22889	16.43	15.94	12.36	9.40	7.19	5.50	4.18
22889	16.69	15.91	12.36	9.39	7.26	5.51	4.18
18788	13.93	13.14	10.28	7.81	6.07	4.53	3.42
13407	10.10	9.49	7.60	5.76	4.44	3.29	2.42
8749	6.61	6.28	5.03	3.82	2.96	2.17	1.60

## Part 7: FWD data for Lane 3; 1,008 passes of C-17 traffic

Note: The force is measured in pounds; the deflections are measured in mils.

Table A7-1. FWD data for Item 1 at 1,008 passes.

Station 1 Center of Test Item 1							
Load(lbs)	D1	D2	D3	D4	D5	D6	D7
23320	6.79	6.30	5.78	5.15	4.43	3.78	3.26
23589	6.76	5.98	5.76	5.07	4.46	3.70	3.20
23716	6.85	6.27	5.72	5.10	4.41	3.75	3.25
19315	5.55	5.07	4.64	4.14	3.61	3.06	2.61
13870	3.99	3.70	3.37	3.04	2.62	2.22	1.91
9014	2.59	2.36	2.16	1.92	1.65	1.39	1.21
Station 2 Center of South Transverse Joint							
Load(lbs)	D1	D2	D3	D4	D5	D6	D7
22233	36.20	2.76	2.59	2.39	2.23	2.01	1.86
22558	34.76	2.86	2.73	2.52	2.35	2.19	2.04
22609	34.44	2.91	2.71	2.54	2.39	2.19	2.01
18652	30.30	2.47	2.33	2.17	2.02	1.85	1.71
13439	24.10	1.97	1.85	1.72	1.57	1.41	1.32
8577	16.86	1.35	1.28	1.15	1.09	0.95	0.85
Station 3 Center of North Transverse Joint							
Load(lbs)	D1	D2	D3	D4	D5	D6	D7
22654	17.33	8.94	7.46	6.29	5.09	4.10	3.34
22831	16.76	8.70	7.54	6.16	5.26	4.12	3.21
22871	16.83	8.84	7.49	6.27	5.16	4.13	3.33
18906	13.30	7.38	6.51	5.15	4.52	3.39	2.66
13669	8.91	5.64	4.90	3.92	3.30	2.56	2.10
8680	5.19	3.82	3.28	2.63	2.09	1.73	2.29
Station 4 Center of East Longitudinal Joint							
Load(lbs)	D1	D2	D3	D4	D5	D6	D7
23180	14.48	9.98	8.51	7.28	6.11	5.06	4.22
23196	14.24	9.95	8.44	7.20	6.03	4.97	4.03
23217	14.27	9.96	8.47	7.20	6.06	5.00	4.05
19231	11.90	8.03	7.06	5.97	5.04	4.13	3.43
13870	8.54	5.94	5.15	4.37	3.67	3.00	2.40
8961	5.45	4.16	3.33	2.80	2.33	1.87	1.30

Table A7-2. FWD data for Item 2 at 1,008 passes.

Station 5 Center of Test Item 2							
Load(lbs)	D1	D2	D3	D4	D5	D6	D7
23545	7.81	7.94	8.12	7.29	5.97	4.72	3.69
23611	7.65	7.78	7.95	7.14	5.88	4.66	3.61
23665	7.64	7.73	7.99	7.12	5.90	4.66	3.57
19258	6.17	6.33	6.48	5.81	4.79	3.81	2.97
13823	4.44	4.43	4.62	4.08	3.40	2.71	2.11
9044	2.78	2.76	2.93	2.54	2.13	1.71	1.34
Station 6 Center of South Transverse Joint							
Load(lbs)	D1	D2	D3	D4	D5	D6	D7
22462	20.64	9.72	8.37	6.85	5.68	4.37	3.35
22648	20.61	9.50	8.44	6.87	5.73	4.36	3.32
22714	20.63	9.46	8.43	6.90	5.70	4.40	3.46
18689	17.16	7.90	7.03	5.78	4.71	3.70	3.01
13582	12.35	6.17	5.20	4.32	3.49	2.74	2.24
8760	7.76	4.18	3.50	2.88	2.33	1.78	1.39
Station 7 Center of North Transverse Joint							
Load(lbs)	D1	D2	D3	D4	D5	D6	D7
22604	20.23	11.87	9.62	7.38	5.29	4.27	3.64
22604	19.32	11.20	9.30	6.91	5.20	4.23	3.50
22637	19.39	11.14	8.91	6.88	5.19	4.21	3.53
18668	16.80	8.94	7.18	5.47	4.17	3.39	2.89
13484	13.43	6.13	5.00	4.01	2.96	2.41	2.05
8661	9.90	3.45	2.93	2.28	1.86	1.54	1.27
Station 8 Center of East Longitudinal Joint							
Load(lbs)	D1	D2	D3	D4	D5	D6	D7
22998	19.13	11.72	9.87	8.50	7.16	5.99	5.04
23064	15.90	11.52	9.71	8.38	7.03	5.86	4.90
23140	15.89	11.52	9.74	8.39	7.05	5.90	4.94
19017	13.26	9.54	8.08	6.96	5.87	4.87	4.04
13714	9.48	6.96	5.95	5.07	4.27	3.54	2.95
8967	6.13	4.55	3.91	3.31	2.78	2.29	1.92

Table A7-3. FWD data for Item 3 at 1,008 passes.

Station 9 Center of Test Item 3							
Load(lbs)	D1	D2	D3	D4	D5	D6	D7
22922	9.06	8.56	8.80	8.40	8.50	7.12	5.70
22987	8.89	8.37	8.70	8.24	8.37	7.02	5.57
23031	8.95	8.57	8.65	8.24	8.39	7.06	5.60
19017	7.41	6.96	7.24	6.79	6.89	5.80	4.60
13779	5.28	5.08	5.29	4.92	4.99	4.21	3.37
8749	3.39	3.08	3.41	3.09	3.15	2.63	2.17
Station 10 Center of South Transverse Joint							
Load(lbs)	D1	D2	D3	D4	D5	D6	D7
22594	16.49	15.26	12.23	9.67	7.27	5.39	4.27
22812	15.50	14.42	11.79	9.30	7.06	5.18	4.11
22801	15.45	14.48	11.75	9.31	7.06	5.20	4.17
18853	12.85	11.96	9.71	7.68	5.83	4.29	3.40
13462	9.28	8.58	7.07	5.56	4.19	3.07	2.52
8847	6.15	5.51	4.66	3.63	2.74	2.00	1.62
Station 11 Center of North Transverse Joint							
Load(lbs)	D1	D2	D3	D4	D5	D6	D7
22429	25.28	15.53	12.96	10.40	8.17	6.09	4.52
22648	23.06	15.28	12.66	10.17	7.99	5.98	4.52
22648	22.94	15.12	12.76	10.06	7.99	5.89	4.39
18613	19.80	12.35	10.41	8.25	6.55	4.83	3.59
13342	15.30	8.63	7.38	5.79	4.59	3.38	2.48
8683	10.86	5.42	4.62	3.59	2.76	2.02	1.56
Station 12 Center of East Longitudinal Joint							
Load(lbs)	D1	D2	D3	D4	D5	D6	D7
22342	28.36	23.21	18.42	14.19	10.78	8.09	6.24
22528	27.54	22.53	18.02	13.82	10.62	7.91	6.06
22517	26.07	22.48	17.82	13.80	10.56	7.84	6.02
18580	23.32	18.78	14.96	11.56	8.90	6.57	5.02
13495	17.70	13.98	11.09	8.58	6.58	4.89	3.73
8399	11.54	9.10	7.37	5.53	4.32	3.13	2.35

REPORT DOCUMENTATION PAGE				Form Approved OMB No. 0704-0188	
Public reporting burden for this collection of information is estimated to average 1 hour per response, including the time for reviewing instructions, searching existing data sources, gathering and maintaining the data needed, and completing and reviewing this collection of information. Send comments regarding this burden estimate or any other aspect of this collection of information, including suggestions for reducing this burden to Department of Defense, Washington Headquarters Services, Directorate for Information Operations and Reports (0704-0188), 1215 Jefferson Davis Highway, Suite 1204, Arlington, VA 22202-4302. Respondents should be aware that notwithstanding any other provision of law, no person shall be subject to any penalty for failing to comply with a collection of information if it does not display a currently valid OMB control number. <b>PLEASE DO NOT RETURN YOUR FORM TO THE ABOVE ADDRESS.</b>					
1. REPORT DATE (DD-MM-YYYY) July 2013		2. REPORT TYPE Final report		3. DATES COVERED (From - To)	
4. TITLE AND SUBTITLE  Minimum Thickness of Concrete Pavement for the F-15 and C-17 Aircraft				5a. CONTRACT NUMBER	
				5b. GRANT NUMBER	
				5c. PROGRAM ELEMENT NUMBER	
6. AUTHOR(S)  Carlos R. Gonzalez, Walter R. Barker, and Alessandra Bianchini				5d. PROJECT NUMBER	
				5e. TASK NUMBER	
				5f. WORK UNIT NUMBER	
7. PERFORMING ORGANIZATION NAME(S) AND ADDRESS(ES)  Geotechnical and Structures Laboratory US Army Engineer Research and Development Center 3909 Halls Ferry Road Vicksburg, MS 39180-6199				8. PERFORMING ORGANIZATION REPORT NUMBER  ERDC/GSL TR-13-34	
9. SPONSORING / MONITORING AGENCY NAME(S) AND ADDRESS(ES)  US Army Corps of Engineers Washington, DC 20314-1000				10. SPONSOR/MONITOR'S ACRONYM(S)  USACE	
				11. SPONSOR/MONITOR'S REPORT NUMBER(S)	
12. DISTRIBUTION / AVAILABILITY STATEMENT Approved for public release; distribution is unlimited.					
13. SUPPLEMENTARY NOTES					
14. ABSTRACT The procedure for the design of military rigid airfield pavements contained in the Unified Facilities Criteria 3-260-02 gives the minimum thickness of airfield concrete pavements as 6 in. The introduction of the C-17 aircraft and the requirement that dowel bars be used as load transfer mechanism at joints for airfield pavements bring into question the validity of the 6 in. minimum thickness. With the objective of updating such minimum thickness criteria, a full-scale test section was constructed and trafficked with wheel loads simulating F-15, B-52, and C-17 aircraft traffic. Test section performance was evaluated by recording the number of passes to failure and by utilizing the falling weight deflectometer testing to measure the stiffness and load transfer capability of joints. In addition, strain gages were installed on the vertical face of a longitudinal joint and on the pavement surface on each side of longitudinal joints. Evaluation of the test section performance and analysis of the strain data supported an Engineer Research and Development Center team recommendation that the minimum pavement thickness be 8 in. for any doweled airfield pavement. The team further recommended that a minimum thickness of 11 in. be established for those pavements supporting C-17 aircraft.					
15. SUBJECT TERMS Rigid pavements Minimum thickness				Strain gauge Accelerated testing Full-scale test section	
16. SECURITY CLASSIFICATION OF:			17. LIMITATION OF ABSTRACT	18. NUMBER OF PAGES	19a. NAME OF RESPONSIBLE PERSON A. Bianchini
a. REPORT Unclassified	b. ABSTRACT Unclassified	c. THIS PAGE Unclassified			19b. TELEPHONE NUMBER (include area code) 601-634-5379